

Supporting Materials

Generalized Interatomic Pair-Potential Function

Jianing Colin Xie^{1,2}, Sudhanshu K. Mishra³, Tapas Kar¹, and Rui-Hua Xie^{4,5}

¹*Department of Chemistry and Biochemistry, Utah State University, Logan, UT 84322, USA*

²*A&M Consolidated High School, College Station, TX 77840, USA*

³*Department of Economics, North-Eastern Hill University, Shillong 793022, India*

⁴*Department of Applied Physics, Xi'an Jiaotong University, Xi'an 710049, China*

⁵*Department of Physics, Hubei University, Wuhan 430062, China*

List of Contents

1.	Covalent Bonding: Neutral Systems.....	3-19
1.1.	H ₂ : Fig.1.1 and Table 1.1	3
1.2.	Li ₂ : Fig.1.2 and Table 1.2	5
1.3.	B ₂ : Fig.1.3 and Table 1.3.....	7
1.4.	C ₂ : Fig.1.4 and Table 1.4.....	8
1.5.	N ₂ : Fig.1.5	9
1.6.	F ₂ : Fig.1.6 and Table 1.6.....	10
1.7.	LiH: Fig.1.7 and Table 1.7	12
1.8.	BeH: Fig.1.8	13
1.9.	LiNa: Fig.1.9 and Table 1.9.....	14
1.10.	InH: Fig.1.10	15
1.11.	NO: Fig.1.11.....	15
1.12.	HCl: Fig.1.12	16
1.13.	OH: Fig.1.13.....	16
1.14.	NH: Fig.1.14.....	17
1.15.	CH: Fig.1.15.....	17
1.16.	CO: Fig.1.16.....	18
1.17.	Si ₂ : Fig.1.17	18
1.18.	SiO: Fig.1.18.....	19
2.	Covalent Bonding: Ionic Systems.....	20-28
2.1.	H ₂ ⁺ : Fig.2.1 and Table 2.1A, Table 2.1B	20
2.2.	HeH ⁺ : Fig.2.2 and Table 2.2	22
2.3.	He ₂ ⁺ : Fig.2.3 and Table 2.3A, Table 2.3B.....	24
2.4.	BeH ⁺ : Fig.2.4. and Table 2.4	26
2.5.	BeH ⁻ : Fig.2.5. and Table 2.5	27
2.6.	LiH ⁻ : Fig.2.6.....	28
3.	Ionic Bonding Systems	29-30
3.1.	NaCl: Fig.3.1. and Table 3.1.	29
4.	van der Waals Binding Systems.....	30-54
4.1.	Triplet states.....	30-32
4.1.1.	H ₂ : Fig.4.1.1	30
4.1.2.	NaK: Fig.4.1.2	31

4.2. Rare-Gas Dimers	32-39
4.2.1. He ₂ : Fig.4.2.1	32
4.2.2. Ne ₂ : Fig.4.2.2	33
4.2.3. Ar ₂ : Fig.4.2.3 and Table.4.2.3	34
4.2.4. Kr ₂ : Fig.4.2.4 and Table 4.2.4.	36
4.2.5. Xe ₂ : Fig.4.2.5 and Table 4.2.5.	38
4.3. Alkaline-Earth Dimers.....	39-42
4.3.1. Ca ₂ : Fig.4.3.1 and Table 4.3.1	39
4.3.2. Sr ₂ : Fig.4.3.2 and Table 4.3.2.....	40
4.3.3. Mg ₂ : Fig.4.3.3.....	42
4.4. Metal-Rare Gas Dimers	43-46
4.4.1. LiHe: Fig.4.4.1	43
4.4.2. LiAr: Fig.4.4.2	43
4.4.3. NaAr: Fig.4.4.3 and Table 4.4.3	44
4.4.4. KAr: Fig.4.4.4	45
4.4.5. NaKr: Fig.4.4.5	45
4.4.6. CaHe: Fig.4.4.6	46
4.5. Group 12 Dimers	46-49
4.5.1. Zn ₂ : Fig.4.5.1	47
4.5.2. Cd ₂ : Fig.4.5.2.....	48
4.5.3. Hg ₂ : Fig.4.5.3	48
4.6. Other van der Waals Dimers	49-54
4.6.1. LiHg: Fig.4.6.1.	49
4.6.2. CdNe: Fig.4.6.2.	50
4.6.3. LiHe ⁻ : Fig.4.6.3.	51
4.6.4. HeH: Fig.4.6.4.	51
4.6.5. NeH: Fig.4.6.5.	52
4.6.6. AgHe: Fig.4.6.6.	53
4.6.7. XeF: Fig.4.6.7.	53
4.6.8. KrF: Fig.4.6.8.	54
5. Meta-Stable Diatomic Dication Systems	54-56
5.1. He ₂ ⁺⁺ : Table 5.1.....	55
5.2. BeH ⁺⁺ : Fig.5.2.....	55
5.3. AlH ⁺⁺ : Fig.5.3.....	56
Appendix A: Notes for Determining Pair-Potential Parameters	57-57
A.1. How to Determine Pair-Potential Parameters	57-57
A.2. List of Pair-Potential Parameters	57-59
Appendix B: Interatomic Pair-Potential Functions (1918~ 2013).....	60-88
B.1. Top Pair-Potential Functions	60-61
B.2. List of Pair-Potential Functions	61-88
References	89-97

1. Covalent Bonding: Neutral Systems

The proposed four-parameter pair-potential function $V(R, \alpha, \beta, \eta, \kappa)$ for the neutral covalent bonding systems is

$$V(R, \alpha, \beta, \eta, \kappa) = \frac{J_1(R, \alpha, \kappa, \eta) + K_1(R, \alpha, \kappa, \beta)}{1 + S_0(R)}, \quad (1)$$

with $J_1(R, \alpha, \kappa, \eta) = e^{-4\alpha R(1+\kappa R)} \left(\frac{1}{R} + \eta\right)$, $K_1(R, \alpha, \kappa, \beta) = e^{-\alpha R(1+\kappa R)} \left(\frac{1}{R} - \beta R\right)$, and $S_0(R) = e^{-R} \left(1 + R + \frac{R^2}{3}\right)$, where R is the nuclear-nuclear distance and $\alpha, \beta, \eta, \kappa$ are adjusting parameters.

1.1. H₂

Here we take the ground state of H₂ as an example. First, we compute the potential energy of the ground-state H₂ by using couple cluster method with single and double excitation (CCSD) [118] and basis set aug-cc-pV5Z (Augmented correlation-consistent core-valence basis sets up to quintuple-zeta quality) that were implemented in Gaussian 09 package [119]. As shown in Fig.1.1, our CCSD/aug-cc-pV5Z calculations are in excellent agreement with the exact data [120]. Then, we fit the CCSD/aug-cc-pV5Z data by using the four-parameter potential function Eq.(1). The Root-Mean-Square (RMS) for this fitting is 0.00046, and four potential parameters are determined to be $\alpha = 1.24179616$, $\beta = 1.91867424$, $\kappa = 0.0478910411$, and $\eta = 2.8004031$. Fig.1.1 presents the fitted potential energy curve (PEC), which agrees well with the exact data [120]. Also, in the short- and large-R regions shown in Fig.1.1(a) and (c), respectively, our four-parameter potential is greatly improved over the three-parameter potential [100].

Recently, Cahill and Parsegian [98] have demonstrated that their developed five-parameter Rydberg-London potential for the ground-state H₂ is five times more accurate than Morse [6], Varshni [34], and Hulburt-Hirschfelder [25] potentials, and are four orders of magnitude more accurate than Lennard-Jones [3] and harmonic potentials. In Fig.1.1, we compare our four-parameter potential with Rydberg-London potential. In the intermediate-R region (Fig.1.1(b)), Rydberg-London potential except a visible deviation in the well bottom overlaps with our four-parameter potential curve. However, Rydberg-London potential [98] in the short-R region (Fig.1.1(a)) is much softer than our four-parameter potential, and displays a discernible deviation in the large-R region (Fig.1.1(c)). This comparison concludes that our four-parameter potential is more accurate than five-parameter Rydberg-London potential.

Rydberg-Klein-Rees (RKR) [121] turning points and vibrational levels provide accurate reference standards for assessing the quality of a potential-energy curve. Thus, we have calculated the vibrational energies for the ground-state H₂ by using the fitted four-parameter potential. The computed results are summarized in Table 1.1 and compared with the literature data. We find that our computed vibrational energies are within a relative error of less than 1% and 3% for $\nu = 0, 1, \dots, 12$ and $\nu = 13, 14$ levels, respectively, compared to experiment [122]. The present results are more accurate than those obtained by using three-parameter potential [100] and five-parameter Rydberg-London potential [98].

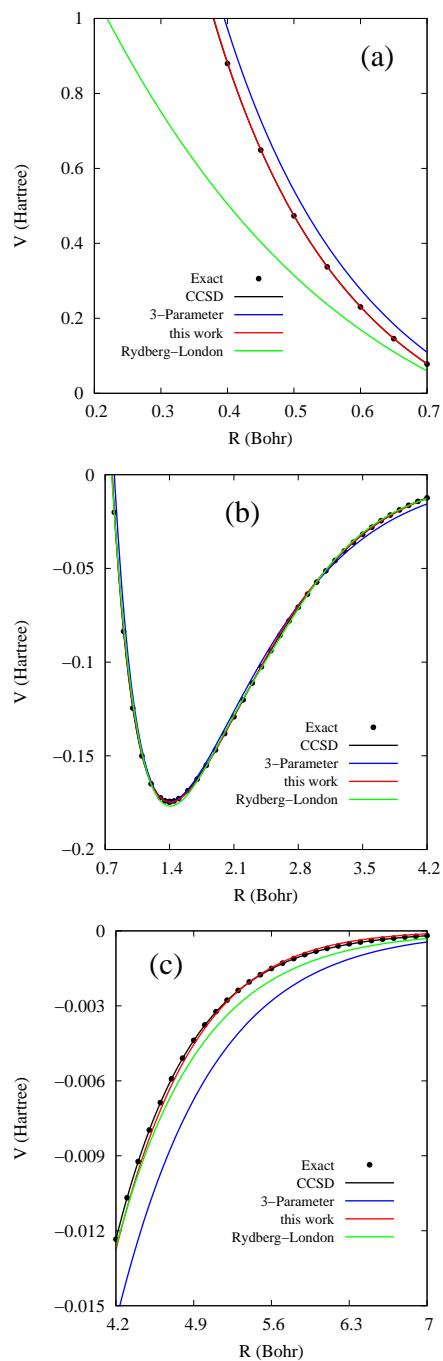


Fig.1.1: The comparison between 4-parameter potential (this work) (Red line, $\alpha = 1.24179616$, $\beta = 1.91867424$, $\kappa = 0.0478910411$, and $\eta = 2.8004031$), 3-parameter potential (Blue line, Ref. [100], $\alpha = 1.5065756$, $\beta = 2.48475652$, and $\gamma = 1.45$), Rydberg-London potential (Green line, Ref. [98], $a = 53.8$, $b = 2.99$, $c = 2.453$, $d = 3.884$, and $e = 47.6$), CCSD/aug-cc-pV5Z (Dark line), and the exact data (Dark filled circles, Ref. [120]) for the ground-state H_2 : (a) Short-R ($0.2 \sim 0.7$ Bohr)(Note: CCSD results overlap with the exact data); (b) Intermediate-R ($0.7 \sim 4.2$ Bohr); (c) Large-R ($4.2 \sim 7$ Bohr) regions.

Table 1.1: The calculated vibrational energies for H_2 using four-parameter (this work, $\alpha = 1.24179616$, $\beta = 1.91867424$, $\kappa = 0.0478910411$, and $\eta = 2.8004031$), three-parameter [100] ($\alpha = 1.5065756$, $\beta = 2.48475652$, $\gamma = 1.45$), and Rydberg-London [98] ($a = 53.8$, $b = 2.99$, $c = 2.453$, $d = 3.884$, and $e = 47.6$) potentials. The value in the parenthesis is the relative error ($\delta = |Theory - Experiment|/Experiment$) of the calculation, compared to experiment [122].

ν	Exp. (Ref. [122]) [eV]	3-Parameter (Ref. [100]) [eV]	Rydberg-London (Ref. [98]) [eV]	4-Parameter (this work) [eV]
0	-4.4774	-4.4628 (0.33%)	-4.5247 (1.06%)	-4.4852 (0.17%)
1	-3.9615	-3.9218 (1.00%)	-3.9779 (0.41%)	-3.9661 (0.12%)
2	-3.4747	-3.4166 (1.67%)	-3.4729 (0.05%)	-3.4750 (0.01%)
3	-3.0166	-2.9465 (2.32%)	-3.0101 (0.22%)	-3.0123 (0.14%)
4	-2.5866	-2.5111 (2.92%)	-2.5856 (0.04%)	-2.5783 (0.32%)
5	-2.1847	-2.1099 (3.42%)	-2.1899 (0.24%)	-2.1734 (0.52%)
6	-1.8110	-1.7427 (3.77%)	-1.8169 (0.33%)	-1.7981 (0.71%)
7	-1.4661	-1.4093 (3.87%)	-1.4673 (0.08%)	-1.4532 (0.88%)
8	-1.1508	-1.1097 (3.57%)	-1.1460 (0.43%)	-1.1396 (0.97%)
9	-0.8665	-0.8439 (2.61%)	-0.8578 (1.00%)	-0.8583 (0.94%)
10	-0.6153	-0.6123 (0.49%)	-0.6068 (1.38%)	-0.6109 (0.71%)
11	-0.4000	-0.4155 (3.88%)	-0.3957 (1.08%)	-0.3994 (0.14%)
12	-0.2245	-0.2543 (13.27%)	-0.2271 (1.16%)	-0.2266 (0.93%)
13	-0.0945	-0.1301 (37.67%)	-0.1031 (9.10%)	-0.0966 (2.25%)
14	-0.0174	-0.0452 (159.77%)	-0.0264 (51.72%)	-0.0169 (2.73%)

1.2. Li_2

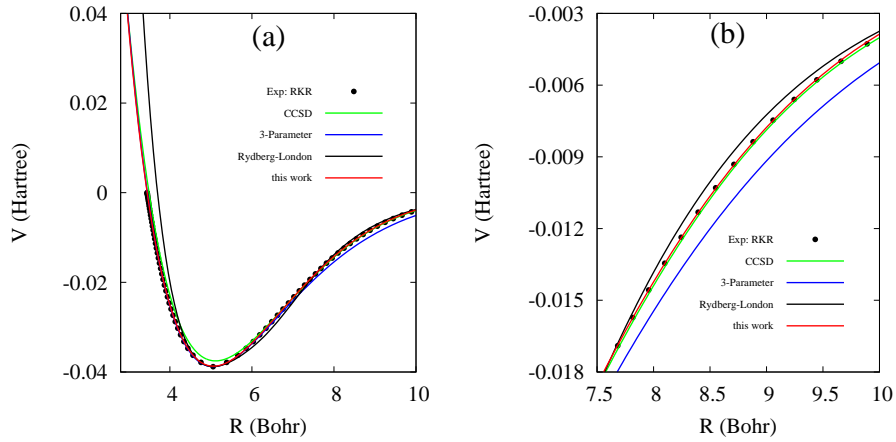


Fig.1.2: The comparison between 4-parameter model potential (Red, this work, $\alpha = 0.221158172$, $\beta = 0.0981516842$, $\kappa = 0.145366735$, and $\eta = 1.19828642$), Rydberg-London potential (Dark line, $a = 199.481$, $b = 1.62$, $c = 0.5101$, $C_6 = 829.33$, $d = 208000$, Ref. [124]), CCSD/6-311++G(3df, 2pd)(Green line, Ref. [100]), 3-parameter model potential (Blue line, $\alpha = 0.585395$, $\beta = 0.73399479$, $\gamma = 0.2125$, Ref. [100]), and the experimental RKR data points (filled circles, Ref. [123].) for the ground state of Li_2 .

The lithium dimer has only 6 electrons and has been one of the most studied diatomic molecules. It is a “light” molecule for which *ab initio* calculations can be of great precision. Its spectroscopic constants are of the same order of magnitude as those of numerous other diatomic

molecules (in contrast to H₂), and its properties are often calculated as a test of theoretical approximations used for heavier molecules. Then the *ab initio* determined parameters are often highly reliable and also can serve as a check of the experimental determinations. For these reasons, Li₂ is a good model for both theoretical and experimental investigations of the interactions in neutral homonuclear diatomic molecules. Here, we take Li₂ as an example, too.

Table 1.2: Calculated vibrational energies for ⁷Li₂ by using the four-parameter potential (this work, $\alpha = 0.221158172$, $\beta = 0.0981516842$, $\kappa = 0.145366735$, and $\eta = 1.19828642$), where $\delta = |Theory - Experiment|/Experiment$ is the relative error of the present calculation, compared to experiment [123].

ν	Exp. (Ref. [123]) [cm ⁻¹]	this work [cm ⁻¹]	δ	ν	Exp. (Ref. [123]) [cm ⁻¹]	this work [cm ⁻¹]	δ
0	175.0320	175.0334	0.001%	19	5790.7056	5810.0379	0.334%
1	521.2611	523.1824	0.369%	20	6022.6578	6041.5448	0.314%
2	862.2642	866.1712	0.453%	21	6246.9482	6265.4344	0.296%
3	1197.9974	1203.9134	0.494%	22	6463.3140	6481.4870	0.281%
4	1528.4128	1536.3202	0.517%	23	6671.3979	6689.4645	0.271%
5	1853.4573	1863.2996	0.531%	24	6870.8931	6889.1075	0.265%
6	2173.0721	2184.7566	0.538%	25	7061.4199	7080.1312	0.265%
7	2487.1914	2500.5927	0.539%	26	7242.5556	7262.2217	0.272%
8	2795.7419	2810.7056	0.535%	27	7413.8431	7435.0293	0.286%
9	3090.6412	3114.9891	0.788%	28	7574.8736	7598.1611	0.307%
10	3395.7978	3413.3326	0.516%	29	7724.9165	7751.1715	0.339%
11	3687.1094	3705.6203	0.502%	30	7863.7083	7893.5477	0.379%
12	3972.4624	3991.7317	0.485%	31	7990.4162	8024.6909	0.429%
13	4251.7309	4271.5400	0.466%	32	8104.4730	8143.8879	0.486%
14	4524.7756	4544.9122	0.445%	33	8205.2323	8250.2681	0.549%
15	4791.4274	4811.7084	0.423%	34	8292.0293	8342.7322	0.611%
16	5051.5343	5071.7806	0.401%	35	8364.3066	8419.8251	0.664%
17	5304.9322	5324.9723	0.378%	36	8421.6123	8479.4715	0.687 %
18	5551.3992	5571.1172	0.355%	37	8463.9648	8518/2744	0.642 %

We fit the RKR data point [123] of the ground state of Li₂ using the four-parameter potential function Eq.(1). The root-mean-square (RMS) for this fitting is 0.0000781, and the potential parameters are determined to be $\alpha = 0.221158172$, $\beta = 0.0981516842$, $\kappa = 0.145366735$, and $\eta = 1.19828642$. In Figure 1.2, we report the fitting results and compare them with Rydberg-London potential [124], *ab initio* CCSD/6-311++G(3df, 2pd) calculation, and the accurate RKR experimental data [123]. The new potential curve for Li₂ agrees very well with experiment RKR data and CCSD/6-311++G(3df, 2pd) calculations. In the repulsive part, we find that our four-parameter potential gives a much better performance than Rydberg-London potential [98]. In the region of $7.5 < R < 10$ shown in Fig.1.2(b), we find that Rydberg-London potential [98] shows a slight deviation from our four-parameter potential and the accurate data, while three-parameter potential [100] displays a large deviation from four-parameter potential curve. We conclude that the four-parameter potential is more accurate than five-parameter Rydberg-London potential [124] and three-parameter potential [100].

Then, we calculate the vibrational energies for the ground-state Li₂ using the four-parameter potential. The calculated results are summarized in Table 1.2. We find that all calculated

vibrational energies are within a relative error of less than 1%, compared to the experimental data [123].

1.3. B₂

The electron-deficient diatomic boron molecule B₂ has long puzzled the scientists. As yet, only six vibrational energy levels are known from experiment [126] for ¹¹B₂ molecule in the ground electronic state. Very recently, Scuseria and colleagues [127] have generated a highly accurate potential energy curve for the ground state of B₂ by using advanced *ab initio* method. In their *ab initio* study, all rotational vibrational levels of the ground state are determined up to the dissociation limit with near-spectroscopic accuracy ($< 10\text{cm}^{-1}$). Using the even-tempered Gaussian (ETG) function, $V(R) = \sum_{k=0}^7 a_k e^{-\alpha\beta^k R^2}$, Scuseria and colleagues [127] have found an exact fitting of their accurate *ab initio* potential curve for the ground-state B₂ and determined the 10 fitting parameters, $\alpha = 0.166$, $\beta = 1.5368$, $a_0 = 8.23987249$, $a_1 = -107.15781150$, $a_2 = 303.54772065$, $a_3 = -1668.82025703$, $a_4 = 2015.42869563$, $a_5 = -353.81494323$, $a_6 = 2257.70466507$, and $a_7 = 3915.44790772$. Both accurate and ETG fitting results are presented in Figure 1.3.

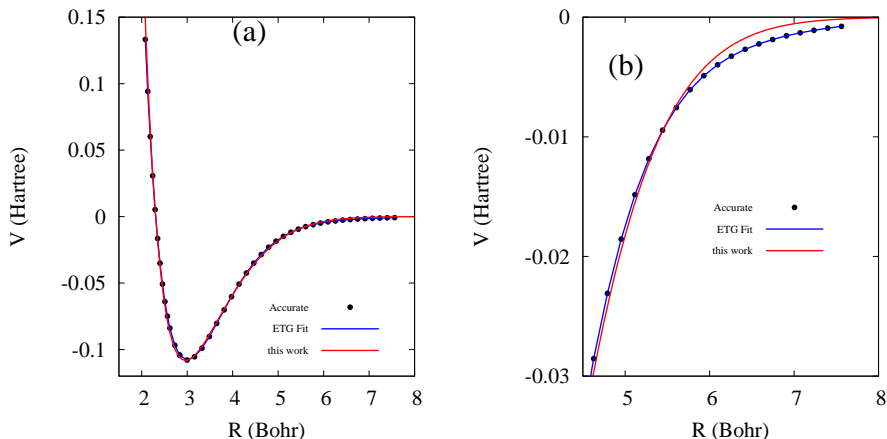


Fig.1.3: The comparison between 4-parameter potential (this work) (Red line, $\alpha = 0.183899426$, $\beta = 0.462900133$, $\kappa = 0.813404073$, and $\eta = 24.2300391$), the fitted result (Blue line, Ref. [127]) by using the Even-Tempered Gaussian (ETG) function, $V(R) = \sum_{k=0}^7 a_k e^{-\alpha\beta^k R^2}$ ($\alpha = 0.166$, $\beta = 1.5368$, $a_0 = 8.23987249$, $a_1 = -107.15781150$, $a_2 = 303.54772065$, $a_3 = -1668.82025703$, $a_4 = 2015.42869563$, $a_5 = -353.81494323$, $a_6 = 2257.70466507$, $a_7 = 3915.44790772$), and the most accurate data (dark filled circles, Ref. [127]) for the ground state of B₂.

Then, we also fit the accurate *ab initio* data of Scuseria and colleagues [127] by using the new potential function given by Eq.(1). The RMS for this fitting is 0.0018, and the fitted parameters are determined to be $\alpha = 0.183899426$, $\beta = 0.462900133$, $\kappa = 0.813404073$, and $\eta = 24.2300391$. Figure 1.3 presents our fitted potential curve. We find that the fitted curve except a slight deviation at $R > 5.5$ Bohr agrees well with the accurate curve.

Then, we calculate the vibrational energies for the ground-state B₂ by using the derived four-parameter potential. The computed results are summarized in Table 1.3. In comparison with the accurate *ab initio* data [127], all calculated vibrational energies except the first two levels ($\nu = 1, 2$) are within the relative error of less than 1% (those for the levels $\nu = 1, 2$ are slightly larger than 1%).

Table 1.3: Calculated vibrational energies for $^{11}\text{B}_2$ by using the four-parameter potential (this work, $\alpha = 0.183899426$, $\beta = 0.462900133$, $\kappa = 0.813404073$, and $\eta = 24.2300391$), where $\delta = |Theory - Accurate|/Accurate$ is the relative error of the present calculation, compared to the accurate data [127].

ν	this work [cm^{-1}]	Accurate [cm^{-1}]	δ	ν	this work [cm^{-1}]	Accurate [cm^{-1}]	δ
0	0.	0.	0.	18	15566.78	15670.66	0.66%
1	1045.11	1031.93	1.27%	19	16226.58	16339.18	0.69%
2	2068.65	2046.35	1.09%	20	16862.16	16982.85	0.71%
3	3070.81	3043.08	0.91%	21	17472.66	17600.88	0.73%
4	4051.72	4021.88	0.74%	22	18059.83	18192.41	0.73%
5	5011.51	4982.51	0.58%	23	18626.90	18756.49	0.69%
6	5950.27	5924.73	0.43%	24	19173.45	19292.11	0.62%
7	6868.07	6848.25	0.29%	25	19692.36	19798.1	0.53%
8	7764.92	7752.78	0.16%	26	20171.69	20273.22	0.50%
9	8640.84	8638.00	0.03%	27	20604.99	20716.06	0.54%
10	9495.79	9503.57	0.08%	28	21008.64	21125.11	0.55%
11	10329.71	10349.13	0.19%	29	21403.24	21498.7	0.44%
12	11142.51	11174.28	0.28%	30	21784.45	21835.08	0.23%
13	11934.08	11978.60	0.37%	31	22138.34	22132.47	0.03%
14	12704.24	12761.64	0.45%	32	22454.39	22389.37	0.29%
15	13452.79	13522.91	0.52%	33	22725.49	22605.03	0.53%
16	14179.48	14261.89	0.58%	34	22945.83	22780.26	0.73%
17	14884.20	14978.01	0.63%	35	23205.37	23024.09	0.79%

1.4. C_2

C_2 molecule is a common intermediate in combustion reactions of carbon containing materials, having first been observed spectroscopically in flames. It plays also a crucial role in the chemistry of the interstellar medium and is found in many extraterrestrial sources such as comets, carbon stars, proto-planetary nebulas, and molecular clouds. Theoretically [128], the ground electronic state $X^1\Sigma_g^+$ of C_2 is known to exhibit anomalous bonding, having two π bonds but no σ bond, which makes the prediction of its potential energy curve a challenging test for quantum chemical methods. In 2004, Abrams and Sherrill [129] reported the most accurate potential energy curve of the ground state of C_2 by performing a full configuration interaction calculation, which exactly solve the electronic Schrödinger equation within the space spanned by a 6 – 31G* Gaussian basis set.

Here we fit the accurate *ab initio* data of Abrams and Sherrill [129] by using the four-parameter potential function given by Eq.(1). The RMS for this fitting is 0.0027, and the fitting parameters are determined to be $\alpha = 0.127145432$, $\beta = 0.967192362$, $\kappa = 1.89580627$, and $\eta = 28.3280362$. Figure 1.4. presents the fitted potential curve, and Table 1.4 compares the fitted potential energies with the accurate potential energies [129]. We find that the fitted curve agrees very well with the accurate data [129].

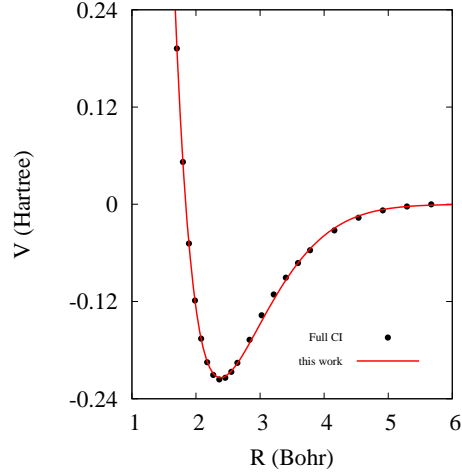


Fig.1.4: Comparison between 4-parameter model (this work) (Red line, $\alpha = 0.127145432$, $\beta = 0.967192362$, $\kappa = 1.89580627$, and $\eta = 28.3280362$) and full configuration interaction calculation (Full CI) (dark filled circles, Ref. [129]) for the ground state of C_2 .

Table 1.4: The fitted potential energies for the ground state of C_2 by using the four-parameter potential (this work) ($\alpha = 0.127145432$, $\beta = 0.967192362$, $\kappa = 1.89580627$, and $\eta = 28.3280362$), compared to the accurate energies (Ref. [129]). All energies are relative to -75.509909 Hartree [129]). Energy and R are in units of Hartree and \AA , respectively.

R	Accurate (Ref. [129])	this work	R	Accurate (Ref. [129])	this work
0.90	0.192291	0.193520	1.50	-0.167216	-0.171464
0.95	0.052244	0.052021	1.60	-0.137019	-0.144248
1.00	-0.048426	-0.049431	1.70	-0.111252	-0.117716
1.05	-0.118736	-0.119608	1.80	-0.090531	-0.093544
1.10	-0.165728	-0.165817	1.90	-0.072506	-0.072529
1.15	-0.194902	-0.193992	2.00	-0.056735	-0.054931
1.20	-0.210564	-0.208838	2.20	-0.032231	-0.029448
1.25	-0.216084	-0.214014	2.40	-0.016548	-0.014472
1.30	-0.214115	-0.212314	2.60	-0.007538	-0.006538
1.35	-0.206746	-0.205840	2.80	-0.002657	-0.002722
1.40	-0.195633	-0.196155	-	-	-

1.5. N_2

N_2 is the most abundant component of the Earth's atmosphere. This fact makes its optical and other properties the topics of great importance. Over the past century, numerous spectroscopic studies have been performed on this system, and a number of high quality *ab initio* studies have been reported for this system. The work of Gdanitz [130], and Li and Paldus [131] reported well-accepted accurate and portable potential energy function for the ground state $X^1\Sigma_g^+$ of N_2 . In this work, we fit the accurate *ab initio* data of Li and Paldus [131] by using the new potential function given by Eq.(1). The RMS for this fitting is 0.00248, and the fitted potential parameters are determined to be $\alpha = 0.151104274$, $\beta = 1.78382371$, $\kappa = 1.99999854$, and $\eta = 42.591009$. Figure 1.5 presents the fitted potential curve and compares with Rydberg-London potential [124]. We find that the fitted 4-parameter potential curve agrees well with

the accurate *ab initio* potential curves (MR-CI [130] and 56R RMR CCSD [131]) and Rydberg-London potential [124].

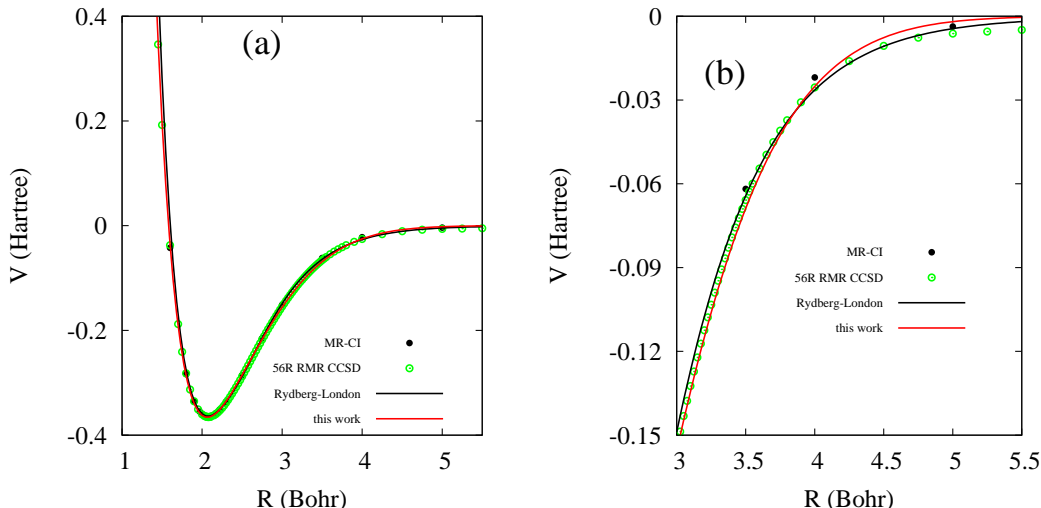


Fig.1.5: Comparison between 4-parameter potential (this work) (Red line, $\alpha = 0.151104274$, $\beta = 1.78382371$, $\kappa = 1.99999854$, and $\eta = 42.591009$), Rydberg-London potential (Dark line, Ref. [124], $a = 3752.644$, $b = 4.3533$, $c = 1.1777$, $C_6 = 14.382$, $d = 34.8$), multiple-reference configuration interaction (MR CI) calculation (dark filled circles, Ref. [130]), and reduced multi-reference coupled-cluster with singles and doubles (RMR CCSD) (Dark green open circles, Ref. [131]) for the ground state of N₂.

1.6. F₂

The first reliable report on the potential energy of the fluorine molecule F₂ is the 1976 paper of Colbourn and co-workers [135], where the absorption spectrum of F₂, in the 780-1020Å range has been photographed at sufficient resolution to allow a rotational analysis of many bands. An analysis of the bands of this system has determined the vibrational levels of the ground state up to the vibrational level of $\nu = 22$. In 2007, Bytautas *et al.* [134] reported the accurate *ab initio* potential energy curve of the ground state of F₂ by performing full configuration interaction (Full CI) calculations. They have also found an accurate analytical expression [103] (i.e., even-Tempered Gaussian (ETG) function): $V(R) = \sum_{k=0}^4 a_k e^{-\alpha\beta^k R^2}$ ($\alpha = 0.41$, $\beta = 2.36$, $a_0 = 0.00533126$, $a_1 = -0.758546$, $a_2 = 4.46776$, $a_3 = -8.12792$, $a_4 = 233913.56201$), by fitting the experimental RKR data points [135].

We have fitted the experimental RKR points [135] of the ground state of F₂ by using the four-parameter potential function given by Eq.(1). The RMS for this fitting reaches 0.0014, and the potential parameters are determined to be $\alpha = 0.029803514$, $\beta = 0.460794341$, $\kappa = 9.99999811$, and $\eta = 54.737768091$. The fitted results are presented in Figure 1.6. The fitted potential curve agrees well with the full CI calculation and experimental RKR data points. To be noted, the equilibrium position ($R_e = 2.6226$ Bohr, $V_{min} = -0.0611474$ Hartree) for this fitting is slightly shifted by 0.05 Bohr in comparison with experiment ($R_e = 2.6705$ Bohr, $V_{min} = -0.0610935761$ Hartree).

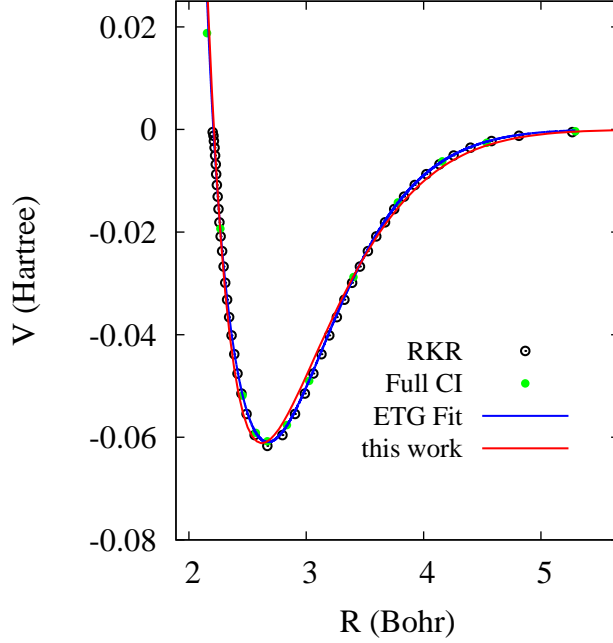


Fig.1.6: The comparison between four-parameter potential (Red line, this work, $\alpha = 0.029803514$, $\beta = 0.460794341$, $\kappa = 9.999999811$, and $\eta = 54.737768091$), accurate full configuration interaction (Full CI) calculation (green filled circles, Ref. [134]), the result (Blue line, Ref. [103]) of fitting the experimental RKR data points by using the Even-Tempered Gaussian (ETG) function, $V(R) = \sum_{k=0}^4 a_k e^{-\alpha \beta^k R^2}$ ($\alpha = 0.41$, $\beta = 2.36$, $a_0 = 0.00533126$, $a_1 = -0.758546$, $a_2 = 4.46776$, $a_3 = -8.12792$, $a_4 = 233913.56201$), and experimental RKR data points (dark open circles, Ref. [135]) for the ground state of F_2 .

Then, we calculate the vibrational energies for the ground-state F_2 using the derived four-parameter potential. The calculated results are summarized in Table 1.6. In comparison with the experimental RKR data [135], all calculated vibrational energies except the first seven levels ($\nu = 1 - 7$) are within the relative error of less than 1% (those for the levels $\nu = 1 - 7$ are less than 4.5%).

Table 1.6: Calculated vibrational energies for $^{19}F_2$ using the four-parameter potential (this work, $\alpha = 0.029803514$, $\beta = 0.460794341$, $\kappa = 9.999999811$, and $\eta = 54.737768091$). Relative $\delta = |Theory - Experiment|/Experiment$ of the present calculation, compared to experiment [135].

ν	this work [cm ⁻¹]	Exp. (Ref. [135]) [cm ⁻¹]	δ %	ν	this work [cm ⁻¹]	Exp. (Ref. [135]) [cm ⁻¹]	δ %	ν	this work [cm ⁻¹]	Exp.(Ref. [135]) [cm ⁻¹]	δ %
0	0	0	0	8	6518.11	6455.17	0.97	16	10963.51	11053.90	0.81
1	931.88	893.90	4.25	9	7187.19	7141.63	0.63	17	11366.25	11468.96	0.89
2	1829.14	1764.15	3.68	10	7824.48	7798.48	0.33	18	11731.35	11842.62	0.93
3	2692.48	2610.22	3.15	11	8429.83	8424.67	0.06	19	12056.85	12172.25	0.94
4	3522.50	3431.53	2.65	12	9003.00	9019.11	0.17	20	12340.24	12452.98	0.90
5	4319.70	4227.43	2.18	13	9543.59	9580.63	0.38	21	12578.05	12678.00	0.78
6	5084.52	4997.19	1.74	14	10051.06	10108.02	0.56	22	12765.12	12830.38	0.50
7	5817.25	5740.05	1.34	15	10524.69	10599.62	0.70				

1.7. LiH

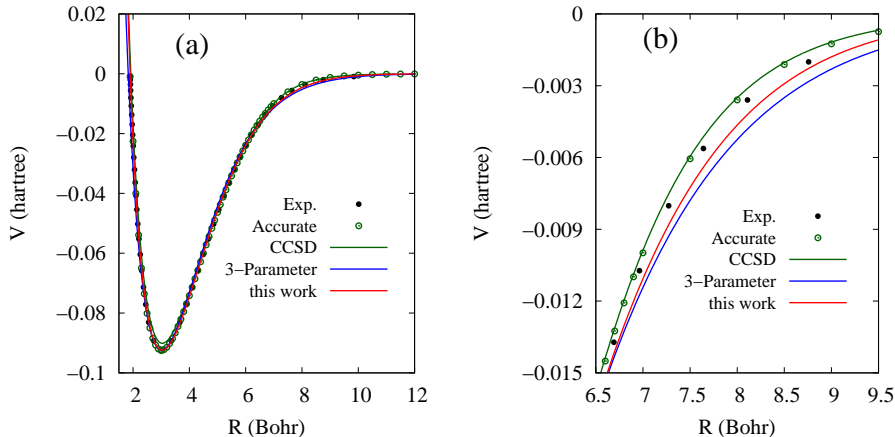


Fig.1.7: Comparison between 4-parameter potential (this work) (Red line, $\alpha = 0.590929935$, $\beta = 0.437032497$, $\kappa = 0.0488894485$, and $\eta = 11.33519$), 3-parameter potential (Blue line, $\alpha = 0.8885591$, $\beta = 1.51479003$, $\gamma = 0.345$, Ref. [100]), CCSD/6-311++G(3df,3pd)(Green line, Ref. [100]), accurate data (Green open circles, Ref. [136]), and experimental RKR data(dark filled circles, Ref. [137].) for the ground state of LiH.

Table 1.7: Calculated vibrational energies for isotopes ${}^7\text{LiH}$ using the four-parameter potential (this work) ($\alpha = 0.590929935$, $\beta = 0.437032497$, $\kappa = 0.0488894485$, and $\eta = 11.33519$) and three-parameter potential ($\alpha = 0.8885591$, $\beta = 1.51479003$, $\gamma = 0.345$, Ref. [100]). The value in the parenthesis is the relative error of the numerical calculation, compared to experiment [137]. Dissociation energy $D_e = 2.515$ eV.

ν	3-Parameter (Ref. [100]) [eV]	this work [eV]	Exp. (Ref. [137]) [eV]	ν	3-Parameter (Ref. [100]) [eV]	this work [eV]	Exp. (Ref. [137]) [eV]
0	-2.4283 (0.02%)	-2.4305 (0.08%)	-2.4287	11	-0.8545 (1.27%)	-0.8606 (0.57%)	-0.8655
1	-2.2594 (0.03%)	-2.2639 (0.17%)	-2.2601	12	-0.7456 (1.13%)	-0.7497 (0.58%)	-0.7541
2	-2.0949 (0.11%)	-2.1.18 (0.22%)	-2.0971	13	-0.6431 (0.77%)	-0.6449 (0.49%)	-0.6481
3	-1.9355 (0.21%)	-1.9441 (0.23%)	-1.9395	14	-0.5471 (0.07%)	-0.5464 (0.20%)	-0.5475
4	-1.7812 (0.34%)	-1.7910 (0.21%)	-1.7873	15	-0.4577 (1.10%)	-0.4545 (0.40%)	-0.4527
5	-1.6321 (0.50%)	-1.6427 (0.15%)	-1.6403	16	-0.3753 (3.05%)	-0.3694 (1.44%)	-0.3642
6	-1.4884 (0.67%)	-1.4993 (0.05%)	-1.4985	17	-0.3001 (6.27%)	-0.2916 (3.25%)	-0.2824
7	-1.3502 (0.85%)	-1.3609 (0.07%)	-1.3618	18	-0.2322 (11.47%)	-0.2213 (6.25%)	-0.2083
8	-1.2175 (1.03%)	-1.2276 (0.21%)	-1.2302	19	-0.1721 (20.43%)	-0.1591 (11.34%)	-0.1429
9	-1.0906 (1.17%)	-1.0997 (0.34%)	-1.1035	20	-0.1200 (37.14%)	-0.1055 (20.61%)	-0.0875
10	-0.9696 (1.26%)	-0.9773 (0.48%)	-0.9820	21	-0.0764 (73.64%)	-0.0614 (39.46%)	-0.0440

Lithium hydride, LiH, has been the object of intense theoretical and spectroscopic study since LiH represents the smallest neutral heteropolar molecule. Its simple electronic structure makes this molecule one of the favorite subjects that spectroscopists and theoretical chemists have extensively studied since 1930s. Highly accurate experimental data are available for this molecule [137]. Among the reported *ab initio* calculations of LiH, one should particularly mention the benchmark ECG (exponentially correlated Gaussian) calculations by Cencek and Rychlewski [138]. Very recently, Tung, Pavanello, and Adamowicz [136] have reported much accurate calculations of the ground-state potential energy curve (PEC) of the LiH molecule performed with all-electron ECG functions with shifted centers. The absolute accuracy of the generated PEC is estimated as not exceeding 0.3 cm^{-1} . Thus, in this paper, we fit the accurate data of Tung, Pavanello, and Adamowicz [136]. The RMS for this fitting is 0.00045, and the potential parameters are determined to be $\alpha = 0.590929935$, $\beta = 0.437032497$, $\kappa = 0.0488894485$, and $\eta = 11.33519$.

In Fig.1.7, we compare the fitted potential curve with three-parameter potential [100], *ab initio* CCSD/6-311++G(3df, 2pd) calculation [100], RKR experimental data [137], and accurate ECG calculations [136] for the ground state of LiH. Our fitted potential curve for LiH except a slight difference at $6.5 < R < 9.5$ agrees very well with experiment, accurate ECG data, and CCSD. As shown in Fig.1.7(b), the four-parameter potential curve is improved over the three-parameter potential [100].

We calculate the vibrational energies for isotopes ^7LiH by using the four-parameter potential. The computed vibrational energies are summarized in Table 1.7. In comparison with experiment [137], our calculated energies by using the four-parameter potential are within the relative error of 1% for $\nu = 0 \sim 15$ and of 1% to 40% for $\nu = 16 \sim 21$, respectively, and are better than those calculated by using the three-parameter potential [100].

1.8. BeH

Beryllium monohydride, BeH, is a small heteronuclear radical. Because it consists of only two nuclei and five electrons, the BeH radical is an attractive benchmark molecule for *ab initio* methods. It has been the subject of numerous theoretical studies (see literature review by Koput [139]). Its ground electronic state has been experimentally characterized [140]. In this work, we fit the experimental data of Ref. [140]. The RMS of this fitting is 0.017, and the potential parameters are determined to be $\alpha = 0.0439935564$, $\beta = 0.372280509$, $\kappa = 4.997$, and $\eta = 0.93473275$. Our fitted potential curve is reported in Fig.1.8, which agrees very well with *ab initio* calculations [139] by using the multi-reference averaged coupled-pair functional method in conjunction with the correlation-consistent core-valence basis sets up to septuple-zeta quality.

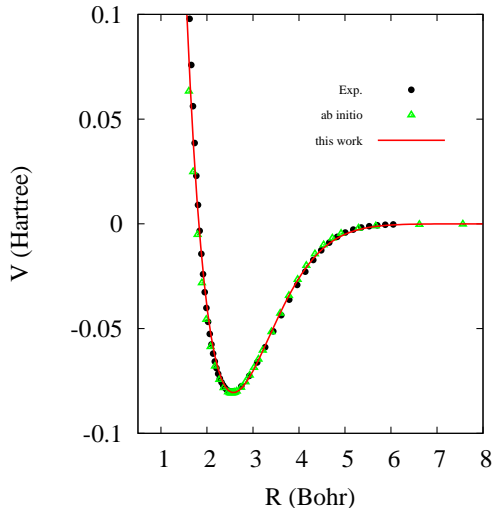


Fig.1.8 Comparison between four-parameter potential (this work) (Red line, $\alpha = 0.0439935564$, $\beta = 0.372280509$, $\kappa = 4.997$, $\eta = 0.93473275$), *ab initio* calculations by using the multi-reference averaged coupled-pair functional (MR-ACPF) method in conjunction with the correlation-consistent core-valence basis sets up to septuple-zeta quality (Green triangle, Ref. [139]), and experimental data (dark filled circles, Ref. [140]) for the ground state of BeH.

1.9. LiNa

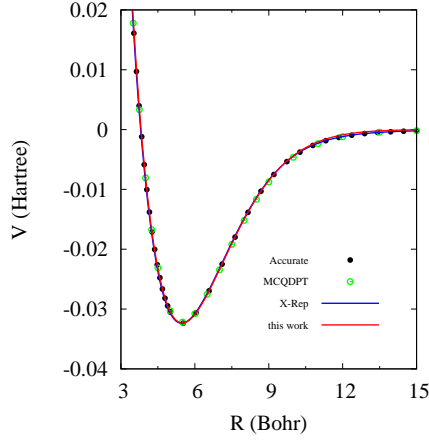


Fig.1.9: Comparison between 4-parameter potential (this work) (Red line, $\alpha = 0.153370182$, $\beta = 0.0750653157$, $\kappa = 0.225977753$, and $\eta = 0.390468193$), multiconfigurational quasi-degenerate perturbation theory (MCQDPT)(Green open circles, Ref. [141]), the X-representation potential (X-Rep)derived from the Laser-induced fluorescence spectroscopy (Blue line, Ref. [142]), and experimental data (Dark filled circles, Ref. [141]), using the simple and well-known extended-Rydberg form $V(R) = -D_e \left(1 + \sum_{k=1}^p a_k \rho^k\right) \exp(-a_1 \rho)$, where $\rho = R - R_e$) for the ground state of LiNa.

The electronic structure of the LiNa molecule was investigated by spectroscopy for the first time in 1971 and later extensively studied by experiment and theory (see the literature review in the most recent work of Tiemann group [142]). In this work, we fit the experimental data of Ref. [141]. The RMS of this fitting is 0.000671, and the potential parameters are determined to be $\alpha = 0.153370182$, $\beta = 0.0750653157$, $\kappa = 0.225977753$, and $\eta = 0.390468193$. The fitted potential curve is reported in Fig.1.9, which agrees very well with multi-configurational quasi-degenerate perturbation theory (MCQDPT) [141], X-representation potential (X-Rep) derived from the Laser-induced fluorescence spectroscopy [142], and experimental data [141] derived by using extended-Rydberg form ($V(R) = -D_e \left(1 + \sum_{k=1}^p a_k \rho^k\right) \exp(-a_1 \rho)$, where $\rho = R - R_e$). Calculated vibrational energies by using the four-parameter potential are listed in Table 1.9. The relative errors of all computed vibrational energies are within less than 1%, compared to experiment [143].

Table 1.9: Calculated vibrational energies for ${}^7\text{LiNa}$ by using the four-parameter potential ($\alpha = 0.153370182$, $\beta = 0.0750653157$, $\kappa = 0.225977753$, and $\eta = 0.390468193$), where $\delta = |Theory - Experiment|/Experiment$ is the relative error of the present calculation, compared to experiment [143].

ν	this work [cm ⁻¹]	Exp. [cm ⁻¹]	δ %	ν	this work [cm ⁻¹]	Exp. [cm ⁻¹]	δ %	ν	this work [cm ⁻¹]	Exp. [cm ⁻¹]	δ %	ν	this work [cm ⁻¹]	Exp. [cm ⁻¹]	δ %
0	0.	0.	0.	11	2595.237	2599.640	0.169	22	4736.697	4743.540	0.14	33	6303.601	6293.203	0.16
1	252.583	253.290	0.27	12	2810.002	2814.700	0.166	23	4905.352	4912.024	0.13	34	6410.347	6395.969	0.22
2	501.983	503.283	0.25	13	3020.979	3025.980	0.165	24	5069.222	5075.554	0.12	35	6509.993	6491.190	0.28
3	748.155	749.956	0.24	14	3228.098	3233.407	0.164	25	5228.180	5233.968	0.11	36	6602.134	6578.532	0.35
4	991.050	993.285	0.22	15	3431.288	3436.903	0.163	26	5382.086	5387.092	0.09	37	6686.290	6657.653	0.43
5	1230.620	1233.236	0.21	16	3630.473	3636.386	0.162	27	5530.793	5534.738	0.07	38	6761.877	6728.210	0.50
6	1466.814	1469.771	0.20	17	3825.572	3831.767	0.161	28	5674.138	5676.705	0.04	39	6828.166	6789.874	0.56
7	1699.579	1702.846	0.19	18	4016.503	4022.951	0.160	29	5811.946	5812.776	0.01	40	6884.204	6842.360	0.61
8	1928.862	1932.418	0.18	19	4203.177	4209.836	0.158	30	5944.022	5942.719	0.02	41	6928.660	6885.486	0.62
9	2154.605	2158.442	0.17	20	4385.501	4392.311	0.155	31	6070.154	6066.285	0.06	42	6959.451	6919.247	0.58
10	2376.751	2380.867	0.17	21	4563.376	4570.256	0.151	32	6190.102	6183.207	0.11				

1.10. InH

Here we report one example for the ground states of group III hydrides. We fit the experimentally determined potential data for the ground-state InH [144]. The RMS of this fitting is 0.00148, and the potential parameters are determined to be $\alpha = 0.399432325$, $\beta = 0.352975842$, $\kappa = 0.126597296$, $\eta = 21.6996589$. The fitted potential curve is reported in Fig.1.10, which agrees very well with experimentally-derived potential data [144].

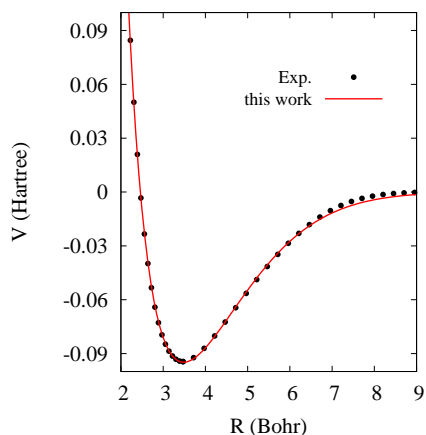


Fig.1.10 Comparison between four-parameter potential (this work) (Red line, $\alpha = 0.399432325$, $\beta = 0.352975842$, $\kappa = 0.126597296$, $\eta = 21.6996589$), and experimentally-derived data (Dark filled circles, Ref. [144]) for the ground state of InH.

1.11. NO

Here we report one example for the ground-state potential of NO. We fit the accurate potential energies determined by Huxley and Murrell [78]. The RMS of this fitting is 0.00221, and the potential parameters are determined to be $\alpha = 0.255622994$, $\beta = 1.40313848$, $\kappa = 1.05129052$, $\eta = 65.1143618$. The fitted potential curve is reported in Fig.1.11, which agrees very well with the accurate data [78]. To be noted, Rydberg-London potential shows a visible deviation from the accurate data at $R = 3 \sim 4$ Bohr.

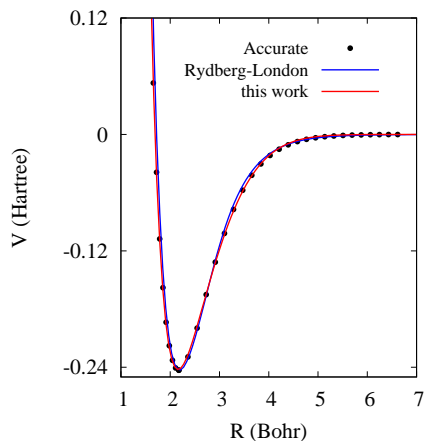


Fig.1.11 Comparison between four-parameter potential (this work) (Red line, $\alpha = 0.255622994$, $\beta = 1.40313848$, $\kappa = 1.05129052$, $\eta = 65.1143618$), Rydberg-London potential (Blue line, $a = 3809.497$, $b = 4.4196$, $c = 1.0943$, $d47.0$, $C_6 = 11.245$, Ref. [124]), and the accurate data (Dark filled circles, Ref. [78]) for the ground state of NO.

1.12. HCl

Here we report the ground-state potential of HCl. We fit the accurate potential energies determined by Huxley and Murrell [78]. The RMS of this fitting is 0.000907, and the potential parameters are determined to be $\alpha = 0.52951669$, $\beta = 0.941428491$, $\kappa = 0.212878625$, $\eta = 42.6912765$. The fitted potential curve is reported in Fig.1.12, which agrees very well with the accurate data [78].

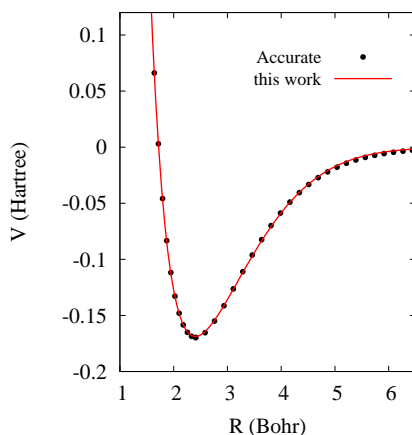


Fig.1.12 Comparison between four-parameter potential (this work) (Red line, $\alpha = 0.52951669$, $\beta = 0.941428491$, $\kappa = 0.212878625$, $\eta = 42.6912765$), and the accurate data (Dark filled circles, Ref. [78]) for the ground state of HCl.

1.13. OH

Here we report the ground-state potential of OH. We fit the accurate potential energies determined by Huxley and Murrell [78]. The RMS of this fitting is 0.0009356, and the potential parameters are determined to be $\alpha = 0.760387114$, $\beta = 1.40066201$, $\kappa = 0.20986805$, $\eta = 39.6142444$. The fitted potential curve is reported in Fig.1.13, which agrees very well with the accurate data [78]. To be noted, Rydberg-London potential [124] is slightly deviated from the accurate data at $R = 3 \sim 4$ Bohr

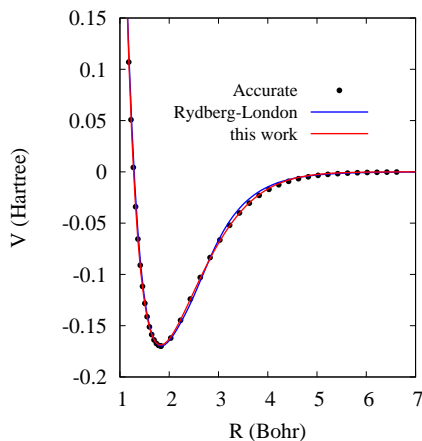


Fig.1.13 Comparison between four-parameter potential (this work) (Red line, $\alpha = 0.760387114$, $\beta = 1.40066201$, $\kappa = 0.20986805$, $\eta = 39.6142444$), Rydberg-London potential (Blue line, $a = 377.804$, $b = 3.6909$, $c = 1.4668$, $d = 32.5$, $C_6 = 6.854$, Ref. [124]) and the accurate data (Dark filled circles, Ref. [78]) for the ground state of OH.

1.14. NH

Here we report the ground-state potential of NH. We fit the accurate potential energies determined by Huxley and Murrell [78]. The RMS of this fitting is 0.000841, and the potential parameters are determined to be $\alpha = 0.641300128$, $\beta = 1.05082101$, $\kappa = 0.269776121$, $\eta = 27.3461228$. The fitted potential curve is reported in Fig.1.14, which agrees very well with the accurate data [78].

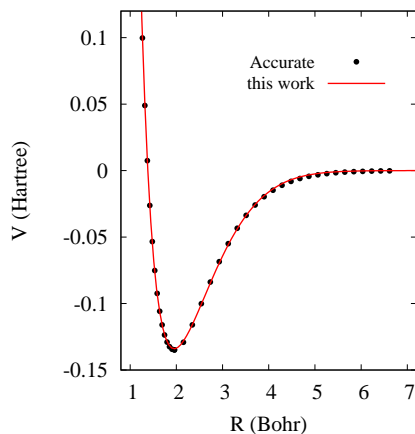


Fig.1.14 Comparison between four-parameter potential (this work) (Red line, $\alpha = 0.641300128$, $\beta = 1.05082101$, $\kappa = 0.269776121$, $\eta = 27.3461228$), and the accurate data (Dark filled circles, Ref. [78]) for the ground state of NH.

1.15. CH

Here we report the ground-state potential of CH. We fit the accurate potential energies determined by Huxley and Murrell [78]. The RMS of this fitting is 0.000841, and the potential parameters are determined to be $\alpha = 0.706575916$, $\beta = 0.980984516$, $\kappa = 0.158091171$, $\eta = 33.8165879$. The fitted potential curve is reported in Fig.1.15, which agrees very well with the accurate data [78].

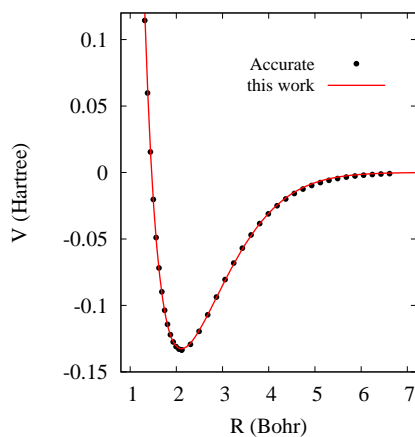


Fig.1.15 Comparison between four-parameter potential (this work) (Red line, $\alpha = 0.706575916$, $\beta = 0.980984516$, $\kappa = 0.158091171$, $\eta = 33.8165879$), and the accurate data (Dark filled circles, Ref. [78]) for the ground state of CH.

1.16. CO

Here we report the ground-state potential of CO. We fit the accurate potential energies determined by Huxley and Murrell [78]. The RMS of this fitting is 0.003586, and the potential parameters are determined to be $\alpha = 0.602412105$, $\beta = 2.49790792$, $\kappa = 0.23540789$, $\eta = 160.846731$. The fitted potential curve is reported in Fig.1.16, which agrees very well with the accurate data [78].

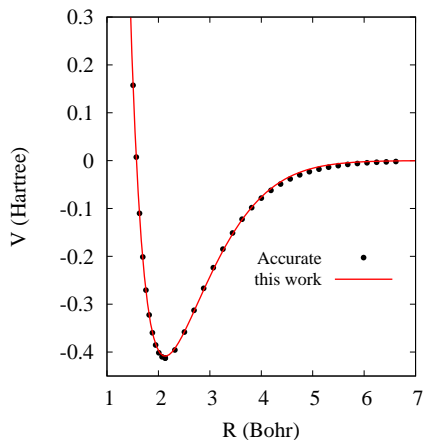


Fig.1.16 Comparison between four-parameter potential (this work) (Red line, $\alpha = 0.602412105$, $\beta = 2.49790792$, $\kappa = 0.23540789$, $\eta = 160.846731$), and the accurate data (Dark filled circles, Ref. [78]) for the ground state of CO.

1.17. Si₂

Here we report the ground-state potential of Si₂. We fit the accurate potential energies determined by Huxley and Murrell [78]. The RMS of this fitting is 0.00181, and the potential parameters are determined to be $\alpha = 0.186283078$, $\beta = 0.325358609$, $\kappa = 0.359889161$, $\eta = 47.3860134$. The fitted potential curve is reported in Fig.1.17, which agrees very well with the accurate data [78].

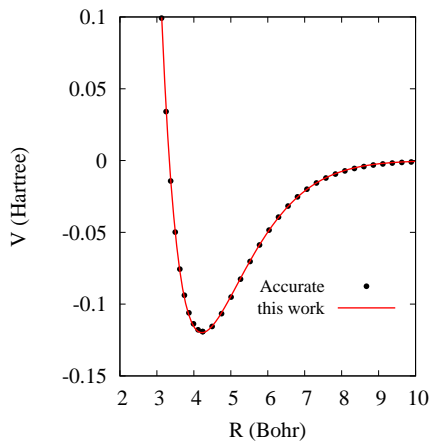


Fig.1.17 Comparison between four-parameter potential (this work) (Red line, $\alpha = 0.186283078$, $\beta = 0.325358609$, $\kappa = 0.359889161$, $\eta = 47.3860134$), and the accurate data (Dark filled circles, Ref. [78]) for the ground state of Si₂.

1.18. SiO

Here we report the ground-state potential of SiO. We fit the accurate potential energies determined by Huxley and Murrell [78]. The RMS of this fitting is 0.0021, and the potential parameters are determined to be $\alpha = 0.520285935$, $\beta = 1.50404553$, $\kappa = 0.151927384$, $\eta = 250.018351$. The fitted potential curve is reported in Fig.1.18, which agrees very well with the accurate data [78].

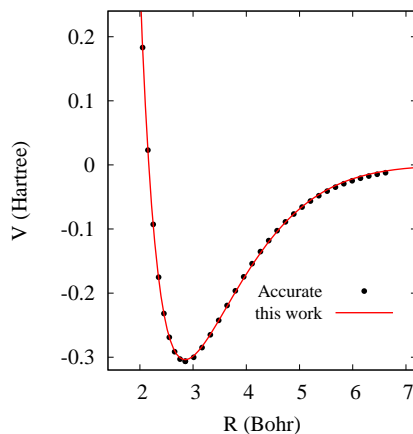


Fig.1.18 Comparison between four-parameter potential (this work) (Red line, $\alpha = 0.520285935$, $\beta = 1.50404553$, $\kappa = 0.151927384$, $\eta = 250.018351$), and the accurate data (Dark filled circles, Ref. [78]) for the ground state of SiO.

2. Covalent Bonding: Ionic Systems

The proposed potential function for ionic covalent bonding systems is

$$V(R, \alpha, \beta, \gamma, \eta, \zeta, \chi) = \frac{J_1(R, \gamma, \zeta, \eta) + K_1(R, \alpha, \zeta, \beta)}{1 + S_0(R)} - I(R, R_e, \chi) \frac{C_4}{R^4} \quad (2)$$

with $J_1(R, \gamma, \zeta, \eta) = e^{-2\gamma R} \left(\frac{\zeta}{R} + \eta \right)$, $K_1(R, \alpha, \zeta, \beta) = e^{-\alpha R} \left(\frac{\zeta}{R} - \beta R \right)$, $S_0(R) = e^{-R} \left(1 + R + \frac{R^2}{3} \right)$, and $I(R, R_e, \chi) = N(R/R_e) \left(1 - e^{-\left(\frac{R}{\chi R_e} \right)^5} \right)$, where $N(R/R_e)$ is a sign function defined as: (i) $N(R/R_e) = +1$ for $R/R_e \geq 10^{-3}$ and (ii) $N(R/R_e) = -1$ for $R/R_e < 10^{-3}$.

2.1. H_2^+

H_2^+ is the simplest one-electron molecule. For this one-electron system, the self-interaction-free Hartree-Fock method is exact (apart from small basis set errors) [146]. In other words, the potential energy curve for the ground-state H_2^+ should approach the exact solution in the limit of infinite basis set size [146]. That is, if one increases the basis set size (for example, including *polarization* and even *diffuse* functions in the trial function), then the potential curve of the ground-state H_2^+ should be improved significantly in all the regions of R [100]. In Fig.2.1, we demonstrate the effect of basis set size by using Hartree-Fock (HF) method implemented in the Gaussian 09 electronic structure package [119]. It is seen that the numerical potential curve for the ground-state H_2^+ , especially in the large- R region, is greatly improved and approaching to the accurate data [145] as the basis size is increased from Gaussian-type basis set 6-311++G(3df, 2pd) (including 2p and 1d polarization functions and diffuse functions) to aug-cc-pV5Z [119].

In this work, we use the new potential function given by Eq.(2) to fit the HF/aug-cc-pV5Z data. The root-mean-square for this fitting is 0.023, and the potential parameters are determined to be $\alpha = \gamma/2 = 1.06464516$, $\beta = 0.921196022$, $\eta = 3.61038634$, $\zeta = 1$, $\chi = 2.572$, and $C_4 = 4.95628851$. The fitting results are presented in Figure 2.1, and Table 2.1A list specified potential energies and compare with the polarization calculation [125], HF results, and accurate data [145]. We find that the fitted results reach an accuracy of less than 5% in the well and large- R regions, compared to the exact value [145]. In the repulsive region, the large error is 6.21% at $R=0.6$ Bohr. For $R > 4$ Bohr, the fitted results are much better than HF/6-311++G(3df, 2pd) calculations, and slightly better than the second-order polarization calculations [125]. As shown in Fig.2.1(a) and (c), the new potential is superior to the three-parameter potential [100].

We calculate the vibrational energies for the ground state H_2^+ using the new potential function. The numerical results are summarized in Table 2.1B. In total, we have obtained 20 vibrational levels as reported in Ref. [147]. The relative error of calculated vibrational energies except the last two levels are less than 2% for the levels $\nu = 0 - 18$, compared to the accurate data [147].

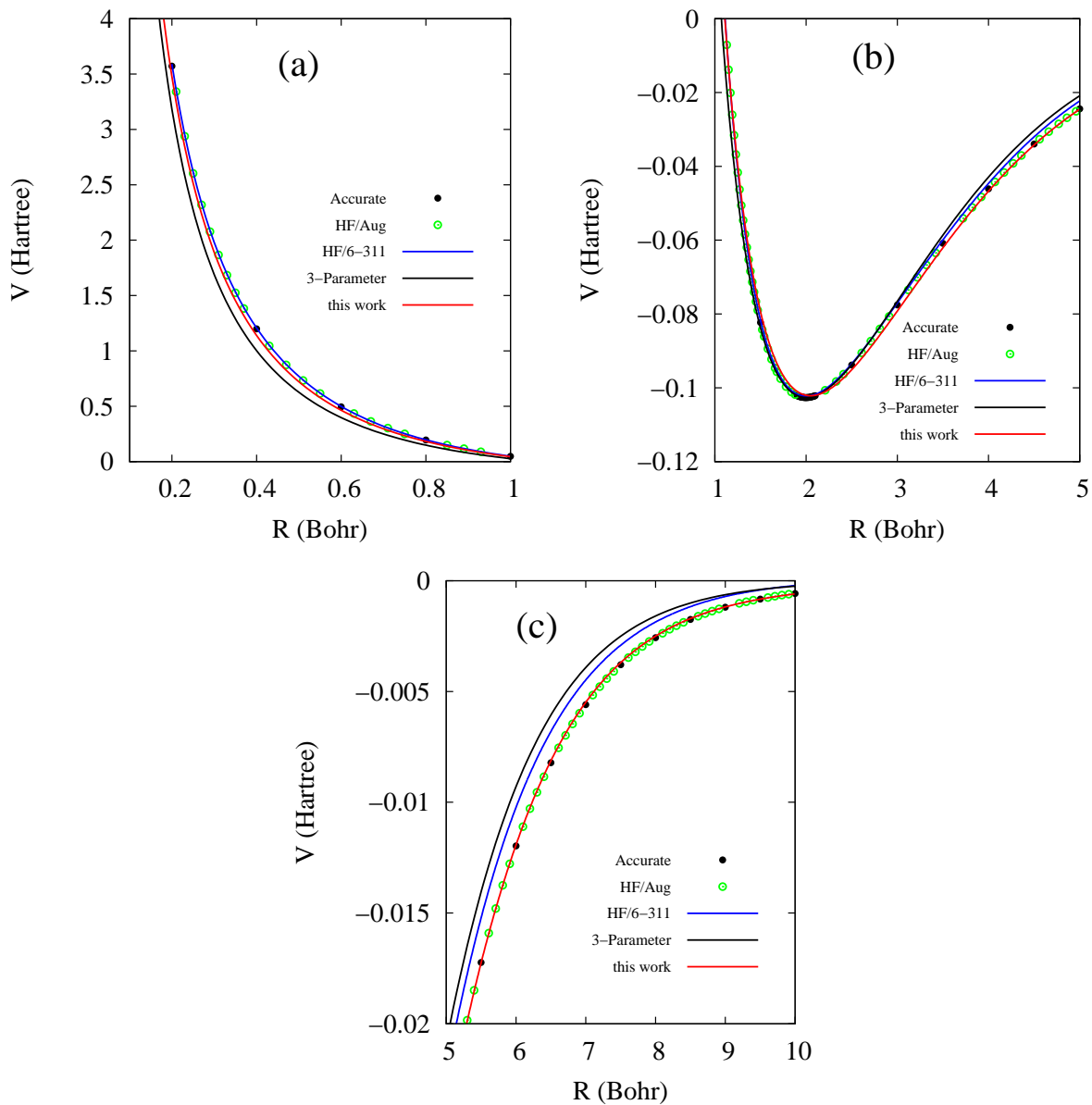


Fig.2.1 Comparison between new derived potential curve (this work) (Red line, $\alpha = \gamma/2 = 1.06464516$, $\beta = 0.921196022$, $\eta = 3.61038634$, $\zeta = 1$, $\chi = 2.572$, $C_4 = 4.95628851$, $R_e = 2.0$), 3-parameter (Dark line, Ref. [100], $\alpha = 1.5065756$, $\beta = 2.48475652$, $\gamma = 1.45$), HF/6-311++G(3df, 2pd) (Blue line, Ref. [100]), HF/aug-cc-pV5Z (Green open circles), and the most accurate data (Dark filled circles, Ref. [145]) for the ground state of one-electron molecule H_2^+ : (a) Repulsive region ($0.08 \sim 1$ Bohr); (b) Intermediate-R region ($1 \sim 5$ Bohr); (c) Large-R region ($5 \sim 10$ Bohr).

Table 2.1A: Comparison of the potential energies of the ground-state H_2^+ derived from the potential function Eq.(2) (this work, $\alpha = \gamma/2 = 1.06464516$, $\beta = 0.921196022$, $\eta = 3.61038634$, $\zeta = 1$, $\chi = 2.572$, $R_e = 2.0$, and $C_4 = 4.95628851$) with accurate data [145] and Hartree-Fock calculations with two basis sets: aug-cc-pV5Z, and 6-311++G(3df, 2pd) [100]. The value in the parenthesis is the relative error of the calculations, compared to the accurate values [145]. Energies and R are in atomic units

R	Perturbation Ref. [125]	New Potential this work	Hartree-Fock 6-311++G(3df, 2pd) (Ref. [100])	Hartree-Fock aug-cc-pV5Z	Exact Ref. [145]
0.2	-	3.4730288 (2.75%)	3.5901913 (0.529%)	3.5731717 (0.053%)	3.5712900
0.4	-	1.1400419 (4.93%)	1.2073537 (0.679%)	1.2001408 (0.078%)	1.1992100
0.6	-	0.4643997 (6.21%)	0.4986432 (0.704%)	0.4956841 (0.106%)	0.4951567
1.0	0.04761 (1.2%)	0.0453453 (5.95%)	0.0493841 (2.427%)	0.0484139 (0.415%)	0.0482137
1.4	-	-0.0669892 (4.28%)	-0.0692730(1.016%)	-0.0698991 (0.122%)	-0.0699843
1.5	-	-0.0793424 (3.62%)	-0.0816883(0.768%)	-0.0822257 (0.115%)	-0.0823205
1.6	-	-0.0882363 (2.96%)	-0.0903713(0.614%)	-0.0908854 (0.049%)	-0.0909300
1.8	-	-0.0985239 (1.73%)	-0.0998017(0.452%)	-0.1002250 (0.029%)	-0.1002544
2.0	-0.1047 (2.0%)	-0.1020067 (0.61%)	-0.1022567(0.368%)	-0.1026223 (0.012%)	-0.1026342
2.2	-	-0.1011692 (0.50%)	-0.1004950(0.168%)	-0.1008402 (0.175%)	-0.1006645
2.5	-	-0.0951008 (1.36%)	-0.0934593(0.388%)	-0.0938368 (0.014%)	-0.0938235
3.0	-0.07880 (1.6%)	-0.0792120 (2.13%)	-0.0770038(0.721%)	-0.0775846 (0.028%)	-0.0775629
3.5	-	-0.0620632 (1.98%)	-0.0599103(1.553%)	-0.0608764 (0.034%)	-0.0608555
4.0	-0.04716 (2.3%)	-0.0467328 (1.41%)	-0.0446260(3.166%)	-0.0460988 (0.030%)	-0.0460849
4.5	-	-0.0342146 (0.81%)	-0.0320165(5.667%)	-0.0339435 (0.010%)	-0.0339400
5.0	-0.02431 (0.5%)	-0.0245167 (0.39%)	-0.0222976(8.692%)	-0.0244142 (0.025%)	-0.0244203
5.5	-	-0.0172460 (0.08%)	-0.0152165(11.694%)	-0.0172195 (0.070%)	-0.0172315
6.0	-0.01162 (2.9%)	-0.0119251 (0.37%)	-0.0102342(14.494%)	-0.0119545 (0.121%)	-0.0119690
6.5	-	-0.0081250 (1.10%)	-0.0068055(17.163%)	-0.0082005 (0.183%)	-0.0082155
7.0	-0.005365 (4.1%)	-0.0054842 (1.96%)	-0.0044778(19.954%)	-0.0055797 (0.256%)	-0.0055940
7.5	-	-0.0036941 (2.61%)	-0.0029110(23.253%)	-0.0037800 (0.343%)	-0.0037930
8.0	-0.002453 (4.5%)	-0.00249938 (2.76%)	-0.0018637(27.494%)	-0.0025590 (0.444%)	-0.0025704
8.5	-	-0.00170690 (2.31%)	-0.0011689(33.099%)	-0.0017371 (0.578%)	-0.0017472

Table 2.1B: Comparison of the vibrational energies for the ground state of H_2^+ calculated using the newly derived potential function (this work)($\alpha = \gamma/2 = 1.06464516$, $\beta = 0.921196022$, $\eta = 3.61038634$, $\zeta = 1$, $\chi = 2.572$, $R_e = 2.0$, and $C_4 = 4.95628851$). The relative error of the calculation is compared to the most accurate data [147]. Energies in atomic units.

ν	This Work	Accurate (Ref. [147])	Relative Error	ν	This Work	Accurate (Ref. [147])	Relative Error
0	-0.0970873714	-0.097411224	0.33%	10	-0.0220911119	-0.02197053	0.54%
1	-0.0873931237	-0.08742784	0.039%	11	-0.0173629703	-0.017272526	0.52%
2	-0.0781750154	-0.078024065	0.19%	12	-0.0131588616	-0.013097364	0.46%
3	-0.0694364449	-0.069180659	0.36%	13	-0.0094885994	-0.009458409	0.31%
4	-0.0611815207	-0.060881381	0.49%	14	-0.00637083681	-0.006373841	0.05%
5	-0.053414961	-0.05311291	0.56%	15	-0.00383761848	-0.003867245	0.76%
6	-0.0461419369	-0.045864811	0.60%	16	-0.0019329211	-0.001967934	1.77%
7	-0.0393678527	-0.039129547	0.60%	17	-0.000697408025	-0.000709201	1.66%
8	-0.0330980705	-0.03290254	0.59%	18	-0.000127254906	-0.000109593	16.11%
9	-0.0273376297	-0.027182285	0.57%	19	-8.9138042E-6	-3.391E-6	162.86%

2.2. HeH^+

Formed by the most abundant elements, the hydrohelium, HeH^+ , plays an important role in astrophysics. According to the standard Big Bang model, the helium hydride ion, HeH^+ , is the first molecule, along with He_2^+ , formed in the Universe. This HeH^+ is a relatively simple hetero-nuclear molecular ion, isoelectronic with H_2 , which makes it of a fundamental significance from the theoretical point of view. The first accurate variational calculations of the Born-Oppenheimer potential of HeH^+ was reported by Wolniewicz [148], and then refined by Kolos and Peek [149] and further by Bishop and Cheung [149]. To date, there have been extensive quantum chemical calculations on this system (see literature review in

Ref. [150, 151]). In the ground electronic state, both electrons are mostly centered around the α nucleus with the proton distance from α being about $R \approx 1.46$ Bohr. Very recently, Pachucki [151] has demonstrated high accuracy calculations for the the ground state of HeH^+ using analytic formulas for two-center two-electron integrals with exponential functions (The potential is obtained in the range of $0.1 \sim 60$ a.u. with precision of about 10^{-12} a.u.).

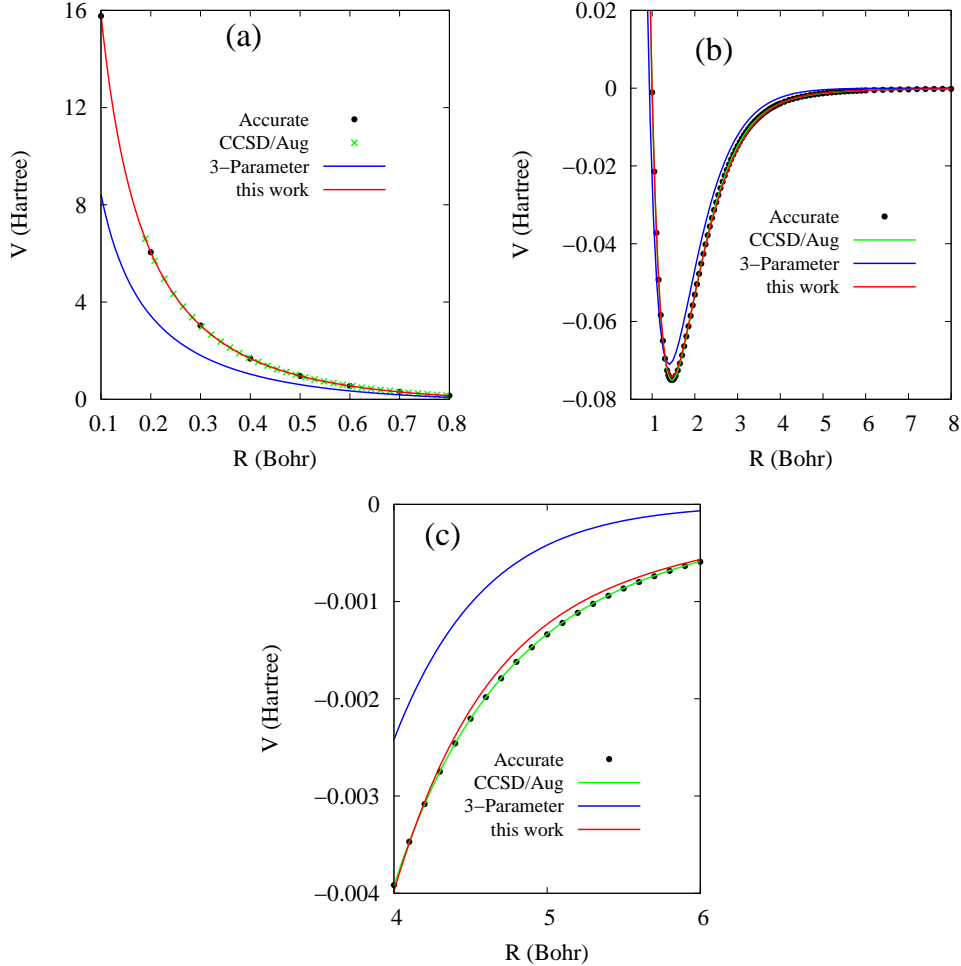


Fig.2.2. The comparison between new potential curve (this work) (Red line, $\alpha = \gamma = 1.94869912$, $\beta = 2.60094136$, $\zeta = 2.04347269$, $\eta = 1.78190656$, $C_4 = 0.709265297$, $\chi = 2.64764358$, and $R_e = 2.042$), CCSD/aug-cc-pV5Z (green line or crossing), 3-parameter model potential (blue line, $\alpha = 2.087114$, $\beta = 3.54492339$, and $\gamma = 1.0$, Ref. [100]), and the most accurate data (dark filled circles, Ref. [151]) for the ground state of HeH^+ : (a) Repulsive region; (b) Attractive region and (c) Enlarged part.

In this work, we first compute the PEC of the ground state of HeH^+ using CCSD/aug-cc-pV5Z and then fit it using the new potential function given by Eq.(2). The RMS for this fitting is 0.0003, and the potential parameters are determined to be $\alpha = \gamma = 1.94869912$, $\beta = 2.60094136$, $\zeta = 2.04347269$, $\eta = 1.78190656$, $C_4 = 0.709265297$, and $\chi = 2.64764358$. Since $C_4 = \alpha_1/2$, the dipole polarizability of He atom is derived to be $\alpha_1 = 2C_4 = 1.418530594$, which agrees well with the literature value ($\alpha_1 = 1.3796$) [152]. The fitting results are presented in Figure 2.2. The fitted PEC except a slight deviation at $R = 4 \sim 6$ Bohr shown in Fig.2.2(c) overlap very well with CCSD/aug-cc-pV5Z data points and the most accurate data [151]. The new potential curve is greatly improved over the three-parameter potential curve [100] in the

repulsive and attractive regions. Then, we calculate the vibrational energies for the ground state HeH^+ , and the numerical results are summarized in Table 2.2. In total, we have obtained 12 vibrational levels as reported in Ref. [150,153]. The relative error of calculated vibrational energies by using the present fitted potential are less than 2% for all the levels $\nu = 0 - 11$, compared to the accurate data [151].

Table 2.2: Comparison of the vibrational energies for the ground state of HeH^+ calculated using the new potential (this work) ($\alpha = \gamma = 1.94869912$, $\beta = 2.60094136$, $\chi = 2.04347269$, $\eta = 1.78190656$, $C_4 = 0.709265297$, $\zeta = 2.64764358$, and $R_e = 2.042$). The relative error of the calculation is compared to the most accurate data [153]. Energies in cm^{-1}

ν	This Work	Accurate (Ref. [153])	Relative Error	ν	This Work	Accurate (Ref. [153])	Relative Error
0	0.	0.	0.	6	12553.3559	12781.3485	1.78%
1	2868.9228	2911.0174	1.45%	7	13563.0243	13765.8454	1.47%
2	5422.8349	5515.2227	1.68%	8	14250.4013	14405.1903	1.07%
3	7666.1656	7810.8577	1.85%	9	14607.3517	14732.6855	0.85%
4	9601.9423	9792.9915	1.95%	10	14722.6704	14848.9097	0.85%
5	11231.4052	11453.4425	1.94%	11	14748.7441	14873.3489	0.84%

2.3. He_2^+

Helium is chemically the least reactive of all of the elements, yet a variety of small helium-containing molecules are known to exist as long-lived or even stable species. These include HeH^+ , He_2 , He_2^+ , and He_2^{++} . Although not very common in the laboratory, many of these molecules are considered to be of astrophysical interest due to the abundance of helium in stellar atmospheres and in interstellar clouds. In this work, we use the new potential function given by Eq.(2) to fit the accurate potential data of the ground-state He_2^+ [154]. The RMS for this fitting is 0.0006, and the potential parameters are determined to be $\alpha = \gamma/2 = 1.5047139$, $\beta = 2.38355439$, $\chi = 0.979471616$, $\eta = 1$, $C_4 = 0.624816071$, and $\zeta = 5.25975522$. The fitting potential curve is presented in Figure 2.3, and some numerical data are listed in Table 2.3A. The fitted potential curve except a slight deviation at $R = 10 \sim 15$ Bohr as shown in Fig.2.3(c) agrees very well with the accurate data [154], and is greatly improved over the three-parameter potential [100]. To be noted, CCSD/aug-cc-pV5Z results show a large deviation in the large-R region, which needs to be improved by increasing the basis size. The calculated vibrational energies for the ground state He_2^+ are summarized in Table 2.3B. The relative errors of calculated vibrational energies are less than 1% for the levels $\nu = 0 - 19$ and 2.8% to 37.3% for the levels $\nu = 20 - 23$, respectively, compared to the accurate data [154].

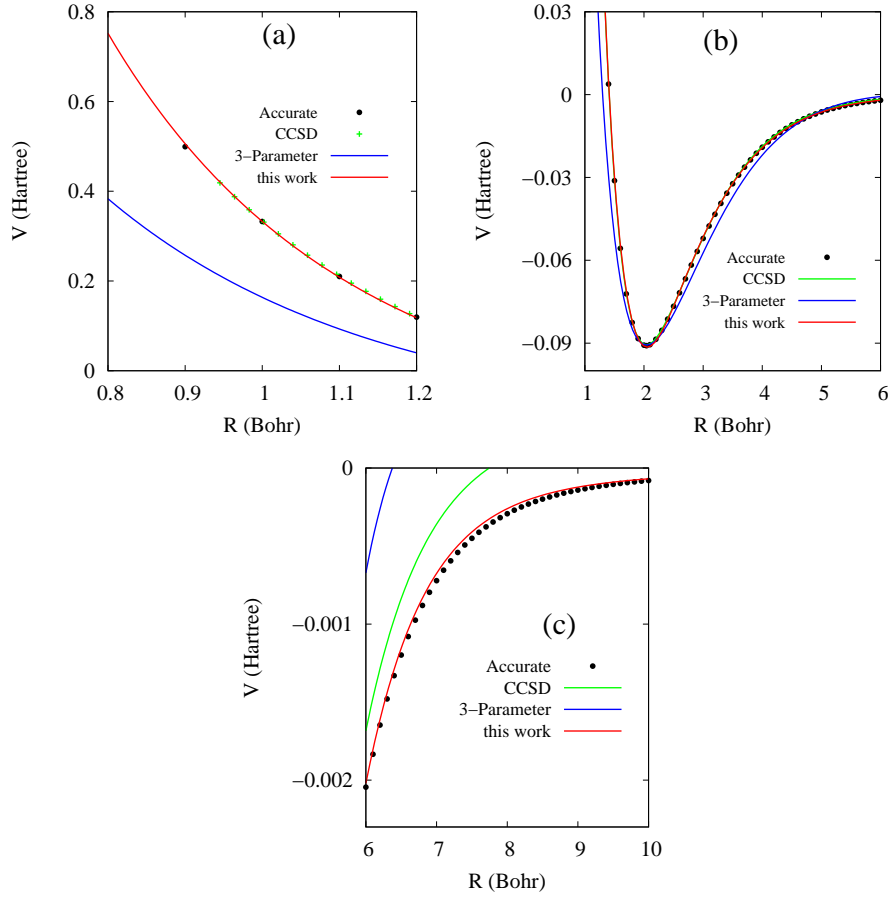


Fig.2.3 Comparison between new potential (this work) (Red line, $\alpha = \gamma/2 = 1.5047139$, $\beta = 2.38355439$, $\chi = 0.979471616$, $R_e = 2.042$, $\eta = 1$, $C_4 = 0.624816071$, and $\zeta = 5.25975522$), CCSD/aug-cc-pV5Z (Green line or crossing), 3-parameter model potential (Blue line, $\alpha = 1.28869$, $\beta = 2.99846884$, and $\gamma = 0.425$, Ref. [100]), and the most accurate data (Dark filled circles, Ref. [154]) for the ground state of He_2^+ : (a) Repulsive region; (b) Attractive region $R = 1 \sim 6$ Bohr; (c) Attractive region $R = 6 \sim 10$ Bohr.

Table 2.3A: Comparison of the potential energies for the ground state of He_2^+ calculated using the new potential function (this work, $\alpha = \gamma/2 = 1.5047139$, $\beta = 2.38355439$, $\chi = 0.979471616$, $R_e = 2.042$, $\eta = 1$, $C_4 = 0.624816071$, and $\zeta = 5.25975522$) with the most accurate data [154]. Energies and R in atomic units.

R	Accurate (Ref. [154])	this work	R	Accurate (Ref. [154])	this work
1.0	0.33268553	0.33268553	8.0	-0.00029280	-0.000260380
2.0	-0.09071740	-0.09111106	9.0	-0.00014135	-0.00012253
2.042	-0.09091977	-0.09142858	10.0	-0.00007999	-0.00006927
3.0	-0.05207816	-0.05154927	11.0	-0.00005077	-0.00004434
4.0	-0.01906935	-0.01925196	12.0	-0.00003466	-0.00003054
5.0	-0.00624850	-0.00635248	13.0	-0.00002478	-0.00002197
6.0	-0.00204495	-0.00202021	14.0	-0.00001830	-0.00001629
7.0	-0.00072159	-0.00067553	15.0	-0.00001383	-0.00001235

Table 2.3B: Comparison of the vibrational energies for the ground state of He_2^+ calculated using the new potential function (this work, $\alpha = \gamma/2 = 1.5047139$, $\beta = 2.38355439$, $\chi = 0.979471616$, $R_e = 2.042$, $\eta = 1$, $C_4 = 0.624816071$, and $\zeta = 5.25975522$). The relative error of the calculation is compared to the most accurate data [154]. Energies in atomic units.

ν	This Work	Accurate Data	Relative Error	ν	This Work	Accurate Data	Relative Error
0	-19205.644	-19116.116	-0.46%	12	-4221.761	-4251.373	0.69%
1	-17530.169	-17487.736	-0.24%	13	-3462.459	-3481.539	0.54%
2	-15929.625	-15929.598	-0.0002%	14	-2776.027	-2786.413	0.37%
3	-14407.352	-14441.8	0.23%	15	-2162.875	-2166.882	0.18%
4	-12965.168	-13024.465	0.45%	16	-1623.707	-1623.937	0.01%
5	-11603.388	-11677.751	0.63%	17	-1159.549	-1158.654	-0.07%
6	-10321.169	-10401.852	0.77%	18	-771.781	-772.152	0.04%
7	-9117.054	-9197.012	0.86%	19	-462.147	-465.491	0.71%
8	-7989.480	-8063.526	0.91%	20	-232.690	-239.384	2.79%
9	-6937.073	-7001.752	0.92%	21	-85.1730	-93.34	8.74%
10	-5958.767	-6012.117	0.88%	22	-17.0682	-22.159	22.97%
11	-5053.811	-5095.127	0.81%	23	-1.826	-2.914	37.31%

2.4. BeH^+

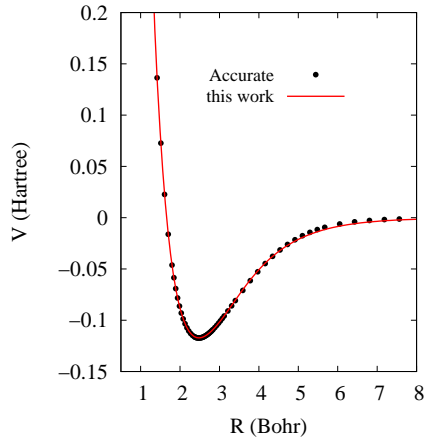


Fig.2.4 The comparison between new potential (Red line, this work, $\alpha = \gamma = 1.19634826$, $\beta = 1.41938735$, $\chi = 1.18705107$, $R_e = 2.476$, $\eta = 18.5564204$, $C_4 = 3.13563906$, and $\zeta = 0.122559941$) and the most accurate data (Dark filled circles, Ref. [155]) for the ground state of BeH^+ .

Although neutral beryllium monohydride (BeH) has attracted considerable experimental and theoretical interest, little is known about its ions (see literature review in a recent paper of Koput [155]). The vibration-rotation energy levels of the BeH^+ cation, BeH^+ , in its ground electronic state were experimentally characterized up to about 2/3 of the dissociation limit. Very recently, Koput has performed a very accurate calculation on the ground-state potential energy of BeH^+ by using the multi-reference averaged coupled-pair functional (MR-ACPF) method in conjunction with the correlation-consistent core-valence basis sets up to septuple-zeta quality. In this work, we use the new potential function given by Eq.(2) to fit the accurate data of Koput [155]. The RMS for this fitting is 0.000691, and the potential parameters are determined to be $\alpha = \gamma = 1.19634826$, $\beta = 1.41938735$, $\chi = 1.18705107$, $\eta = 18.5564204$, $C_4 = 3.13563906$, and $\zeta = 0.122559941$. The fitted potential curve is presented in Figure 2.4. It agrees well with the accurate data [155]. In Table 2.4, we listed the computed vibrational

energies for the ground state of BeH^+ using the fitted potential. The relative errors for all the computed energies, compared to experiment [156], are less than 1%.

Table 2.4.: Comparison of the vibrational energies for the ground state of BeH^+ calculated by using the fitted potential (this work) ($\alpha = \gamma = 1.19634826$, $\beta = 1.41938735$, $\chi = 1.18705107$, $R_e = 2.476$, $\eta = 18.5564204$, $C_4 = 3.13563906$, and $\zeta = 0.122559941$). The relative error of the calculation is compared to the experimental data [155]. Energies in cm^{-1} .

ν	This Work	Exp.(Ref. [156])	Relative Error	ν	This Work	Exp. (Ref. [156])	Relative Error
0	0.	0.	0.0%	6	11664.294	11601.723	0.53%
1	2134.680	2140.097	0.25%	7	13305.207	13236.008	0.52%
2	4198.855	4199.289	0.01%	8	14844.418	14779.843	0.43%
3	6188.898	6176.402	0.20%	9	16277.216	16230.761	0.28%
4	8100.181	8070.164	0.37%	10	17600.128	17585.969	0.086%
5	9927.284	9879.148	0.48%				

2.5. BeH^-

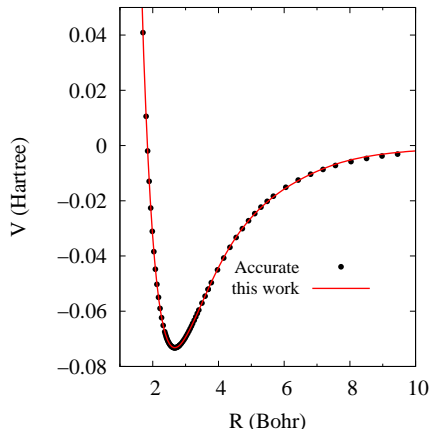


Fig.2.5 The comparison between new potential (this work) (Red line, $\alpha = \gamma = 1.16789295$, $\beta = 1.18495346$, $\chi = 2.17836477$, $R_e = 2.669$, $\eta = 12.6045998$, $C_4 = 18.4984266$, and $\zeta = 1.26131762$) and the accurate data (dark filled circles, Ref. [155]) for the ground state of BeH^- .

Neutral beryllium monohydride (BeH) and its cation were experimentally characterized. In contrast, there is no experimental information available about properties of the BeH anion, except for the adiabatic electron affinity of the BeH molecule. Nevertheless, very recently, Koput has performed a very accurate calculation on the ground-state potential energy of BeH^- by using the multi-reference averaged coupled-pair functional (MR-ACPF) method in conjunction with the correlation-consistent core-valence basis sets up to septuple-zeta quality. The predicted vibration-rotation energy levels for the BeH anion can be useful in a future experimental detection of this species. In this work, we use the new potential function given by Eq.(2) to fit the accurate data of Koput [155]. The RMS for this fitting is 0.0001115, and the potential parameters are determined to be $\alpha = \gamma = 1.16789295$, $\beta = 1.18495346$, $\chi = 2.17836477$, $\eta = 12.6045998$, $C_4 = 18.4984266$, and $\zeta = 1.26131762$. The fitting potential curve is presented in Figure 2.5. It agrees well with the accurate data [155]. In Table 2.5, we listed the computed vibrational energies for the ground state of BeH^- using the fitted potential.

The relative errors for all the energies, compared to accurate theoretical calculation [155], are less than 0.5%.

Table 2.5.: Comparison of the vibrational energies for the ground state of BeH^- calculated by using the new potential (this work) ($\alpha = \gamma = 1.16789295$, $\beta = 1.18495346$, $\chi = 2.17836477$, $R_e = 2.669$, $\eta = 12.6045998$, $C_4 = 18.4984266$, and $\zeta = 1.26131762$). The relative error of the calculation is compared to the accurate theoretical data [155]. Energies in cm^{-1} .

ν	This Work	Theory (Ref. [155])	Relative Error
0	0.	0.	0.%
1	1551.51	1549.84	0.10%
2	3003.25	2997.78	0.18%
3	4355.60	4344.74	0.25%
4	5609.04	5592.09	0.30%
5	6764.29	6741.84	0.33%

2.6. LiH^-

As the simplest stable molecular anion, LiH^- was the focus of several theoretical studies involving a variety of techniques during the year 1975 to 1978 [158]. Later, it was extensively studied both theoretically and experimentally (see Table I and literature review in Ref. [157]). The Gellene group [157] has performed a very accurate calculation on the ground-state potential energy of LiH^- by using multi-reference configuration interaction in the single and double space (MRCISD). In this work, we use the new potential function given by Eq.(2) to fit the accurate potential data of the ground-state LiH^- [157]. The RMS for this fitting is 0.0001115, and the potential parameters are determined to be $\alpha = \gamma = 0.981753027$, $\beta = 0.981349042$, $\chi = 2.39811679$, $\eta = 1$, $C_4 = 64.6224785$, and $\zeta = 3.6729584$. The fitting potential curve is presented in Figure 2.6. It agrees well with the accurate data [157].

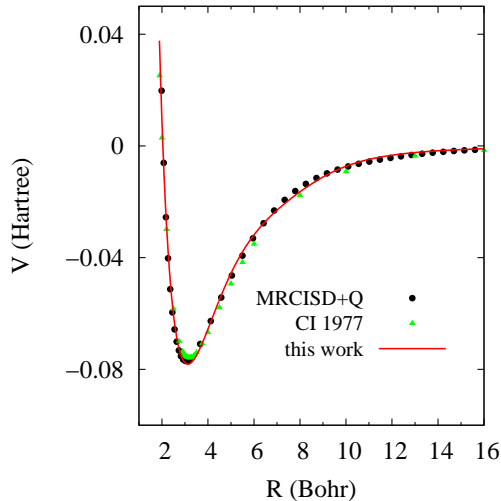


Fig.2.6 The comparison between new potential (this work) (Red line, $\alpha = \gamma = 0.981753027$, $\beta = 0.981349042$, $\chi = 2.39811679$, $R_e = 3.153$, $\eta = 1$, $C_4 = 64.6224785$, and $\zeta = 3.6729584$), configuration interaction (CI) calculations (Green triangle, Ref. [158]), multi-reference configuration interaction in the single and double space (MRCISD) (Dark filled circles, Ref. [157]) for the ground state of LiH^- .

3. Ionic Bonding Systems

The proposed potential function for the ionic bonding systems is

$$V(R, \alpha, \beta, \gamma, \eta, \zeta, \chi) = \frac{J_1(R, \gamma, \zeta, \eta) + K_1(R, \alpha, \zeta, \beta)}{1 + S_0(R)} - I(R, R_e, \chi) \left[\frac{Z^2}{R} + \frac{C_4}{R^4} + \frac{C_6}{R^6} + \frac{C_7}{R^7} \right] \quad (3)$$

with $J_1(R, \gamma, \zeta, \eta) = e^{-2\gamma R} \left(\frac{\zeta}{R} + \eta \right)$, $K_1(R, \alpha, \zeta, \beta) = e^{-\alpha R} \left(\frac{\zeta}{R} - \beta R \right)$, $S_0(R) = e^{-R} \left(1 + R + \frac{R^2}{3} \right)$, and $I(R, R_e, \chi) = N(R/R_e) \left(1 - e^{-\left(\frac{R}{\chi R_e}\right)^5} \right)$, where $N(R/R_e)$ is a sign function defined as: (i) $N(R/R_e) = +1$ for $R/R_e \geq 10^{-3}$ and (ii) $N(R/R_e) = -1$ for $R/R_e < 10^{-3}$. Z is the charge number. C_4 , C_6 and C_7 are related to the polarizabilities of the ions and are available in the literature.

3.1. NaCl

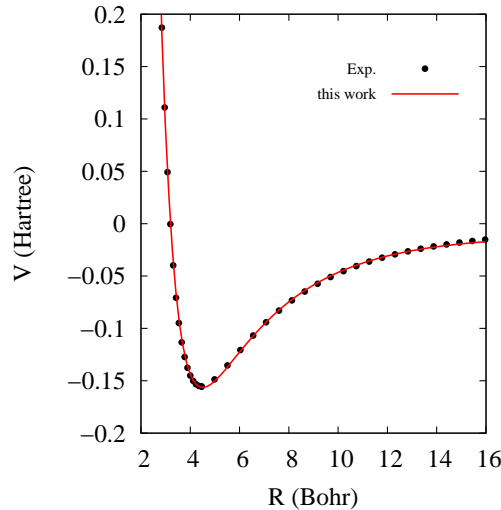


Fig.3.1. The comparison between the new potential (this work) (Red line, $\alpha = \gamma/2 = 0.449611907$, $\beta = 0.130590627$, $\eta = 125.509261$, $\chi = 7.29009261$, $R_e = 4.4628$, $C_4 = 2.09988569 \times 10^{-6}$, $C_6 = 2008637.94$, $C_7 = 99999986.1$, $\zeta = 1$) and the experimental data (Dark filled circles, Ref. [159]) for the ground state of NaCl.

In this work, we fit the experimentally-determined potential [159] of the ground state of NaCl. We take C_4 , C_6 , and C_7 as fitting parameters. The RMS for this fitting is 0.00248, and the determined potential parameters are $\alpha = \frac{\gamma}{2} = 0.449611907$, $\beta = 0.130590627$, $\eta = 125.509261$, $\chi = 7.29009261$, $C_4 = 2.09988569 \times 10^{-6}$, $C_6 = 2008637.94$, $C_7 = 99999986.1$, $\zeta = 1$. As shown in Fig.3.1., the fitted curve agrees well with experiment [159]. We compute the vibrational energies for isotopes Na^{35}Cl and Na^{37}Cl and obtain in total, 463 and 467 vibrational levels, respectively. Table 3.1 compares the computed vibrational energies with experimentally-determined ones. It is found that our computed vibrational energies are in good agreement with experiment [159].

Table 3.1: The calculated vibrational energies for isotopes Na³⁵Cl (in total, 463 levels, up to $\nu = 462$) and Na³⁷Cl (in total, 467 levels, i.e., up to $\nu = 466$) using the model potential ($\alpha = \gamma/2 = 0.449611907$, $\beta = 0.130590627$, $\eta = 125.509261$, $\chi = 7.29009261$, $R_e = 4.4628$, $C_4 = 2.09988569E - 006$, $C_6 = 2008637.94$, $C_7 = 99999986.1$, $\zeta = 1$), compared to the energies determined in experiment [159].

Na ³⁵ Cl			Na ³⁷ Cl		
ν	this work [cm ⁻¹]	Exp. [cm ⁻¹]	ν	this work [cm ⁻¹]	Exp. [cm ⁻¹]
0	0	0	0	0	0
1	362.464	361.15111	1	358.595	357.29437
2	721.667	718.80343	2	713.996	711.16501
3	1077.631	1072.99164	3	1066.229	1061.6469
4	1430.381	1423.75018	4	1415.316	-
5	1779.941	1771.11401	5	1761.281	-
6	2126.335	2115.11780	6	2104.144	-
7	2469.587	2455.79490	7	2443.932	-
8	2809.720	2793.17600	8	2780.666	-
9	3146.759	-	9	3114.369	-

4. van der Waals Binding Systems

The proposed potential function for the non-covalent van der Waals binding systems is

$$V(R, \alpha, \beta, \eta, \chi) = \frac{J_1(R, \alpha, \eta) + K_1(R, \alpha, \beta)}{1 + S_0(R)} - I(R, R_e, \chi) \sum_n \frac{C_n}{R^n} \quad (4)$$

with $J_1(R, \alpha, \eta) = e^{-\alpha R} \left(\frac{1}{R} + \eta \right)$, $K_1(R, \alpha, \beta) = e^{-\alpha R} \left(\frac{1}{R} - \beta R \right)$, $S_0(R) = e^{-R} \left(1 + R + \frac{R^2}{3} \right)$, and $I(R, R_e, \chi) = N(R/R_e) \left(1 - e^{-\left(\frac{R}{\chi R_e}\right)^5} \right)$, where $N(R/R_e)$ is a sign function defined as: (i) $N(R/R_e) = +1$ for $R/R_e \geq 10^{-3}$ and (ii) $N(R/R_e) = -1$ for $R/R_e < 10^{-3}$.

4.1. Triplet States

4.1.1. H₂

This is the only system for which an exact *ab initio potential* is available within the Born-Oppenheimer approximation. We use Eq.(4) and the dispersion coefficient of Ref. [80] to fit the exact potential energies of Kolos and Wolniewicz [160]. The RMS of this fitting is 0.00704, and the potential parameters are determined to be $\alpha = 1.80886753$, $\beta = 0.80476915$, $\eta = 19.5353848$, and $\chi = 0.94375137$. In Fig.4.1.1, we compared the fitted potential curve with the exact *ab initio results* of Kolos and Wolniewicz [160], Tang-Toennies potential (TT1984) [80], perturbation calculation (TTY1994) [161], and three-parameter model potential [100]. The fitted potential curve is in excellent agreement with the exact *ab initio* data and perturbation calculation. In the short-R range and in the large-R region, the present potential is greatly improved over the three-parameter potential [100]. To be noted, in the repulsive region at $R < 6$ Bohr, the TT1984 Potential [80] is much harder than the exact potential curve.

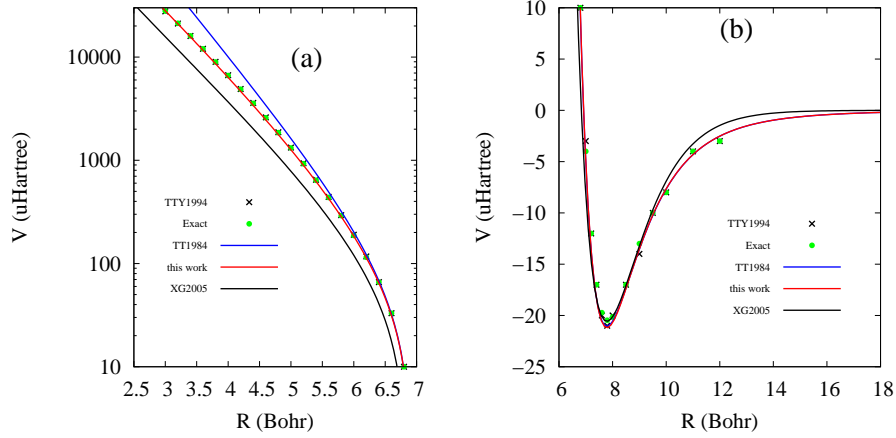


Fig.4.1.1: Comparison between the present potential curve (this work) (Red line, $\alpha = 1.80886753$, $\beta = 0.80476915$, $\eta = 19.5353848$, $\chi = 0.94375137$, $R_e = 7.8$, $C_6 = 6.499$, $C_8 = 124.4$, and $C_{10} = 3286.0$), three-parameter model potential (Dark line, $\alpha = 0.978$, $\beta = 0.02228$, and $\gamma = 0.874$, Ref. [100]), perturbation calculation (TTY1994)(Dark cross, Ref. [161]), Tang-Toennies potential (TT1984) (Blue line, $A = 9.3$, $b = 1.664$, $C_6 = 6.499$, $C_8 = 124.4$, and $C_{10} = 3286.0$ Ref. [80]), and exact data (Green filled circles, Ref. [160]) for the triplet $H_2(^3\Sigma_u)$ state. (a) Repulsive region (Energy in log scale) and (b) attractive region.

4.1.2. NaK

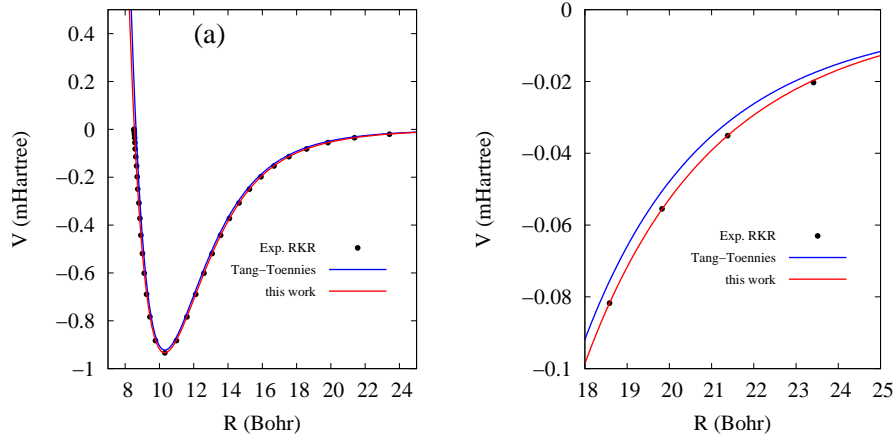


Fig.4.1.2 Comparison of the triplet-state $a^3\Sigma^+$ of NaK of the present work (this work) (Red line, $\alpha = 0.581007114$, $\beta = 0.169441107$, $\eta = 1.27758572$, $\chi = 1.86032252$, $R_e = 10.315$, $C_6 = 2410.0$, $C_8 = 229050.0$, and $C_{10} = 24680000.0$) with Tang-Toennies potential (Blue line, $A = 3.829$, $b = 0.7573$, $C_6 = 2410.0$, $C_8 = 229050.0$, $C_{10} = 24680000.0$, $C_{12} = 3.015 \times 10^9$, $C_{14} = 4.175 \times 10^{11}$, $C_{16} = 6.555 \times 10^{13}$ Ref. [80]) and experimental RKR points [162].

The $^3\Sigma^+$ states of the alkali dimers are another chemically different class of systems which can be used to test the potential models. Breford and Engelke [162] observed laser-induced fluorescence from the $^3\Pi_1$ state into the $a^3\Sigma^+$ state in NaK and determined an RKR potential up to high energies very close to the dissociation limit for $a^3\Sigma^+$. Thus, we fit their RKR data points by using the potential function Eq.(4) and the dispersion coefficients $C_6 = 2410.0$, $C_8 = 229050.0$, and $C_{10} = 24680000.0$ of Ref. [80]. The RMS for this fitting is 0.00928, and the potential parameters are determined to be $\alpha = 0.581007114$, $\beta = 0.169441107$, $\eta =$

1.27758572, $\chi = 1.86032252$. The fitted potential curve is presented in Fig.4.1.2. It agrees well with the RKR data points. To be noted, as shown in Fig.4.1.2(b), Tang-Toennies potential shows obvious deviations from the RKR data at $R = 18 \sim 25$ Bohr.

4.2. Rare-Gas Dimers

4.2.1. He₂

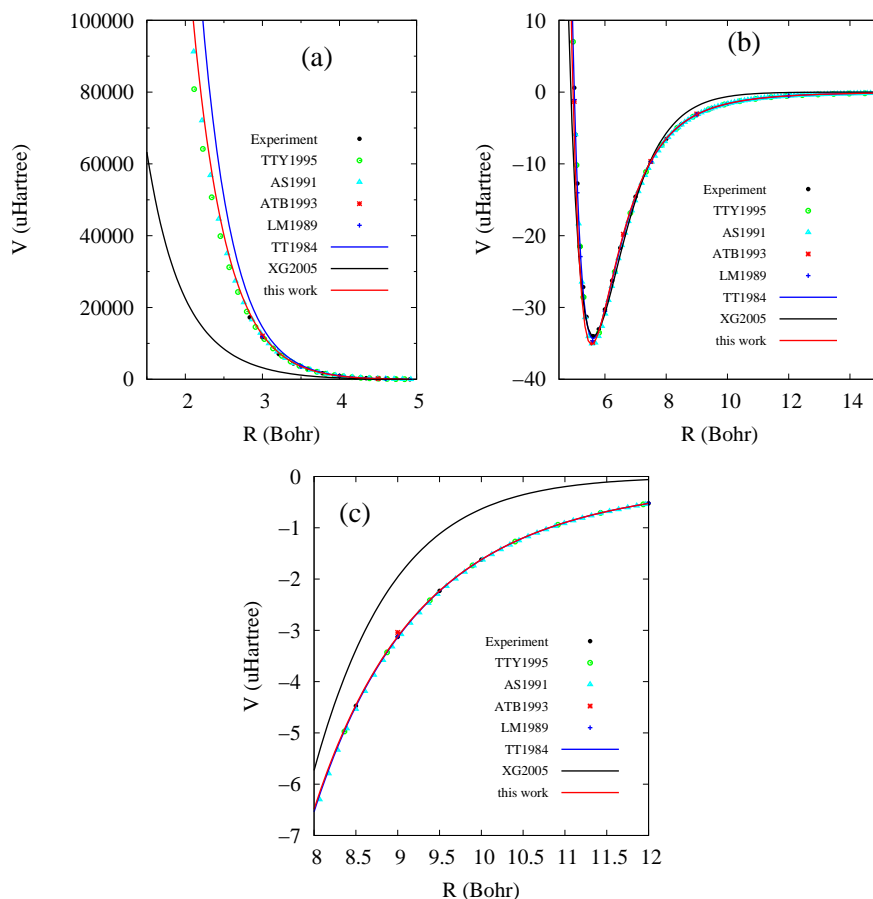


Fig.4.2.1: The comparison between the present potential (Red line, this work, $\alpha = 2.34281426$, $\beta = 1.427609211$, $\eta = 24.9327859$, $\chi = 0.705917281$, $R_e = 5.613$, $c_6 = 1.461$, $c_8 = 14.11$, $c_{10} = 183.5$), three-parameter potential (XG2005) (Dark line, $\alpha = 1.313$, $\beta = 0.04200863$, $\gamma = 1.4$, Ref. [100]), Tang-Toennies potential (TT1984) (Blue line, $A = 22.16$, $b = 2.388$, $c_6 = 1.461$, $c_8 = 14.11$, $c_{10} = 183.5$, Ref. [80]), quantum Monte Carlo calculation (ATB1993) (Red star, Ref. [168]), LM2M2 potential (AS1991) (Cyan triangle, Ref. [167]), variational LM2 (LM1989) (Blue cross, Ref. [166]), Tang-Toennies-Yiu potential (TTY1995) (Green open circle, $D = 7.449$, $\beta = 1.3443$, $c_6 = 1.461$, $c_8 = 14.11$, $c_{10} = 183.5$, Ref. [90]), and experimental data (Dark filled circles, Ref. [165]) for the ground-state He₂. (a) $R = 1.5 \sim 5$ Bohr (Energy in log scale); (b) $R = 5 \sim 15$ Bohr; and (c) $R = 8 \sim 12$ Bohr;.

The interatomic potentials between members of the rare gas family of atoms provide the largest class of chemically identical atoms which interact via van der Waals potentials [163]. He₂ is probably the atom-atom system which has been studied most extensively, both theoretically and experimentally. Two very accurate refined potentials based on the combined

evaluation of both bulk and molecular beam scattering data were proposed by Aziz and co-workers [164] and Feltgen and co-workers [165]. Having only four electrons in closed shells, He_2 is ideally suited for a theoretical study.

Here we fit the accurate potential data of the ground-state He_2 [167] by using the potential function Eq.(4) and the dispersion coefficients $c_6 = 1.461$, $c_8 = 14.11$, $c_{10} = 183.5$ of Ref. [80]. The RMS for this fitting is 0.00134, and the potential parameters are determined to be $\alpha = 2.34281426$, $\beta = 1.427609211$, $\eta = 24.9327859$, and $\chi = 0.705917281$. The results are reported in Fig.4.2.1 and compared with literature data. We find that the new potential curve in the short- and large-R regions has been greatly improved over the three-parameter potential curve [100]. At all the interaction regions, the new potential curve is in excellent agreement with experiment [165] and calculations of Tang-Toennies-Yiu [169], variational LM-2 [166], and LM2-M2 [167] potentials, and quantum Monte Carlo [168]. For $R < 3.5$ Bohr, we find that Tang-Toennies potential [80] is slightly harder than the experimental curve.

4.2.2. Ne_2

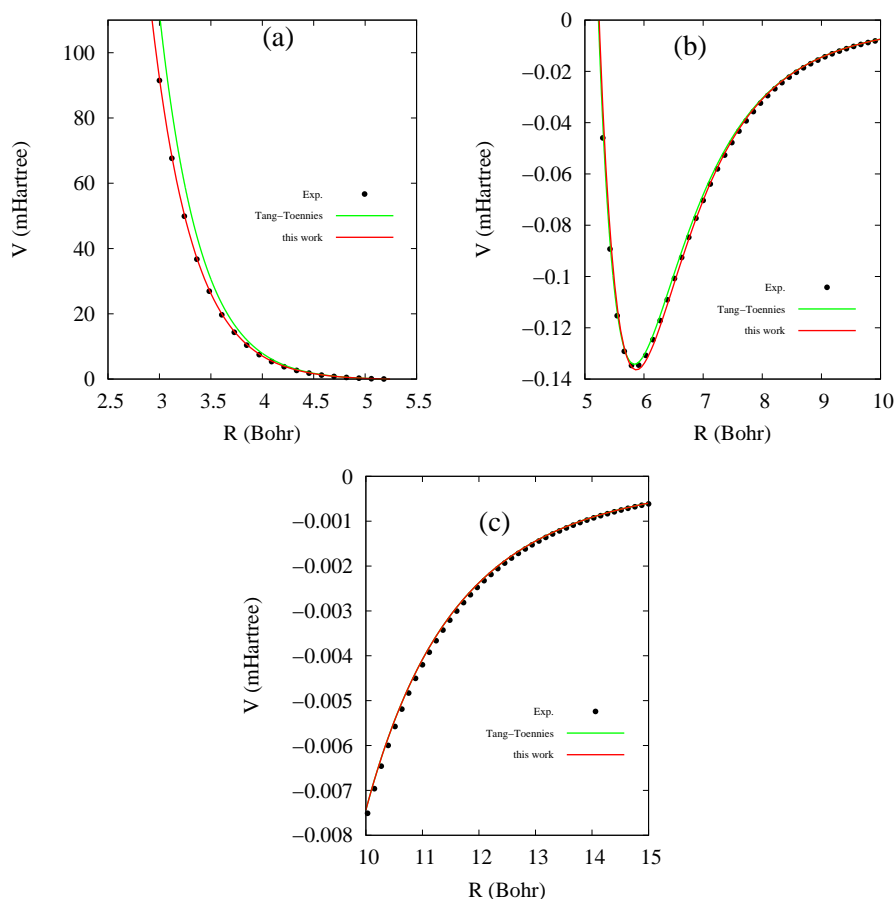


Fig.4.2.2 Comparison of the ground-state potential curve of Ne_2 of the present work (this work) (Red line, $\alpha = 2.57804505$, $\beta = 3.59526654$, $\eta = 302.992153$, $\chi = 0.898113069$, $R_e = 5.840$, $C_6 = 6.383$, $C_8 = 90.34$, and $C_{10} = 1536.0$) with HFD-B experimental data (Dark filled circles, Ref. [171]), Tang-Toennies potential curve (Green line, $A = 951.8$, $b = 1.681$, $C_6 = 6.383$, $C_8 = 90.34$, and $C_{10} = 1536.0$, Ref. [175]).

Aziz and Slaman [171] constructed an accurate potential energy curve for the ground state of Ne_2 . It accurately reflects the position of the high-energy repulsive region of the potential required by the high-energy beam data, includes values of dispersion coefficients C_6 , C_8 and C_{10} , and has the ability to reproduce highly accurate viscosity values. The potential is a significant improvement over the XC-2, XC-3 and HFD-C2 potential of Aziz *et al.* [170], which were considered to be the best among the potentials available in the literature (See literature reviews in Ref. [171]). In this work, we fit the accurate potential curve of Aziz and Slaman [171]. The RMS for this fitting is 0.0148, and the determined potential parameters are $\alpha = 2.57804505$, $\beta = 3.59526654$, $\eta = 302.992153$, and $\chi = 0.898113069$. The fitted potential curve is presented in Fig.4.2.2. It agrees very well with the accurate data [171]. To be noted, Tang-Toennies potential [175] is slightly harder than the accurate data. The spacings $\Delta G_{\nu+1/2}$ of vibrational energies calculated by using the fitted potential are listed in Table 4.2.2 and compared with literature data. It agrees well with experiment [172] and other calculations by HFD-B, HFD-C2, and XC-2. [171], and is much better than Lennard-Jones potential [3], extended Rydberg -van der Waals potential [79] and Tang-Toennies potential [80].

Table 4.2.2: Computed vibrational energies E_ν and spacings $\Delta G_{\nu+1/2}$ by using the new potential, compared with HFD [171], HFD-C2 [171], XC-2 [171] and experiment [172]. All in units of cm^{-1} . The vibrational spacings for the potentials, xR-vdW (extended Rydberg -van der Waals potential [79]), TT (Tang-Toennies potential [80]), mTT (modified Tang-Toennies potential [91]), and LJ (Lennard-Jones potential [3]), are from Ref. [177].

ν	E_ν	$\Delta G_{\nu+1/2}$								
	this work	this work	HFD-B Ref. [171]	HFD-C2 Ref. [171]	XC-2 Ref. [171]	xR-vdW Ref. [177]	TT Ref. [177]	mTT Ref. [177]	LJ Ref. [177]	Exp. Ref. [172]
0	0	14.199	13.84	13.79	13.45	11.026	13.001	13.502	10.442	13.7 ± 0.5
1	14.199	2.989								
2	17.188									

4.2.3. Ar_2

The interatomic potential for Ar_2 is as well characterized as that for many common stable diatomics, experimentally by using several spectroscopic techniques and theoretically by using ab initio techniques [173]. The most accurate potential energy curve of its ground state was experimentally determined by Aziz [174]. Thus, we use Eq.(4) and the dispersion coefficients C_6 , C_8 and C_{10} of Ref. [175] to fit directly the accurate data of Aziz [174]. The RMS of this fitting is 0.0151, and the potential parameters are determined to be $\alpha = 1.5069144$, $\beta = 19.2457331$, $\eta = 126.019972$, and $\chi = 1.28100922$. Our fitted potential curve is presented in Fig.4.2.3, which agrees very well with the accurate data [174]. As shown in Fig.4.2.3(a), Tang-Toennies potential [175] is much harder, and CCSD/daug-cc-pV5Z-33211 calculations [173] is slightly harder than the accurate data [174]. Overall, the new potential is greatly improved over the three-parameter potential [100] in all the regions.

Cahill and Parsegian [98] have compared Rydberg-London (RL) potential for the ground-state Ar_2 with Lennard-Jones (LJ) potential [3]. They pointed out that the LJ potential curve matched at the potential minimum is too deep for $R > 8.5$ Bohr (4.5 \AA), and too hard for $R < 5.671$ Bohr (3 \AA) [98]. Does it matter that LJ fails to fit the Ar-Ar interaction? Cahill and Parsegian [98] found that the dimensionless second virial coefficient B_2/R_e^3 of Ar_2 calculated

by using RL and LJ potentials at room temperature are -0.499 and -0.899 , which differ from the experimental value of -0.552 [176] by 9.6% and 63%, respectively. Thus, LJ fitting with only two parameters is not as accurate as RL fitting [98].

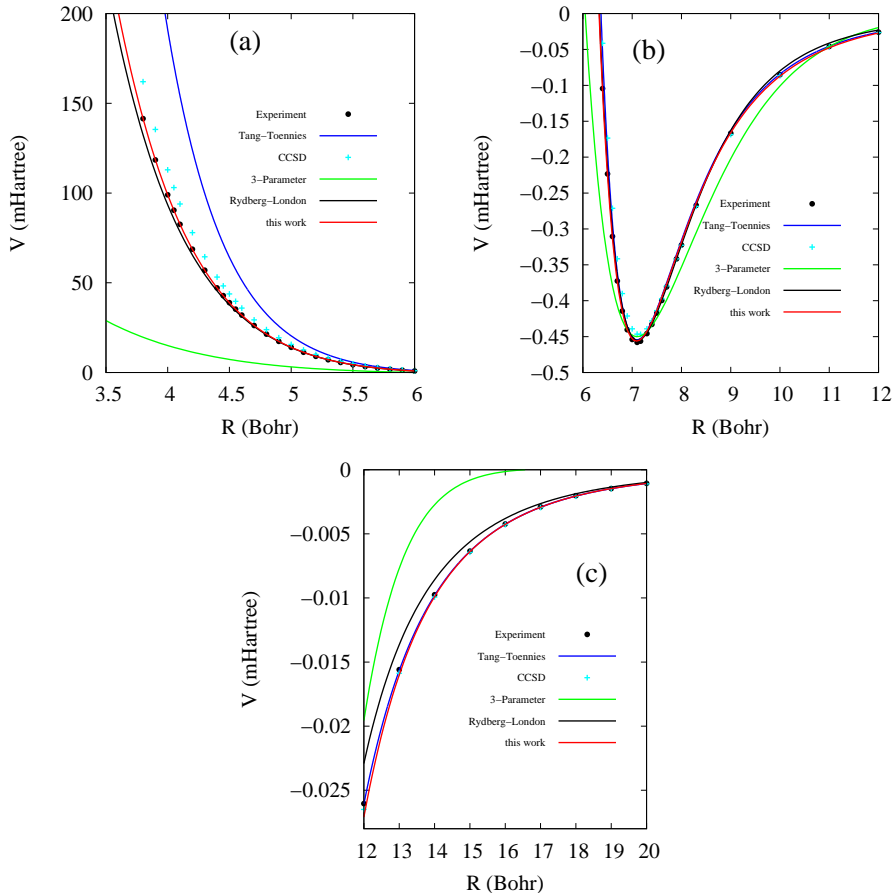


Fig.4.2.3 Comparison of the ground-state potential curve of Ar_2 : The present work (this work) (Red line, $\alpha = 1.5069144$, $\beta = 19.2457331$, $\eta = 126.019972$, $\chi = 1.28100922$, $R_e = 7.10$, $C_6 = 64.3$, $C_8 = 1623$, and $C_{10} = 49060$) with CCSD/daug-cc-pV5Z-33211 calculations (Cyan cross, Ref. [173]), experimental data (Dark filled circles, Ref. [174], Tang-Toennies potential (Blue line, $A = 748.3$, $b = 2.031$, $C_6 = 64.3$, $C_8 = 1623$, and $C_{10} = 49060$, Ref. [175]), Rydberg-London potential (Dark line, $a = 1720$, $b = 2.6920$, $c = 0.2631$, $d = 37.943$, $e = 177588$, Ref. [98]), and three-parameter potential (Green line, $\alpha = 0.8706$, $\beta = 0.403498$, $\gamma = 0.38$, Ref. [100]).

Then, is the accuracy of RL potential important in the liquid phase where additivity is only approximate? Cahill and Parsegian [98] have significantly tested whether the lack of complete additivity in the liquid phase obscures the advantages of the RL potential over the LJ potential. They calculated the heats of vaporization $\Delta_{vap}H$ of Ar at their boiling points and atmospheric pressure by using RL and LJ potentials in Monte Carlo simulation [98]. RL and LJ potentials gave $\Delta_{vap}H = 0.0694, 0.0787$ eV (per atom), which differ from the experimental value of 0.0666 eV [176] by 4.2% and 18%, respectively. Clearly, the errors due to a lack of additivity are of the order of 4% [98], while the errors due to the defect of the LJ potential are about 18% [98]. Their analysis has shown that even in the liquid phase, limited additivity is less of a problem than the defects of the LJ potential [98]. Thus, they concluded that RL potential

represents weak noncovalent bonds better than LJ potential [98]. How is the accuracy of our new potential function Eq.(4), compared to RL potential? In the intermediate-R region, as shown in FIG.4.2.3(b), RL potential curve except a visible deviation at $10 < R < 12$ overlaps well with our potential curve and the accurate data. In the repulsive region shown in Fig.4.2.3(a), RL curve is slightly softer than the accurate data and our potential (to be noted, RL converges to a finite value as R goes to 0). In the large-R region shown in Fig.4.2.3(c), RL potential displays a discernible deviation at $R = 12 \sim 16$ Bohr. It shows that our potential function is more accurate than RL potential.

Further, we calculate the vibrational energies for the ground state of Ar_2 using the new potential function. The results are summarized in Table 4.2.3 and compared with those obtained by using other potential functions. Our results are in excellent agreement with experiment [174] and HFD calculations [66], and are more accurate than those obtained by using RL [98], Tang-Toennies [80], and Lennard-Jones [3] potentials.

Table 4.2.3: Computed vibrational energies E_ν and spacings $\Delta G_{\nu+1/2}$ among them by using the present potential for Ar_2 , compared to theoretical and experimental data available in the literature. All energies in cm^{-1} . The abbreviation for potential functions are: HFD (Hartree-Fock dipersion potential [66]), xR-vdw (extended Rydberg -van der Waals potential [79]), TT (Tang-Toennies potential [80]), mTT (modified Tang-Toennies potential [91]), RL (Rydberg-London potential [98]), and LJ (Lennard-Jones potential [3]).

ν	Present Potential		$\Delta G_{\nu+1/2}$								$\Delta G_{\nu+1/2}$		
	E_ν	$\Delta G_{\nu+1/2}$	<i>ab initio</i> Ref. [173]	<i>ab initio</i> Ref. [178]	<i>ab initio</i> Ref. [181]	<i>ab initio</i> Ref. [182]	HFD Ref. [177]	xR-vdw Ref. [177]	TT Ref. [177]	mTT Ref. [177]	RL Ref. [98]	LJ Ref. [177]	Exp. Ref. [174, 179]
0	0	25.902	25.29	25.50	25.69	25.75	25.503	20.793	23.184	25.247	25.914	19.277	25.69±0.01
1	25.902	20.550	20.12	20.14	20.57	20.48	20.378	17.638	19.463	20.506	20.956	16.356	20.58±0.02
2	46.453	15.427	15.18	15.06	15.57	15.44	15.602	14.566	15.742	15.388	16.037	13.633	15.58±0.02
3	61.880	10.799	10.58	10.63	10.91	10.79	10.691	11.620	12.022	10.553	11.255	11.118	10.91±0.03
4	72.678	6.918	6.57	6.68	6.83	6.76	6.674	8.856	8.301	6.275	6.80	8.824	6.84±0.07
5	79.597	3.796	3.40	3.56	-	-	4.001	6.350	4.580	3.921	3.309	6.763	-
6	83.392	1.494	-	1.42	-	-	-	-	-	-	1.105	-	-
7	84.886												

4.2.4. Kr_2

In this work, we fit the accurate potential curve of HFD-B experimental data for the ground-state Kr_2 presented in Ref. [183] and use the dispersion coefficients $C_6 = 129.6$, $C_8 = 4187$, and $C_{10} = 155500$ of Ref. [175]. The RMS for this fitting is 0.0269, and the determined potential parameters are $\alpha = 1.69712234$, $\beta = 5.28825134$, $\eta = 246.375269$, $\chi = 0.85643772$. We present the fitted potential curve in Fig.4.2.4. It agrees very well with HFD-B data [183]. To be noted, Tang-Toennies potential [175] is slightly harder than the accurate data. Rydberg-London potential [98] in the repulsive region has a slight deviation from the HFD-B data, and has a large deviation at $R = 12 \sim 17$ Bohr. It concludes that our present potential is more accurate than Rydberg-London and Tang-Toennies potentials. In Table 4.2.4, we list the spacings of vibrational energies calculated by using the present potential and compare them with the literature data. We find that our results agree well with experiment [184, 185].

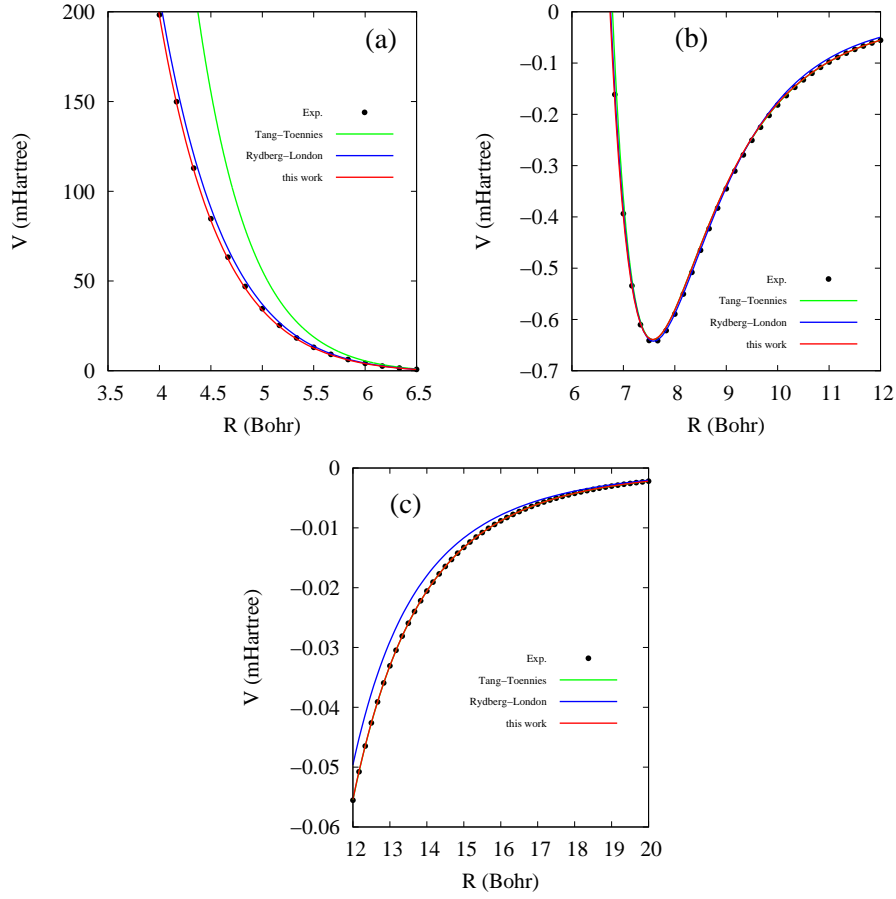


Fig.4.2.4 Comparison of the ground-state potential curve of Kr_2 of the present work (this work) (Red line, $\alpha = 1.69712234$, $\beta = 5.28825134$, $\eta = 246.375269$, $\chi = 0.85643772$, $R_e = 7.58$, $C_6 = 129.6$, $C_8 = 4187$, and $C_{10} = 155500$) with Rydberg-London potential (Blue line, $a = 2499$, $b = 2.5249$, $c = 0.2466$, $d = 78.214$, $e = 199064$, Ref. [98]), HFD-B experimental data (Dark filled circles, Ref. [183]), Tang-Toennies potential curve (Green line, $A = 832.4$, $b = 1.865$, $C_6 = 129.6$, $C_8 = 4187$, and $C_{10} = 155500$, Ref. [175]).

Table 4.2.4: Comparison of our computed vibrational spacings for Kr_2 with experiment and theory. All values are given in cm^{-1} . The vibrational spacings for the potentials, xR-vdW (extended Rydberg -van der Waals potential [79]), TT (Tang-Toennies potential [80]), mTT (modified Tang-Toennies potential [91]), RL (Rydberg-London potential [98]), and LJ (Lennard-Jones potential [3]), are from Ref. [177].

Transition	Exp.	Exp.	this work	xR-vdW	TT	mTT	RL	LJ
	Ref. [184]	Ref. [185]						
0-1	21.56±0.54	21.175±0.01	21.53	23.707	21.471	21.098	21.560	21.704
1-2	19.09±0.57	19.093±0.02	19.38	20.940	19.307	19.420	19.543	19.106
2-3	16.76±0.60		17.22	18.220	17.144	16.981	17.484	16.642
3-4	14.76±0.75		15.07	15.563	14.980	15.232	15.426	14.318
4-5	12.23±0.51		12.95	12.996	12.817	12.447	13.374	12.142
5-6	10.49±0.50		10.90	10.554	10.653	10.201	11.340	10.120
6-7	8.92±0.44		8.95	8.276	8.490	8.734	9.339	8.258
7-8	6.92±0.63		7.14	6.210	6.327	6.560	7.401	6.565
7-9	5.54±0.30		5.48	4.401	4.163	5.103	5.572	5.047

4.2.5. Xe₂

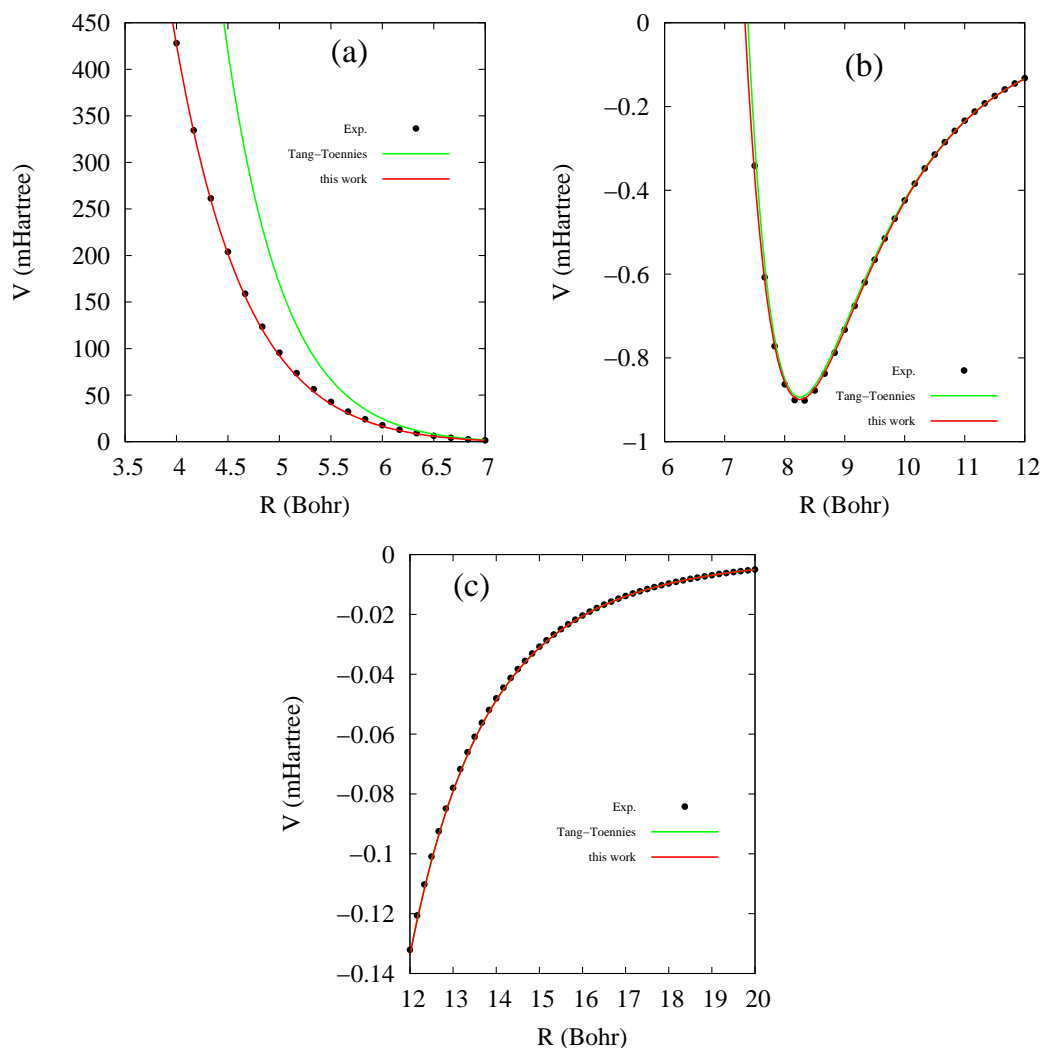


Fig.4.2.5 Comparison of the ground-state potential curve of Xe₂ of the present work (this work) (Red line, $\alpha = 1.45493289$, $\beta = 15.1518022$, $\eta = 248.22859$, $\chi = 0.876419067$, $R_e = 8.25$, $C_6 = 285.9$, $C_8 = 12810$, and $C_{10} = 619800$) with HFD-B experimental data (Dark filled circles, Ref. [183]), Tang-Toennies potential curve (Green line, $A = 951.8$, $b = 1.681$, $C_6 = 285.9$, $C_8 = 12810$, and $C_{10} = 619800$, Ref. [175]).

In this work, we fit the accurate potential curve of HFD-B experimental data for the ground-state Xe₂ presented in Ref. [183] and use the dispersion coefficients $C_6 = 285.9$, $C_8 = 12810$, and $C_{10} = 619800$ of Ref. [175]. The RMS for this fitting is 0.0213, and the determined potential parameters are $\alpha = 1.45493289$, $\beta = 15.1518022$, $\eta = 248.22859$, $\chi = 0.876419067$. We present the fitted potential curve in Fig.4.2.5. It agrees very well with HFD-B data [183]. Similar to Kr₂, Tang-Toennies potential [175] is harder than the HFD-B data in the repulsive region. It concludes that our present potential is more accurate than Tang-Toennies potential. In Table 4.2.5, we list the spacings of vibrational energies calculated by using the present potential and compare them with the literature data. We find that our results agree well with experiment [184, 185].

Table 4.2.5: Comparison of our computed vibrational energy spacings for Xe₂ with experimental and other theoretical data. All values are given in cm⁻¹. The vibrational spacings for the potentials, xR-vdW (extended Rydberg -van der Waals potential [79]), TT (Tang-Toennis potential [80]), and LJ (Lennard-Jones potential [3]), are from Ref. [177].

Transition	Exp. (Ref. [186])	Modified exp-6 (Ref. [187])	CCSD (Ref. [180])	this work	xR-vdW (Ref. [177])	TT (Ref. [177])	LJ (Ref. [177])
0-1	19.90±0.30	20.71	18.65	19.50	20.911	19.643	21.488
1-2	18.55±0.30	19.27	17.50	18.37	18.856	18.358	19.370
2-3	17.20±0.30	17.48	16.35	17.23	16.845	17.092	17.343
3-4	16.17±0.30	16.22	15.20	16.08	15.101	15.849	15.408
4-5	14.63±0.30	14.71	14.05	14.93	14.868	14.629	13.570
5-6	13.70±0.30	13.30	12.92	13.78	12.922	13.435	11.830
6-7	12.63±0.30	12.10	11.79	12.62	11.004	12.271	10.194
7-8	11.33±0.30	10.80	10.68	11.48	9.123	11.141	8.664
8-9	10.15±0.30	9.52	9.59	10.35	7.297	10.045	7.244
9-10	8.95±0.30	8.49	8.52	9.24	5.563	8.990	5.939
10-11	7.83±0.30	7.44	7.49	8.17			
11-12	6.79±0.30	6.46	6.49	7.14			
12-13	5.83±0.30	5.66	5.54	6.15			
13-14	4.93±0.30	4.73	4.63	5.22			
14-15	4.11±0.30	3.96	3.81	4.35			

4.3. Alkaline-Earth Dimers

Alkaline-earth metals attract both experimental and theoretical research in the field of cold atom interactions. Cooling and trapping of several species (Mg, Ca) was motivated by the use of group-II atoms for realization of optical frequency standards and by the perspective for achievement of quantum degeneracy. Presently cooling techniques are developed for Ca with which microkelvin and even nanokelvin temperatures were reported.

An important problem for making reliable theoretical predictions on cold collision phenomena in this area is to obtain accurate interaction potentials for alkaline-earth dimers. Contrary to the alkali metals, the available spectroscopic information is by no means complete and often with insufficient accuracy.

4.3.1. Ca₂

The $X^1\Sigma_g^+$ state of Ca₂ has been the subject of several investigations since the early experimental study of the so-called green system by Balfour and Whitlock [188] in 1975, where vibrational levels up to the 7th level were observed. In 1980, Vidal [189] extended the spectroscopic data on the X state of Ca₂ using the laser induced fluorescence technique and derived new sets of Dunham coefficients for the X and B states describing a total of 5846 observed lines covering vibrational levels from $\nu = 0$ to 34. A potential-energy curve for the ground state of Ca₂ based on the inverted perturbation approach (IPA) was determined, which allowed the extrapolation of the ground-state dissociation energy from experimental data. The calculated eigenenergies of this IPA potential, however, do not agree with the term energies calculated with the Dunham coefficients within the $0.03 - cm^{-1}$ uncertainty. Later, in 2000, Tiemann group [190] reported on an accurate determination of the Ca₂ ground-state potential-energy curve.

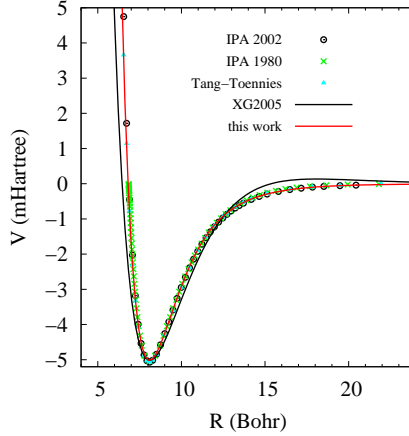


Fig.4.3.1 Comparison of the ground-state potential curve of Ca_2 of the present work ($\alpha = 0.838362902$, $\beta = 2.96505942$, $\eta = 21.2098198$, $\chi = 1.75753763$, $R_e = 8.081$, $C_6 = 2121$, $C_8 = 223000$, and $C_{10} = 21320000$) with the IPA data points in 1980 (Ref. [189]), IPA data points in 2002 (Ref. [190]), Tang-Toennies potential ($A = 28.23$, $b = 0.9987$, $C_6 = 2121$, $C_8 = 223000$, and $C_{10} = 21320000$, Ref. [191]), and three-parameter potential [100].

Table 4.3.1.: Comparison of computed vibrational energies for $^{40}\text{Ca}_2$ with experiment [189]. All values are given in cm^{-1} .

ν	this work	Exp.(Ref. [189])	ν	this work	Exp.(Ref. [189])	ν	this work	Exp.(Ref. [189])
0	32.39	32.26	12	647.27	650.28	24	994.07	992.55
1	93.67	95.17	13	686.47	688.84	25	1011.07	1009.75
2	153.14	155.94	14	723.80	725.51	26	1026.38	1025.31
3	210.81	214.58	15	759.25	760.30	27	1040.04	1039.24
4	266.66	271.12	16	792.81	793.24	28	1052.14	1051.57
5	320.68	325.59	17	824.49	824.35	29	1062.74	1062.32
6	372.88	377.99	18	854.28	853.64	30	1071.93	1071.50
7	423.24	428.35	19	882.20	881.15	31	1079.77	1079.14
8	471.76	476.69	20	908.25	906.88	32	1086.33	1085.27
9	518.43	523.03	21	932.44	930.87	33	1091.66	1089.89
10	563.24	567.40	22	954.79	953.13	34	1095.83	1093.04
11	606.19	609.81	23	975.32	973.68	-	-	-

Using Eq.(4) and the dispersion coefficients C_6 , C_8 and C_{10} of Ref. [191], we fit the accurate data of Ref. [190]. The RMS of this fitting is 0.0116, and the potential parameters are determined to be $\alpha = 1.24946345$, $\beta = 2.67596495$, $\eta = 29.910735$, and $\chi = 1.34122874$. The fitted potential curve is presented in Fig.4.3.1 and agrees very well with the IPA data [189,190] and Tang-Toennies potential [191]. The present potential is greatly improved over the three-parameter potential in all the regions [100]. In Table 4.3.1., we list the computed vibrational energies by using the present potential for $^{40}\text{Ca}_2$. It agrees very well with experiment [189].

4.3.2. Sr_2

Over the past decades the Sr_2 molecule has been the subject of many different studies. Currently there is high interest in ultracold ensembles of strontium atoms and high-precision spectroscopy on strontium, because it could be a candidate for an optical frequency standard (see literature review in Ref. [192]). Recently, Tiemann group has derived precise potentials

for the ground-state of Sr_2 by high-resolution Fourier-transform spectroscopy of fluorescence progressions from single-frequency laser excitation of Sr_2 produced in a heat pipe at very high temperature (950 °C).

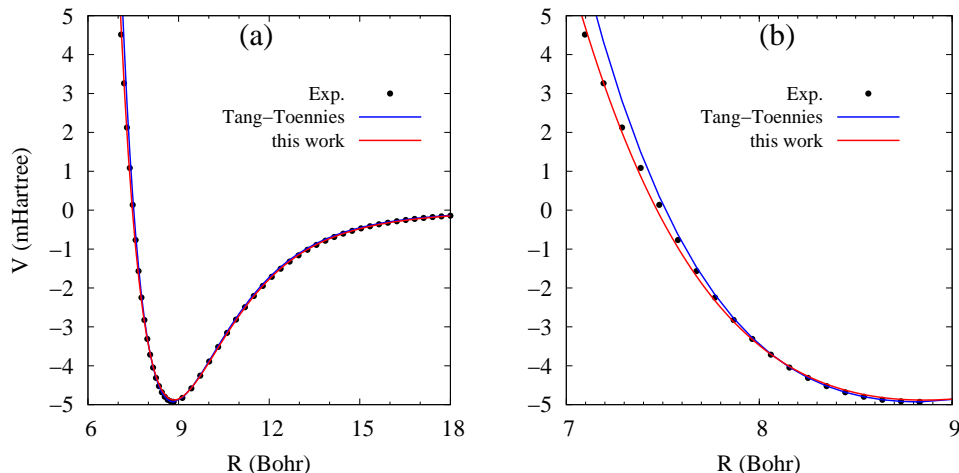


Fig.4.3.2. Comparison of the ground state of Sr_2 of the present work (this work) (Red line, $\alpha = 0.766237652$, $\beta = 2.72708084$, $\eta = 21.152344$, $\chi = 1.76518642$, $R_e = 8.828$, $C_6 = 3103.0$, $C_8 = 379200.0$, $C_{10} = 42150000.0$) with the experimental data (Dark filled circles, Ref. [192]) and Tang-Toennies potential (Blue line, $A=44.73$, $b=0.9699$, $C_6 = 3103.0$, $C_8 = 379200.0$, $C_{10} = 42150000.0$, Ref. [193]). (a) Full scale. (b) Enlarged in the repulsive region.

Table 4.3.2.: Computed vibrational energies (in units of cm^{-1}) for $^{88}\text{Sr}_2$. All values are relative to the energy of the first vibrational level $\nu = 0$. Dissociate energy $D_e = 1081.82\text{cm}^{-1}$ [195].

ν	E_ν								
0	0.	13	441.62	26	761.94	39	958.47	52	1041.36
1	38.18	14	470.62	27	781.46	40	968.57	53	1043.97
2	75.68	15	498.90	28	800.24	41	977.98	54	1046.12
3	112.47	16	526.45	29	818.27	42	986.72	55	1047.86
4	148.57	17	553.28	30	835.58	43	994.82	56	1049.21
5	183.96	18	579.39	31	852.14	44	1002.27	57	1050.23
6	218.65	19	604.77	32	867.97	45	1009.11	58	1050.95
7	252.63	20	629.42	33	883.07	46	1015.35	59	1051.43
8	285.91	21	653.34	34	897.44	47	1021.01	60	1051.72
9	318.48	22	676.53	35	911.08	48	1026.12	61	1051.88
10	350.34	23	698.98	36	924.00	49	1030.69	62	1051.94
11	381.48	24	720.71	37	936.20	50	1034.74		
12	411.91	25	741.69	38	947.69	51	1038.29		

In this work, we use Eq.(4) and the dispersion coefficients of Ref. [193] to fit the experimental data of Sr_2 [192]. The RMS of this fitting is 0.0674, and the potential parameters are determined to be $\alpha = 0.766237652$, $\beta = 2.72708084$, $\eta = 21.152344$, $\chi = 1.76518642$. The fitted potential curve, as shown in Fig.4.3.2., is in excellent agreement with the experimentally determined potential [192]. In the repulsive wall (Fig.4.3.2(b), shows discernible, increased differences from the experimental data [192] with decreasing R in the region of $R < 8$ Bohr. Using the fitted potential, we got in total 63 vibrational levels which are listed in Table 4.3.2.

This is in agreement with a recent experiment [194], where a two-photon photoassociative spectroscopy of ultracold ^{88}Sr has determined the binding energy of the last vibrational level $\nu = 62$. Meanwhile, very recently, ground state levels as high as $\nu = 60$ (outer turning point at 23 \AA and 0.1 cm^{-1} below the asymptote) have also been observed by Fourier-transform spectroscopy of fluorescence progressions [195], which support our calculations.

4.3.3. Mg_2

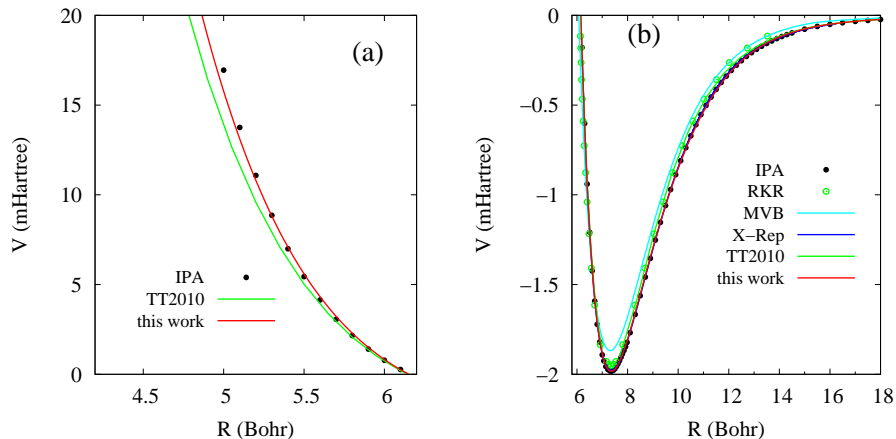


Fig.4.3.3 Comparison of the ground-state potential curve of Mg_2 : The present work (this work) (Red line, $\alpha = 1.24946345$, $\beta = 2.67596495$, $\eta = 29.910735$, $\chi = 1.34122874$, $R_e = 7.354$, $C_6 = 627$, $C_8 = 41500$, and $C_{10} = 2757000$) with the RKR data points (Green open circles, Ref. [196]), IPA potential (Dark filled circles, Ref. [197]), X-representation of the potential energy curves (Blue line, Ref. [198]), Tang-Toennies potential (Green line, $A = 7.3486$, $b = 1.0475$, $C_6 = 627$, $C_8 = 41500$, and $C_{10} = 2757000$, Ref. [199]), and *ab initio* multi-configuration valence bond (MVB) calculation (cyan line, Ref. [200]).

There are several ways to obtain the interaction potential of the ground-state Mg_2 . First, a Rydberg-Klein-Rees (RKR) potential [196] has been constructed from the measurement of the rovibrational levels. Second, Vidal and Scheingraber [197] have improved upon the RKR analysis [196] by applying a variational procedure based on the inverted perturbation approach (IPA). As shown in Fig.4.3.3, there is a slight difference between RKR and IPA data points in the attractive region. Very recently, Tiemann group [198] has investigated the $A^1 \Sigma_u^+ - X^1 \Sigma_g^+$ UV spectrum of Mg_2 with high resolution Fourier-transform spectroscopy, and achieved a very accurate PEC for the ground-state Mg_2 , i.e., the X-representation PEC shown in Fig.4.3.3, which overlaps exactly with the IPA data points. Using Eq.(4) and the dispersion coefficients C_6 , C_8 and C_{10} of Ref. [198], we fit the accurate data of Ref. [198]. The RMS of this fitting is 0.00534, and the potential parameters are determined to be $\alpha = 1.24946345$, $\beta = 2.67596495$, $\eta = 29.910735$, and $\chi = 1.34122874$. Fig.4.3.3 presents our fitted PEC. Except a slight deviation in the repulsive region, the fitted PEC overlaps quite well with the IPA points. To be noted, Tang-Toennies potential [199] is getting softer and softer in the repulsive region (see Fig.4.3.3(a)) as R decreases, and shows a slight deviation from the IPA points in the attractive region. In comparison with the other PECs, *ab initio* multi-configuration valence bond (MVB) calculation [200] shows some deviations from the IPA data points [197] and X-representation PEC [198], but is close to the RKR points [196].

4.4. Metal-Rare Gas Dimer

4.4.1. LiHe

Using Eq.(4) and the dispersion coefficients C_6 , C_8 and C_{10} of Ref. [201], we fit the potential energy curve of the ground-state LiHe [201]. The root-mean-square of this fitting is 0.0416, and the potential parameters are determined to be $\alpha = 1.279007516$, $\beta = 0.00616$, $\eta = 7.690378437$, $\chi = 0.906530719$. The fitted potential curve is presented in Fig.4.4.1, which agrees well with Ref. [201]. The present potential is greatly improved over the three-parameter potential [100].

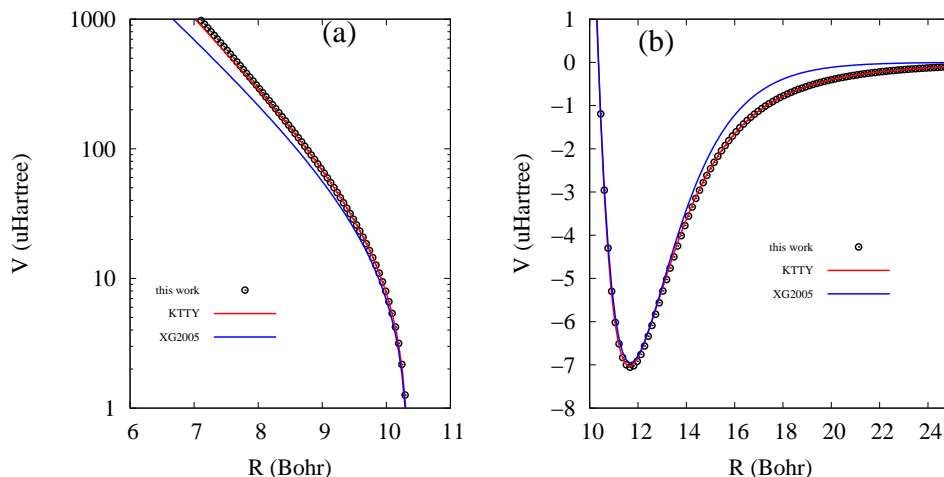


Fig.4.4.1. Comparison of the ground-state potential curve of LiHe of the present work (this work) ($\alpha = 1.2471927$, $\beta = 0.100442894$, $\eta = 7.96945502$, $\chi = 0.931774366$, $R_e = 11.645$, $C_6 = 22.507$, $C_8 = 1083.2$, and $C_{10} = 72602.1$) with KTTY potential curve ($A = 2.430857$, $b_1 = 1.04911$, $b_2 = 0.00381298$, $C_6 = 22.507$, $C_8 = 1083.2$, and $C_{10} = 72602.1$, Ref. [201]) and three-parameter potential ($\alpha = 0.7047$, $\beta = 0.00969121$, $\gamma = 1.04$, Ref. [100]).

4.4.2. LiAr

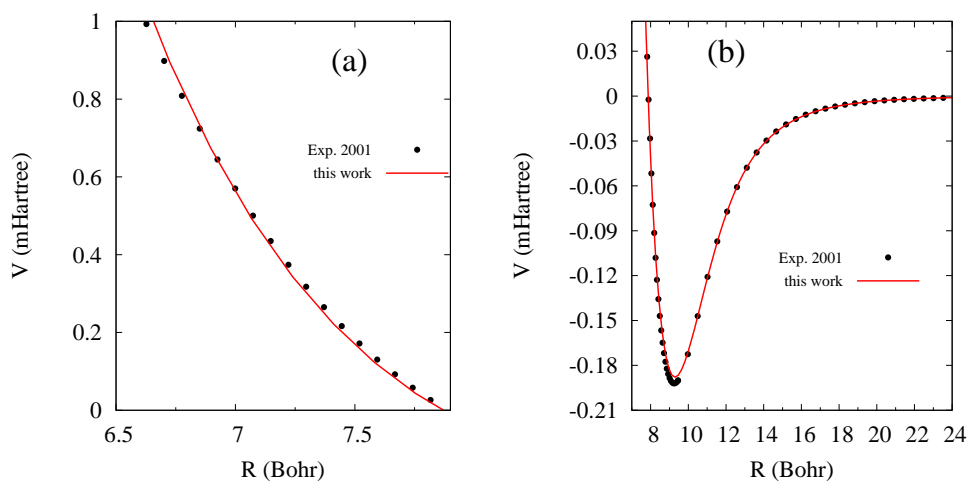


Fig.4.4.2. Comparison of the ground-state potential curve of LiAr of the present work ($\alpha = 0.756392786$, $\beta = 0.0101626292$, $\eta = 5.01705619E - 011$, $\chi = 0.973713149$, $R_e = 9.251$, $C_6 = 174.439002$, $C_8 = 16211.717$, $C_{10} = -648740.115$) with experiment [203].

Using Eq.(4) and the dispersion coefficients C_6 , C_8 and C_{10} of Ref. [203], we fit the experimentally determined potential data of the ground-state LiAr [203]. The RMS of this fitting is 0.00787, and the potential parameters are determined to be $\alpha = 0.756392786$, $\beta = 0.0101626292$, $\eta = 5.01705619 * 10^{-11}$, $\chi = 0.973713149$. The fitted potential curve is presented in Fig.4.4.2, which agrees well with Ref. [203]. We have computed the vibrational energies for the ground state of ${}^7\text{Li}^{40}\text{Ar}$. The computed energies, referencing to the lowest level, are 0., 15.7675926, 25.9838635, 30.6602299 cm^{-1} , which are in good agreement with experimental values (0, 16.0876, 26.4140, 31.1668 cm^{-1}) [203].

4.4.3. NaAr

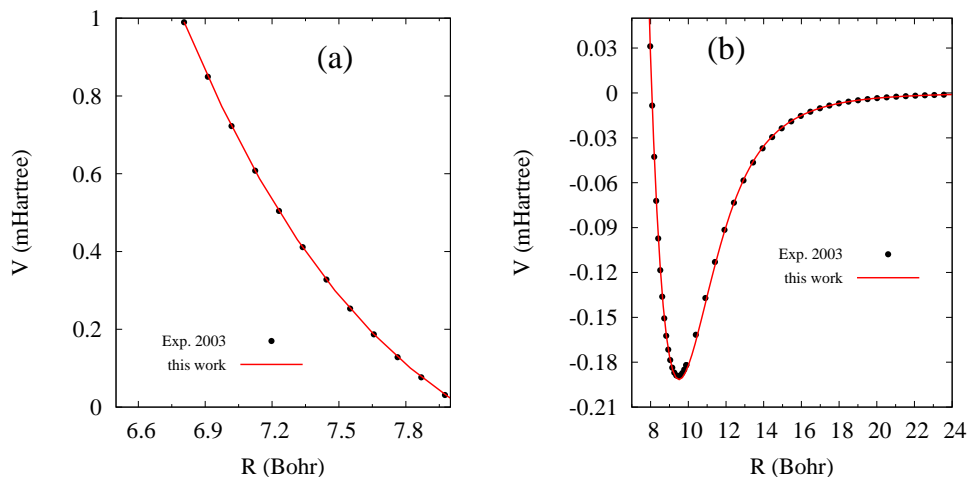


Fig.4.4.3. Comparison of the ground-state potential curve of NaAr of the present work ($\alpha = 1.05262069$, $\beta = 6.76650021 * 10^{-5}$, $\eta = 2.6312004$, $\chi = 0.977308837$, $R_e = 9.464$, $C_6 = 146.291942$, $C_8 = 37301.7153$, $C_{10} = -2839043.74$, and $C_{12} = 98879551$) with experiment [204].

Table 4.4.3: Comparison of ${}^{23}\text{Na}^{40}\text{Ar}$ vibrational energies (cm^{-1}) of present work with experiments [204–206]. The relative errors are compared to Ref. [204].

ν	Exp.(Ref. [204])	present work	Ref. [205]	Ref. [206]
0	0	0	0	0
1	11.243	11.321 (0.69%)	11.243 (0.0%)	11.244 (0.01%)
2	20.311	20.589 (1.37%)	20.308 (0.01%)	20.290 (0.10%)
3	27.137	27.592 (1.68%)	27.134 (0.01%)	26.710 (1.57%)
4	31.722	32.243 (1.64%)	31.720 (0.01%)	31.180 (1.71%)
5	34.219	34.749 (1.55%)	-	-
6	35.086	35.627 (1.31%)	-	-

Using Eq.(4) and the dispersion coefficients C_6 , C_8 and C_{10} of Ref. [204], we fit the experimentally-determined potential curve of Ref. [204]. The RMS of this fitting is 0.00133, and the potential parameters are determined to be $\alpha = 1.05262069$, $\beta = 6.76650021 * 10^{-5}$, $\eta = 2.6312004$, and $\chi = 0.977308837$. The fitted potential curve is presented in Fig.4.4.3., which agrees well with the experimental data [204]. We have computed the vibrational energies for the ground state of ${}^{23}\text{Na}^{40}\text{Ar}$ and listed in Table 4.4.3. The relative errors of the present calculations by using the new potential are less than 2%.

4.4.4. KAr

Using Eq.(4) and the dispersion coefficients C_6 , C_8 and C_{10} of Ref. [207], we fit the experimentally-determined potential curve of the ground-state KAr [207]. The RMS of this fitting is 0.00651, and the potential parameters are determined to be $\alpha = 0.784386108$, $\beta = 0.110425294$, $\eta = 1.25453368$, $\chi = 0.902759495$. The fitted potential curve is presented in Fig.4.4.4., which agrees well with the experimental data [204].

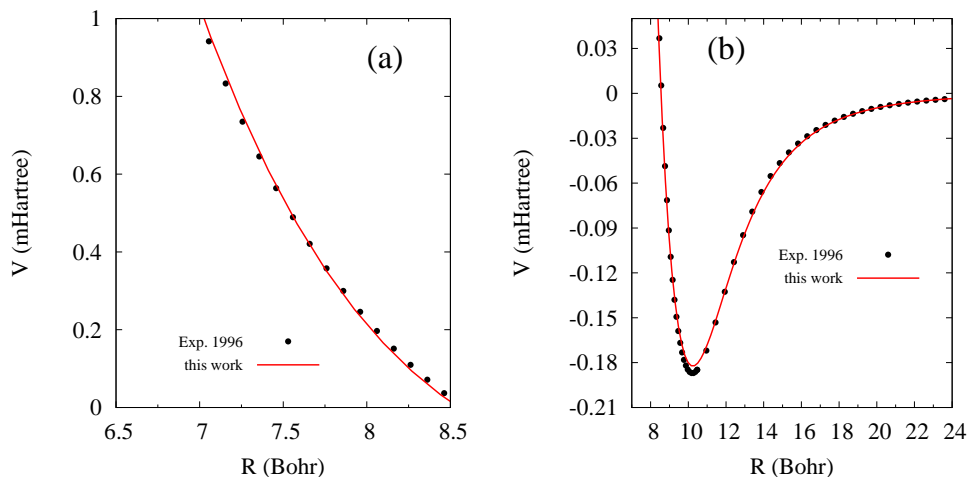


Fig.4.4.4. Comparison of the ground-state potential curve of KAr of the present work ($\alpha = 0.784386108$, $\beta = 0.110425294$, $\eta = 1.25453368$, $\chi = 0.902759495$, $R_e = 10.2155$, $C_6 = 813.707004$, $C_8 = -92544.8751$, and $C_{10} = 5201954.29$) with experiment [207].

4.4.5. NaKr

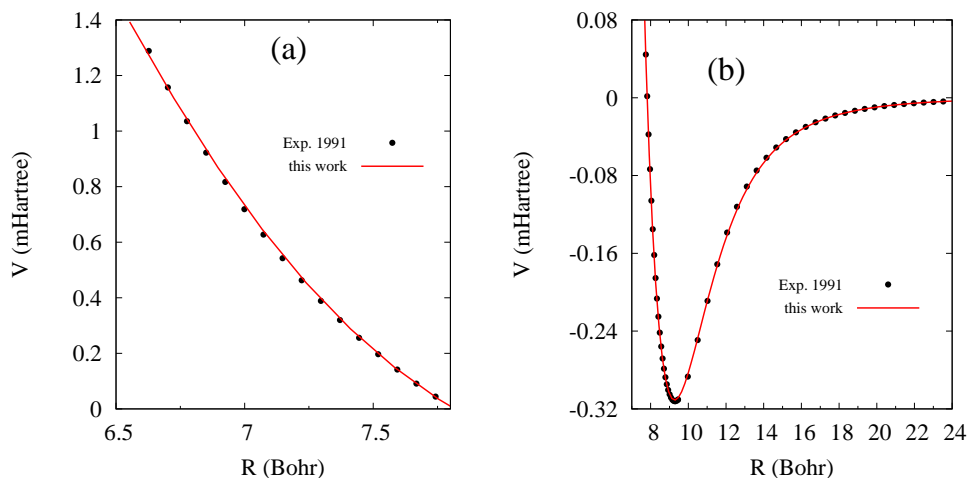


Fig.4.4.5. Comparison of the ground-state potential curve of NaKr of the present work ($\alpha = 1.03555444$, $\beta = 1.51652775$, $\eta = 17.7782338$, $\chi = 0.665157117$, $R_e = 9.297$, $C_6 = 774.161953$, $C_8 = -71575.4863$, and $C_{10} = 3137439.55$) with experiment [208].

Using Eq.(4) and the dispersion coefficients C_6 , C_8 and C_{10} of Ref. [208], we fit the experimentally-determined potential data of the ground-state NaKr [208]. The RMS of this

fitting is 0.00437, and the potential parameters are determined to be $\alpha = 1.03555444$, $\beta = 1.51652775$, $\eta = 17.7782338$, $\chi = 0.665157117$. The fitted potential curve is presented in Fig.4.4.5., which agrees well with the experimental data [208].

4.4.6. CaHe

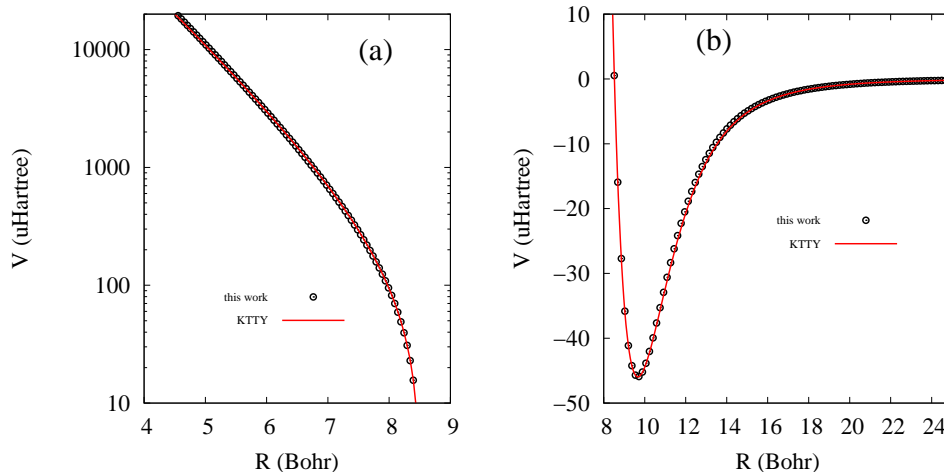


Fig.4.4.6 Comparison of the ground-state potential curve of CaHe of the present work (this work) ($\alpha = 1.279007516$, $\beta = 0.00616$, $\eta = 7.690378437$, $\chi = 0.906530719$, $R_e = 9.64$, $C_6 = 46.8$, $C_8 = 1835$, and $C_{10} = 118500$) with Kleinekathöfer potential curve (KTTY) ($A = 3.19$, $b_1 = 1.053$, $b_2 = 0.00745$, $C_6 = 46.8$, $C_8 = 1835$, and $C_{10} = 118500$, Ref. [209]).

Using Eq.(4) and the dispersion coefficients C_6 , C_8 and C_{10} of Ref. [209], we fit the potential energy curve of the ground-state CaHe [209]. The RMS of this fitting is 0.02, and the potential parameters are determined to be $\alpha = 1.279007516$, $\beta = 0.00616$, $\eta = 7.690378437$, $\chi = 0.906530719$. The fitted potential curve is presented in Fig.4.4.6, which agrees very well with Ref. [209].

4.5. Group 12 Dimers

Diatomic molecules formed from two closed shell atoms are van der Waals molecules such as dimers (Zn_2 , Cd_2 , Hg_2) of group 12 atoms, the so-called battery elements, with outer electronic configuration $nd^{10}(n+1)s^2$. These dimers have been investigated for a long time, and are of interest for a variety of reasons [210]. A large number of papers on the interatomic potential energies of these dimers have been published (see review in Ref. [211]). Experimentally, Hg_2 potential is probably the most extensively studied among these three dimers. Not until late 1980s, efficient cooling of the mercury dimers by supersonic expansion made it possible to resolve the vibrational and rotational spectra of the absorption bands for transitions from ground state to excited states. Since much higher temperature is required to vaporize cadmium and zinc, Cd_2 and Zn_2 are less extensively studied than Hg_2 . Nevertheless, recent laser spectroscopies of Cd_2 and Zn_2 seem to give reliable values of ω_e and D_e of the electronic ground states. But the equilibrium distances R_e of these dimers are less certain.

4.5.1 Zn₂

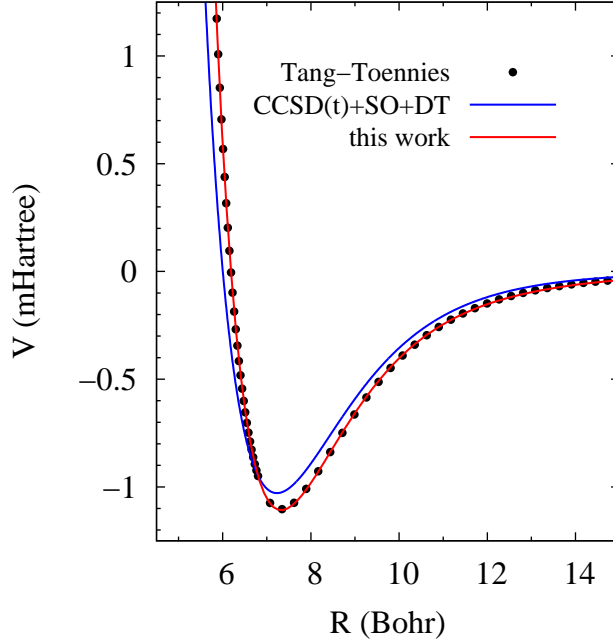


Fig.4.5.1. Comparison of the ground-state potential curve of Zn₂ of the present work (this work) ($\alpha = 0.951854441$, $\beta = 0.845807252$, $\eta = 5.17252173$, $\chi = 1.65593701$, $R_e = 7.323$, $C_6 = 359$, $C_8 = 13500$, and $C_{10} = 640000$) with the recent CCSD calculations ($a_6 = -840.0$, $a_7 = 0.0$, $a_8 = 1120945.16929225$, $a_9 = -40566470.5207570$, $a_{10} = 600462536.497241$, $a_{11} = -4601554475.95170$, $a_{12} = 19363653998.2602$, $a_{13} = -42652938535.8249$, and $a_{14} = 38570620352.9465$, Ref. [212]) and Tang-Toennies potential ($A = 7.63$, $b = 1.1489$, $C_6 = 359$, $C_8 = 13500$, and $C_{10} = 640000$, Ref. [211]).

For the ground state of Zn₂, we use Eq.(4) and the dispersion coefficients C_6 , C_8 and C_{10} of Wei *et al.* [211] to fit the Tang-Toennies potential curve derived recently by Wei *et al.* [211]. The RMS of this fitting is 0.00455, and the potential parameters are determined to be $\alpha = 0.951854441$, $\beta = 0.845807252$, $\eta = 5.17252173$, $\chi = 1.65593701$. In Fig.4.5.1, we present the fitted potential curve, which agrees very well with Ref. [211]. The recent CCSD calculations of Pahl *et al.* [212] are fitted with a function form of extended Lenard-Jones potential $V(R) = \sum_{k=6}^{k=14} a_k/R^k$. Their calculations [212] estimated the dispersion coefficient C_6 to be 514 and set $a_6 = C_6$. The value of C_6 is about 40 percent larger than the accurate literature data (359 [211]). On the other hand, the two terms corresponding to C_8 and C_{10} in Ref. [212] have a positive sign. Thus, it is expected that the potential of Pahl *et al.* [212] does not have the same long range behavior as the Tang-Toennies potential [211]. Near the potential minimum, the potential of Pahl *et al.* [212] is not too different from the Tang-Toennies potential [211].

4.5.2 Cd₂

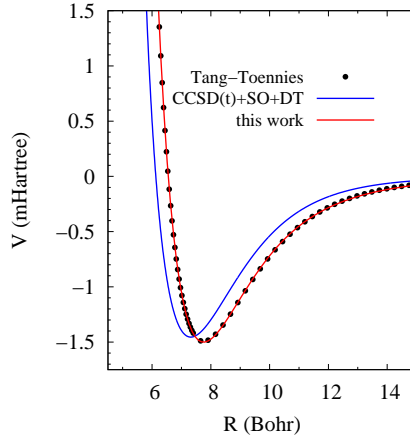


Fig.4.5.2. Comparison of the ground-state potential of Cd₂ derived from the new function ($\alpha = 0.905436963$, $\beta = 1.13619161$, $\eta = 7.52670062$, $\chi = 1.63815301$, $R_e = 7.752$, $C_6 = 686$, $C_8 = 28900$, and $C_{10} = 1537000$) with the recent CCSD calculations ($a_6 = -840.0$, $a_7 = 0.0$, $a_8 = 1975089.60438597$, $a_9 = -72973282.5105466$, $a_{10} = 1110874391.15603$, $a_{11} = -8804084660.52397$, $a_{12} = 38464166968.9086$, $a_{13} = -88181906149.4874$, and $a_{14} = 83111453189.9489$, Ref. [212]), and Tang-Toennies potential ($A = 10.26$, $b = 1.0842$, $C_6 = 686$, $C_8 = 28900$, and $C_{10} = 1537000$, Ref. [211]).

For the ground state of Cd₂, we use Eq.(4) and the dispersion coefficients C_6 , C_8 and C_{10} of Wei *et al.* [211] to fit the recent results of Wei *et al.* [211], where the interaction potential is described by the Tang-Toennies potential model. The RMS of this fitting is 0.0069 and the potential parameters are determined to be $\alpha = 0.905436963$, $\beta = 1.13619161$, $\eta = 7.52670062$, and $\chi = 1.63815301$. In Fig.4.5.2, we present the fitted potential curve, which agrees very well with Ref. [211]. The recent CCSD calculations of Pahl *et al.* [212] are fitted with a function form of extended Lenard-Jones potential $V(R) = \sum_{k=6}^{14} a_k/R^k$. In the CCSD calculation, Pahl *et al.* [212] estimated the dispersion coefficient C_6 to be 840 and set $a_6 = C_6$. This value is twenty percent larger than the accurate literature data, 686. On the other hand, the two terms corresponding to C_8 and C_{10} have a positive sign. Thus, the potential of Pahl *et al.* [212] does not have the same long range behavior as the Tang-Toennies potential [211]. Nevertheless, it is not clear whether this will affect the shape of the potential near the potential minimum. The experimental minimum of Czajkowski and Koperski [213] seems to agree with the Tang-Toennies potential, while the more recent experiment of Strojecki *et al.* [214] seems to agree better with the calculations of Pahl *et al.* [212].

4.5.3 Hg₂

There are many theoretical studies on the potential of the ground-state Hg₂. The most extensive one is probably the recent theoretical calculation of Pahl *et al.* [215]. They have carried out a coupled cluster calculation with single, double, and perturbative triple excitations CCSD (T), at the complete basis set limit, including correction for the full triples and spin-orbit interactions. The CCSD(T)+SO+ ΔT data points of their calculation were fitted with the analytic form of extended Lenard-Jones potential $V(R) = \sum_{k=6}^{14} a_k/R^k$.

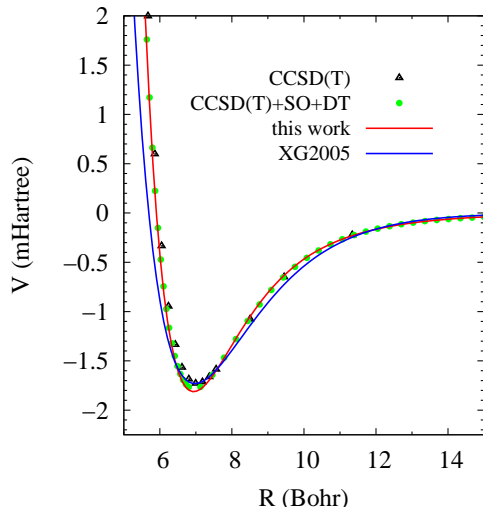


Fig.4.5.3. Comparison of the ground-state potential of Hg_2 fitted by using the new function (this work) ($\alpha = 1.06270654$, $\beta = 2.29004018$, $\eta = 13.8969565$, $\chi = 1.58681219$, $R_e = 6.955$, $C_6 = 392$, $C_8 = 12920$, and $C_{10} = 537000$) with the recent CCSD(T)+SO+ ΔT calculations ($a_6 = -392.0$, $a_7 = 0.0$, $a_8 = 513051.995806700$, $a_9 = -19598874.8141078$, $a_{10} = 282773699.594663$, $a_{11} = -2026379590.56904$, $a_{12} = 7793899858.68874$, $a_{13} = -15443502105.5180$, and $a_{14} = 12400089118.4353$, Ref. [215]), and CCSD(T) calculation (Ref. [216]).

In this work, we use Eq.(4) and the dispersion coefficients C_6 , C_8 and C_{10} of Ref. [217] to fit the potential data calculated by using CCSD(T)+SO+ ΔT [215]. The root-mean-square of our fitting is 0.0073, and the potential parameters are determined to be $\alpha = 1.06270654$, $\beta = 2.29004018$, $\eta = 13.8969565$, and $\chi = 1.58681219$. In Fig.4.5.3, we present the fitted curve and compare it with the recent CCSD(T) calculations of Munro *et al.* [216]. In the CCSD(T)+SO+ ΔT calculation, Pahl *et al.* [215] estimated the dispersion coefficient C_6 to be the accurate data, -392, and set $a_6 = C_6$. Thus, the potential of Pahl *et al.* [215] has the same long range behavior as the Tang-Toennies potential [217]. The present potential is also greatly improved over the three-parameter potential [100].

4.6. Other van der Waals Dimers

4.6.1. LiHg

A $^2\Sigma^+$ van der Waals bond of the system LiHg is formed by the 1S_0 Hg atom with the $^2S_{1/2}$ Li atom. It is known that LiHg shows an anomalous behavior both with respect to shape and magnitude of the well parameters compared to the other alkali-mercury systems. An accurate potential for the ground-state LiHg has been obtained by Buck *et al.* [218]. Thus, we fit their accurate potential curve by using the potential function Eq.(4) and the dispersion coefficients $C_6 = 443.0$, $C_8 = 25400.0$, $C_{10} = 1840000.0$ of Ref. [80]. The RMS for this fitting is 0.0633, and the potential parameters are determined to be $\alpha = 1.00277412$, $\beta = 0.884046581$, $\eta = 4.15797715$, $\chi = 2.08111888$. The fitted curve is presented in Fig.4.6.1. It agrees well with experiment [218]. To be noted, Tang-Toennies potential shows an obvious deviation from experiment at $R = 8 \sim 11$ Bohr.

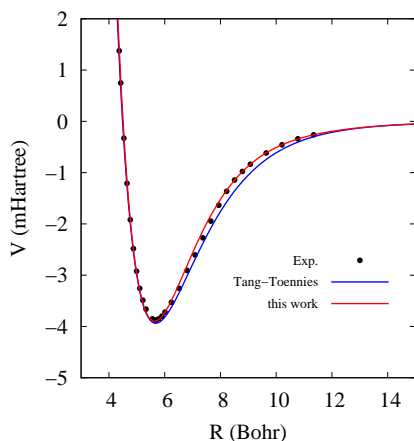


Fig.4.6.1. Comparison of the ground-state potential of LiHg of the present work (Red line, this work, $\alpha = 1.00277412$, $\beta = 0.884046581$, $\eta = 4.15797715$, $\chi = 2.08111888$, $R_e = 5.671$, $C_6 = 443.0$, $C_8 = 25400.0$, $C_{10} = 1840000.0$) with Tang-Toennies potential curve (Blue line, $A = 2.246$, $b = 1.012$, $C_6 = 443.0$, $C_8 = 25400.0$, $C_{10} = 1840000.0$, $C_{12} = 1.68 \times 10^8$, $C_{14} = 1.95 \times 10^{10}$, $C_{16} = 2.85 \times 10^{12}$ Ref. [80]) and experiment [218].

4.6.2. CdNe

The weakly bound van der Waals molecules of Group 12 (Zn, Cd, Hg) and rare gas (He, Ne, Ar, Kr, Xe) atoms have been studied by Koperski et al. (see literature review in Ref. [219]). Here we take CdNe as an example. We fit the experimentally determined potential data of the ground-state CdNe [219]. The RMS of this fitting is 0.001127, and the potential parameters are determined to be $\alpha = 1.19957532$, $\beta = 1.63773977$, $\eta = 11.8338502$, $\chi = 1.06487289$ (note: the dispersion of C_6 taken from Ref. [219]). The fitted potential agrees well with experiment [219]. In comparison with the three-parameter model potential [100], the new potential is greatly improved in the repulsive region (see Fig.4.6.2(a)).

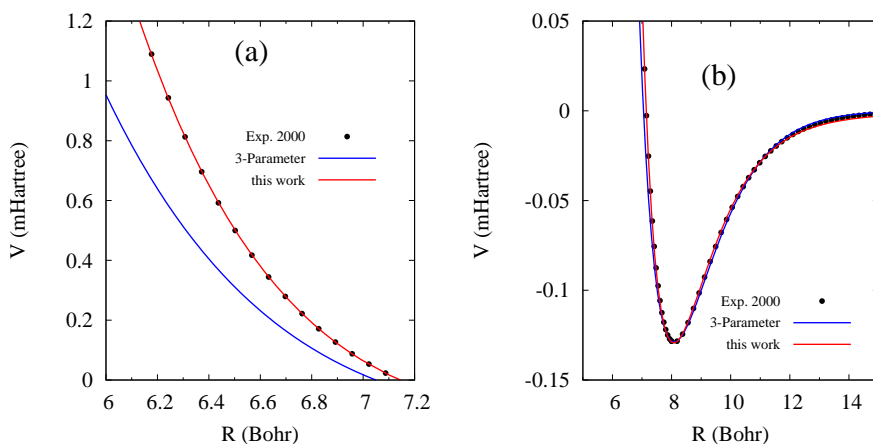


Fig.4.6.2. Comparison of the ground state of CdNe of the present work (red line, this work, $\alpha = 1.19957532$, $\beta = 1.63773977$, $\eta = 11.8338502$, $\chi = 1.06487289$, $R_e = 8.091$, $C_6 = 31.810688$) with three-parameter potential curve (blue line, $\alpha = 0.893146$, $\beta = 0.33243839$, $\gamma = 0.4$, Ref. [100]) and experiment (dark filled circles, Ref. [219]). (a) Repulsive region. (b) Attractive region.

4.6.3. LiHe⁻

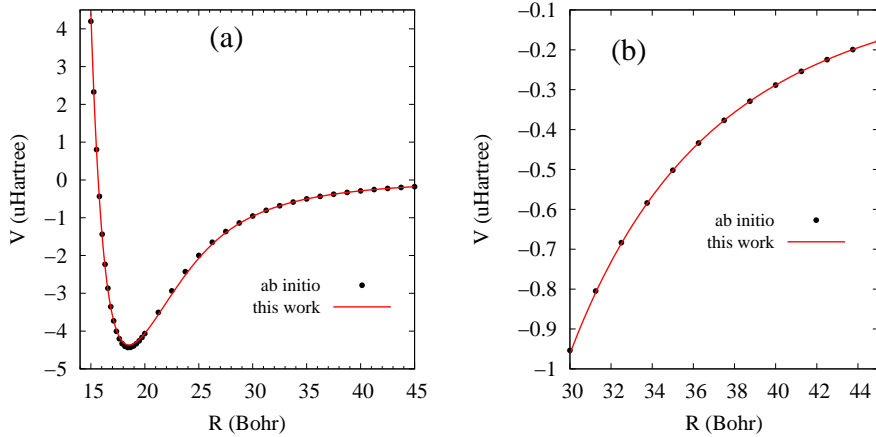


Fig.4.6.3. Comparison of the ground state of LiHe⁻ of the present work (red line, this work, $\alpha = 0.651021658$, $\beta = 0.0311407995$, $\eta = 0.509474386$, $\chi = 1.03618203$, and $R_e = 18.5$) with the *ab initio* data of Ref. [220]. (a) Full curve. (b) Enlarged Large-R part.

The He+Li⁻ interaction potential can generate interest in a variety of contexts beyond the general considerations associated with all weakly bound systems (for details, refer to the literature review in Ref. [220]). We fit the accurate potential data of the ground-state LiHe⁻ [220]. In our potential function, the C_4/R^4 term describes the ion-induced dipole interaction given by $-z^2\alpha_1/(2R^4)$. The R^{-6} term describes the ion-induced quadrupole and dispersion interaction given by $-z^2\alpha_2/(2R^6) - C_6/R^6$. The R^{-8} term describes the ion-induced octopole, the ion-hyperpolarizability, and the dispersion interaction given by $-z^2\alpha_3/(2R^8) - z^2\gamma_1/(24R^8) - C_8/R^8$. These values are (all in atomic units): $C_6 = 70.365674$, $C_8 = 6111.8844$, $\alpha_1 = 1.38272$, $\alpha_2 = 2.428246$, $\alpha_3 = 10.62$, and $\gamma_1 = 48.28598$. The root-mean-square for this fitting is 0.0435, and the potential parameters are determined to be: $\alpha = 0.651021658$, $\beta = 0.0311407995$, $\eta = 0.509474386$, and $\chi = 1.03618203$. The fitted potential curve is presented in Fig.4.6.3, which is in excellent agreement with the *ab initio* data [220]. To be noted, if we also take α_1 as the fitting parameter, then we have $\alpha_1 = 1.34036506$ as well as $\alpha = 0.648801132$, $\beta = 0.0254107349$, $\eta = 0.422241742$, and $\chi = 1.01883999$. The fitted value $\alpha_1 = 1.34036506$ is in good agreement with the data $\alpha_1 = 1.38272$ obtained in Ref. [220].

4.6.4. HeH

Numerous calculations have been made on the potential curve of the ground-state HeH (see literature review in Ref. [221, 222]). Here we use Eq.(4) to fit the potential data of Tang-Toennies [221]. The RMS of this fitting is 0.0001608, and the potential parameters are determined to be $\alpha = 1.58803424$, $\beta = 0.579296416$, $\eta = 3.22806569$, $\chi = 1.22237816$ (The dispersion coefficients taken from Ref. [221]). The fitted potential curve, as shown in Fig.4.6.4, agrees well with Tang-Toennies potential. In comparison with Tang-Toennies potential, the potential energies calculated by RCCSD/EVEN-II (the H and He EVEN basis sets were obtained by extending each of the standard H and He aug-cc-pV5Z basis sets by one diffuse function of each type in the standard even-tempered way) show about 10% deviation around the energy minimum, but agree well in the large-R region.

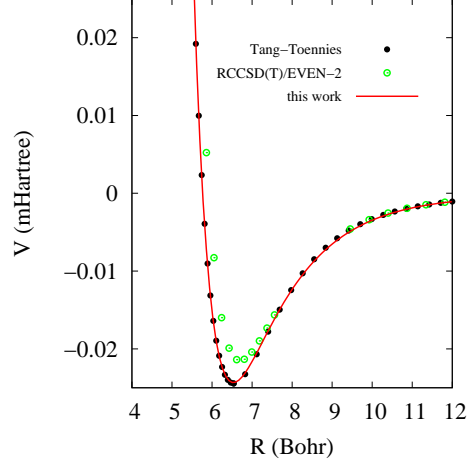


Fig.4.6.4. Comparison of the ground-state potential of HeH of the present work (this work) (Red line, $\alpha = 1.58803424$, $\beta = 0.579296416$, $\eta = 3.22806569$, $\chi = 1.22237816$, $R_e = 6.5406$, $C_6 = 2.81$, $C_8 = 41.74$, $C_{10} = 874.2$, $Nmax = 5$) with Tang-Toennies potential (Dark filled circles, $A = 4.474$, $b = 1.834$, $C_6 = 2.81$, $C_8 = 41.74$, $C_{10} = 874.2$, $Nmax = 8$ Ref. [221]) and RCCSD/EVEN-II calculations (Green open circles, Ref. [222]).

4.6.5. NeH

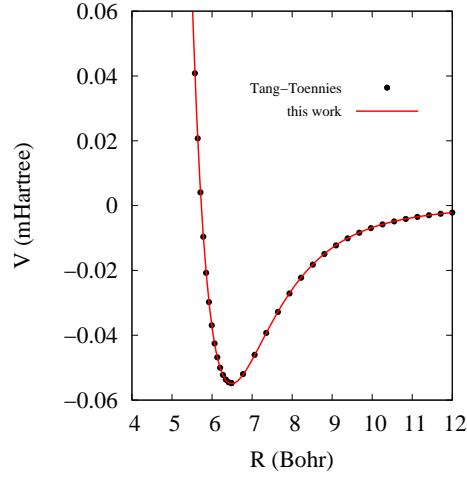


Fig.4.6.5. Comparison of the ground-state potential of NeH of the present work (this work) (Red line, $\alpha = 1.99549877$, $\beta = 0.000214356648$, $\eta = 28.3976811$, $\chi = 0.590250099$, $R_e = 6.4839$, $C_6 = 5.71$, $C_8 = 92.59$, $C_{10} = 2007.0$, $Nmax = 5$) with Tang-Toennies potential (Dark filled circles, $A = 11.78$, $b = 1.873$, $C_6 = 5.71$, $C_8 = 92.59$, $C_{10} = 2007.0$, $Nmax = 8$, Ref. [221]).

Numerous calculations have been made on the potential curve of the ground-state NeH (see literature review in Ref. [221]). Here we use Eq.(4) to fit the potential data of Tang-Toennies [221]. The RMS of this fitting is 0.000217, and the potential parameters are determined to be $\alpha = 1.99549877$, $\beta = 0.000214356648$, $\eta = 28.3976811$, $\chi = 0.590250099$ (The dispersion coefficients taken from Ref. [221]). The fitted potential curve, as shown in Fig.4.6.5., agrees well with Tang-Toennies potential.

4.6.6. AgHe

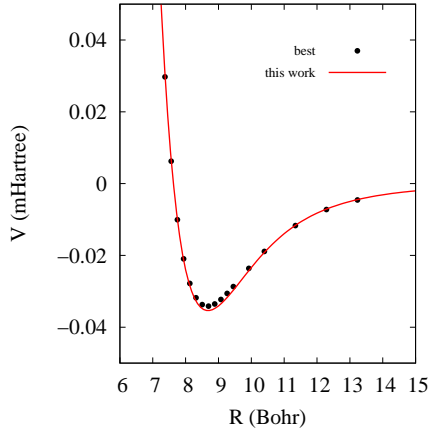


Fig.4.6.6. Comparison of the ground-state potential of AgHe of the present work (this work) (Red line, $\alpha = 1.3969125$, $\beta = 0.00679322993$, $\eta = 4.4391844$, $\chi = 0.909659481$, $R_e = 8.669$, $C_6 = 19.75$, $C_8 = 641.3$, $C_{10} = 22020.0$) with the best data (Dark filled circles, Ref. [223]).

The interactions of neutral coinage metals (Au, Ag, Cu) with the rare gas atoms have been studied intensively in recent years (see literature review in Ref. [223]). In 2008, AgHe dimer was detected in the lab [224]. Very recently, Gardner *et al.* [223] have provided in their supplementary materials the best extrapolated potential energy curves of the ground states of the dimers X-Rg (X=Cu, Ag, Au, Rg=He, Ne, Ar, Kr, Xe, Rn). Thus, in this work, we use Eq.(4) and the dispersion coefficients of Ref. [225] to fit the best potential data of the ground-state AgHe [223]. The RMS of this fitting is 0.000818, and the potential parameters are determined to be $\alpha = 1.3969125$, $\beta = 0.00679322993$, $\eta = 4.4391844$, and $\chi = 0.909659481$. The fitted potential curve, as shown in Fig.4.6.6., agrees well with the best potential energies of Gardner *et al.* [223]. Using the fitted potential, we got one vibrational level with the energy of -0.0102874 mHartree (Relative to the bottom of the potential well, our calculated vibrational energy is 0.0238376 mHartree (5.232 cm^{-1}), which is in excellent agreement with the calculated value of 5.2 cm^{-1} [226]).

4.6.7. XeF

Active interest in the rare gas halides has been motivated both by the peculiar nature of the bonding involved, and by the use of their molecular bands to obtain UV laser action [227,228]. In particular, among the rare gas halides, XeF is remarkably different from the others. Its ground-state potential curve shows a large curvature, which implies a very abrupt onset of repulsion, and has a large well depth and a short bond length. In this work, we take it as an example for rare gas halides. We use Eq.(4) and the dispersion coefficients of Ref. [79] to fit the potential energy curve of the ground state of XeF experimentally determined by Lee group [229] using the exp-spline-Morse-spline-van der Waals form [51]. The RMS of this fitting is 0.0111, and the potential parameters are determined to be $\alpha = 3.44058805$, $\beta = 30202.8963$, $\eta = 125046.845$, $\chi = 1.29988247$. The fitted potential curve, as shown in Fig.4.6.7., agrees well with experiment.

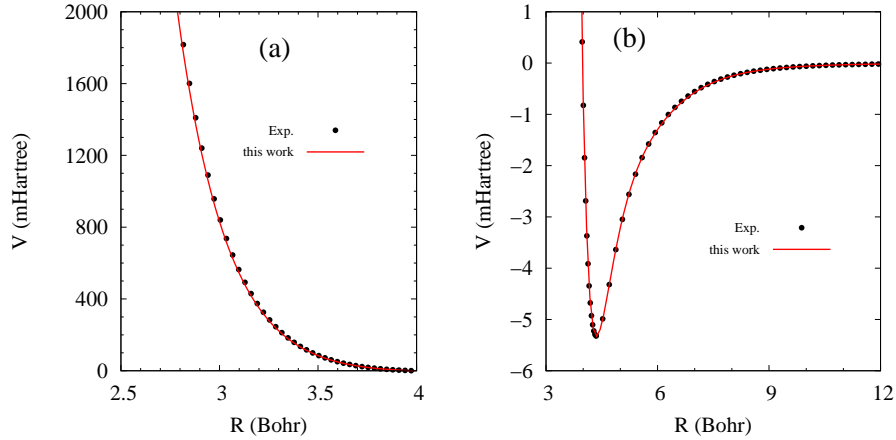


Fig.4.6.7. Comparison of the ground state of XeF of the present work (this work) (red line, $\alpha = 3.44058805$, $\beta = 30202.8963$, $\eta = 125046.845$, $\chi = 1.29988247$, $R_e = 4.3478$, $C_6 = 51.1212328$, $C_8 = 971.8541$) with the experimentally-determined potential data (dark filled circles, Ref. [229]).

4.6.8. KrF

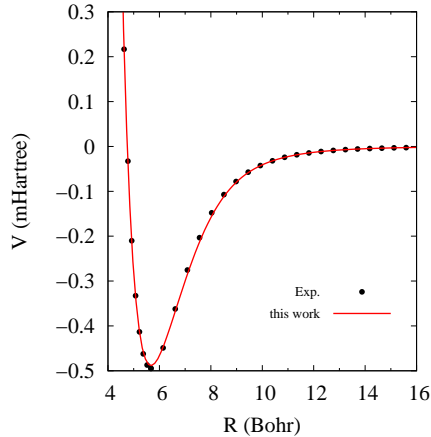


Fig.4.6.8. Comparison of the ground state of KrF of the present work (this work) (red line, $\alpha = 1.88310506$, $\beta = 1.326016$, $\eta = 14.6602054$, $\chi = 1.1394956$, $R_e = 5.6711$, $C_6 = 35.1954218$, $C_8 = 584.676487$) with the experimentally-determined potential data (dark filled circles, Ref. [230]).

In this work, we take KrF as one more example for rare gas halides. We use Eq.(4) and the dispersion coefficients of Ref. [79] to fit the potential energy curve of the ground state of KrF experimentally determined by Lee group [230] using the exp-spline-Morse-spline-van der Waals form [51]. The RMS of this fitting is 0.00457, and the potential parameters are determined to be $\alpha = 1.88310506$, $\beta = 1.326016$, $\eta = 14.6602054$, $\chi = 1.1394956$. The fitted potential curve, as shown in Fig.4.6.8., agrees well with experiment [230].

5. Meta-Stable Systems

The proposed potential function for the meta-stable systems is given by

$$V(R, \alpha, \beta, \gamma, \zeta, q) = \frac{J_1(R, \gamma, \zeta, q) + K_1(R, \alpha, \beta, \zeta, q)}{1 + S_0(R)} \quad (5)$$

with $J_1(R, \gamma, \zeta, q) = e^{-2\gamma R} \left(\frac{\zeta}{R^q} + \eta \right)$, $K_1(R, \alpha, \beta, \zeta, q) = e^{-\alpha R} \left(\frac{\zeta}{R^q} - \beta R \right)$, and $S_0(R) = e^{-R} \left(1 + R + \frac{R^2}{3} \right)$

5.1. He₂⁺⁺

Table 5.1.: Comparison of the spacings $\Delta G_\nu = E_{\nu+1} - E_\nu$ (in units of cm⁻¹) of the vibrational energies E_ν of the potential well with the most accurate data [237]. The value in the parenthesis is the relative error compared to the accurate data [237].

⁴ He ₂ ⁺⁺			³ He ⁴ He ⁺⁺		
ν	this work	Accurate (Ref. [237])	ν	this work	Accurate (Ref. [237])
0	3068.555 (0.57%)	3051.29	0	3285.664 (0.48%)	3269.92
1	2774.238 (0.42%)	2785.81	1	2952.595(0.002%)	2952.65
2			2		

5.2. BeH⁺⁺

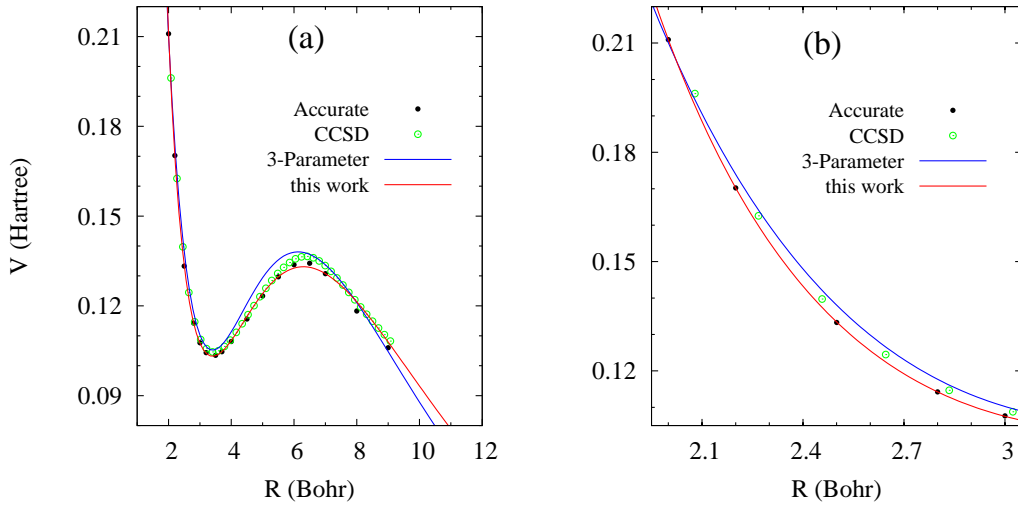


Fig.5.2. The comparison between the present potential potential (this work) (Red line, $\alpha = 0.614371674$, $\beta = 0.883328762$, $\gamma = 0.109403265$, $\zeta = 1.64081594$, and $q = 2.9011314$), three-parameter model potential (Blue line, $\alpha = 0.687$, $\beta = 1.43632004$, $\gamma = 0.1185$, Ref. [100]), CCSD/6-311++G(3df,3pd)(Green cross, Ref. [100]), and the most accurate data (dark filled circles, Ref. [238]) for the meta-stable diatomic dication BeH⁺⁺. The barrier near R =6 Bohr. (a) Full scale. (b) Enlarged in the repulsive region.

In this work, we use Eq.(5) to fit the accurate data of Ref. [238]. The RMS of this fitting is 0.00114, and the potential parameters are determined to be $\alpha = 0.614371674$, $\beta = 0.883328762$, $\gamma = 0.109403265$, $\zeta = 1.64081594$, and $q = 2.9011314$. In Fig.5.2(a)(b), we present the fitted potential curve and compare it with CCSD/6-311++G(3df,3pd) [100], three-parameter potential [100], and the accurate data [238]. The present potential agrees well with accurate data [238]. In the barrier and repulsive regions, the present potential is better than CCSD/6-311++G(3df,3pd) calculations [100], and is greatly improved in the accuracy over the three-parameter potential [100].

5.3. AlH^{++}

In this work, we use Eq.(5) to fit the CCSD/6-311++G(3df, 2pd) data of Ref. [100]. The RMS of this fitting is 0.00214, and the potential parameters are determined to be $\alpha = 0.423212447$, $\beta = 0.217842583$, $\gamma = 0.0280432067$, $\zeta = 6.04865744$, and $q = 4.3704501$. Fig.5.3 presents the fitted potential, which is compared with CCSD/6-311++G(3df,3pd) [100] and three-parameter potential [100]. In the repulsive and barrier regions, the present potential is greatly improved over the three-parameter potential.

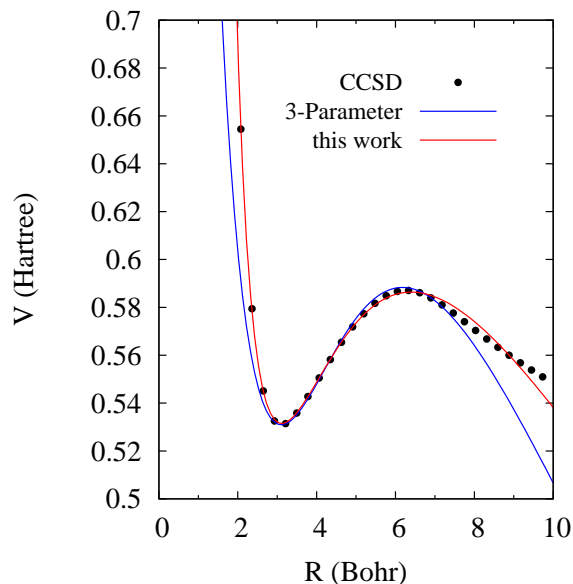


Fig.5.3. The comparison between four-parameter model potential (Red line, this work, $\alpha = 0.423212447$, $\beta = 0.217842583$, $\gamma = 0.0280432067$, $\zeta = 6.04865744$, and $q = 4.3704501$), three-parameter model potential (Blue line, $\alpha = 0.585984$, $\beta = 0.79669152$, $\gamma = 0.0365$, Ref. [100]), and CCSD/6-311++G(3df,3pd)(Dark filled circles, Ref. [100]) for the meta-stable diatomic dication AlH^{++} . The barrier near $R = 6$ Bohr.

Appendix A: Notes for Determining Pair-Potential Parameters

A.1. How to Determine Pair-Potential Parameters

The parameters of the proposed potential function may be estimated by a suitable method. When estimating the reliability of the interatomic potential obtained, it is necessary to take into account not only the measurement errors but also the approximate nature of the formulae, which connect the measured characteristics with the interatomic potential. Also, it is necessary to bear in mind that the function is over-determined and nonlinear in parameters. As a result, different sets of proposed parameters can give the same precision when fitted to experimental data. Our purpose in this study is to provide a few-parameter analytical function form to uniformly describe the potential energy of diatomic systems. Thus, we try to define pair-potential parameters as few as possible. Here are some notes for determining pair-potential parameters.

- **Note 1:** For cases that need coefficients C_6 , C_8 , and C_{10} , check the literature whether accurate values are available (the higher-order coefficients C_{2n} ($n \geq 6$) can be derived by $C_{2n} = (\frac{C_{2n-2}}{C_{2n-4}})^3 C_{2n-6}$ [80]). If they are not available, C_n may be used as a potential parameter for fitting.
- **Note 2:** For ionic covalent bonding, ionic bonding, and van der Waals systems, the damping parameter χ can be set as a fitting parameter. As demonstrated in section 2, 3 and 4, it seems that χ varies from system to system and cannot be fixed as a constant.
- **Note 3:** We provide a Non-Linear Least-Squares Fitting (NLLSF) Fortran program¹ for users to determine potential parameters (For the Fortran program, we provide two examples, H_2 and Ar_2 . Go to the following web link to download the package <http://www.nehu-economics.info/Fortran-Computer-Programs-with-Help.html> The package includes input and output files). It is not a black-box code. Users need to define how many fitting parameters the potential function has and to provide the input file. For other inputs, user can use the default values.
- **Note 4:** Users may use other NLLSF program that is available. For example, Matlab and gnuplot provide functions for solving NLLSF problems.
- **Note 5:** Contact us for any problem during the fitting process.

A.2. List of Pair-Potential Parameters

In this section, the determined potential parameters for neutral covalent bonding systems studied in section 1, ionic covalent bonding systems studied in section 2, van der Waals binding systems studied in section 4, and diatomic dications studied in section 5 are listed in Table A1, A2, A3, and A4, respectively.

¹To credit one of our authors, S. K. Mishra, who developed this program, please cite the following reference: S. K. Mishra, "Performance of Differential Evolution Method in Least Squares Fitting of Some Typical Nonlinear Curves", Journal of Quantitative Economics, 5(1), 140-177 (2007).

Table A1: Potential parameters α , β , κ , and η determined for neutral covalent diatomic systems by using Eq.(1). All in atomic units

Molecule	α	β	κ	η
H ₂	1.24179616	1.91867424	0.0478910411	2.8004031
Li ₂	0.221158172	0.0981516842	0.145366735	1.19828642
B ₂	0.183899426	0.462900133	0.813404073	24.2300391
C ₂	0.127145432	0.967192362	1.89580627	28.3280362
N ₂	0.151104274	1.78382371	1.99999854	42.591009
F ₂	0.029803514	0.460794341	9.999999811	54.737768091
Si ₂	0.186283078	0.325358609	0.359889161	47.3860134
LiH	0.590929935	0.437032497	0.0488894485	11.33519
BeH	0.0439935564	0.372280509	4.997	0.93473275
LiNa	0.153370182	0.0750653157	0.225977753	0.390468193
InH	0.399432325	0.352975842	0.126597296	21.6996589
NO	0.255622994	1.40313848	1.05129052	65.1143618
HCl	0.52951669	0.941428491	0.212878625	42.6912765
OH	0.760387114	1.40066201	0.20986805	39.6142444
NH	0.641300128	1.05082101	0.269776121	27.3461228
CH	0.706575916	0.980984516	0.158091171	33.8165879
CO	0.602412105	2.49790792	0.23540789	160.846731
SiO	0.520285935	1.50404553	0.151927384	250.018351

Table A2: Potential parameters α , β , γ , η , ζ , χ and C_4 determined for ionic covalent bonding systems by using Eq.(2). R_e is from the literature data. All in atomic units

Molecule	α	β	γ	η	ζ	χ	C_4	R_e
H ₂ ⁺	1.06464516	0.921196022	2 α	3.61038634	1	2.572	4.95628851	2.0
HeH ⁺	1.94869912	2.60094136	α	1.78190656	2.04347269	2.64764358	0.709265297	2.042
He ₂ ⁺	1.5047139	2.38355439	α	1	5.25975522	0.979471616	0.624816071	2.042
BeH ⁺	1.19634826	1.41938735	α	18.5564204	0.122559941	1.18705107	3.13563906	2.476
BeH ⁻	1.16789295	1.18495346	α	12.6045998	1.26131762	2.17836477	18.4984266	2.669
LiH ⁻	0.981753027	0.981349042	α	1	3.6729584	2.39811679	64.6224785	3.153

Table A3: Potential parameters α , β , η and χ determined for van der Waals weakly binding systems using Eq.(4). R_e and C_n ($n = 6, 8, 10$) are taken from literature. All in atomic units

Molecule	α	β	η	χ	R_e	C_6	C_8	C_{10}	Literature
H ₂	1.80886753	0.80476915	19.5353848	0.94375137	7.8	6.499	124.4	3286.0	Ref. [80]
NaK	0.581007114	0.169441107	1.27758572	1.86032252	10.315	2410.0	229050.0	24680000.0	Ref. [80]
He ₂	2.34281426	1.427609211	24.9327859	0.705917281	5.613	1.461	14.11	183.5	Ref. [90]
Ne ₂	2.57804505	3.59526654	302.992153	0.898113069	5.840	6.383	90.34	1536.0	Ref. [175]
Ar ₂	1.5069144	19.2457331	126.019972	1.28100922	7.10	64.3	1623	49060	Ref. [175]
Kr ₂	1.69712234	5.28825134	246.375269	0.85643772	7.58	129.6	4187	155500	Ref. [175]
Xe ₂	1.45493289	15.1518022	248.22859	0.876419067	8.25	285.9	12810	619800	Ref. [175]
Ca ₂	0.838362902	2.96505942	21.2098198	1.75753763	8.081	2121	223000	21320000	Ref. [191]
Mg ₂	1.24946345	2.67596495	29.910735	1.34122874	7.354	627	41500	2757000	Ref. [199]
Sr ₂	0.766237652	2.72708084	21.152344	1.76518642	8.828	3103.0	379200.0	42150000.0	Ref. [193]
LiHe	1.2471927	0.100442894	7.96945502	0.931774366	11.645	22.507	1083.2	72602.1	Ref. [201]
CaHe	1.279007516	0.00616	7.690378437	0.906530719	9.64	46.8	1835	118500	Ref. [209]
LiAr	0.756392786	0.0101626292	5.01705619E-011	0.973713149	9.251	174.439002	-16211.717	648740.115	Ref. [203]
NaAr	1.05262069	6.76650021E-5	2.6312004	0.977308837	9.464	146.291942	-37301.7153	2839043.74	Ref. [204]
KAr	0.784386108	0.110425294	1.25453368	0.902759495	10.2155	813.707004	-92544.8751	5201954.29	Ref. [207]
NaKr	1.03555444	1.51652775	17.7782338	0.665157117	9.297	774.161953	-71575.4863	3137439.55	Ref. [208]
Zn ₂	0.951854441	0.845807252	5.17252173	1.65593701	7.323	359	13500	640000	Ref. [211]
Cd ₂	0.905436963	1.13619161	7.52670062	1.63815301	7.752	686	28900	1537000	Ref. [211]
Hg ₂	1.06270654	2.29004018	13.8969565	1.58681219	6.955	392	12920	537000	Ref. [217]
LiHg	1.00277412	0.884046581	4.15797715	2.08111888	5.671	443.0	25400.0	1840000.0	Ref. [80]
CdNe	1.19957532	1.63773977	11.8338502	1.06487289	8.091	31.810688	-	-	Ref. [219]
LiHe ⁻	0.651021658	0.0311407995	0.509474386	1.03618203	18.5	70.365674	6111.8844	-	Ref. [220]
HeH	1.58803424	0.579296416	3.22806569	1.22237816	6.5406	2.81	641.74	874.2	Ref. [221]
NeH	1.99549877	0.000214356648	28.3976811	0.590250099	6.4839	5.71	92.59	2007.0	Ref. [221]
AgHe	1.3969125	0.00679322993	4.4391844	0.909659481	8.669	19.75	641.3	22020.0	Ref. [225]
XeF	3.44058805	30202.8963	125046.845	1.29988247	4.3478	51.1212328	971.8541	-	Ref. [79]
KrF	1.88310506	1.326016	14.6602054	1.1394056	5.6711	35.1954218	584.676487	-	Ref. [79]

Table A4: Potential parameters α , β , γ , ζ and q determined for diatomic dications using Eq.(5). All in atomic units

Molecule	α	β	γ	ζ	q
He ₂ ⁺⁺	2.19893097	21.3316218	0.279984035	3.6828207	0.712005705
BeH ⁺⁺	0.614371674	0.883328762	0.109403265	1.64081594	2.9011314
AlH ⁺⁺	0.423212447	0.217842583	0.0280432067	6.04865744	4.3704501

Appendix B: Interatomic Pair-Potential Functions (1918-2013)

B.1. Top Pair-Potential Functions

Fig.B.1. presents the total citations of pair-potential functions developed from 1918 to 2013, and Table B.1. list top pair-potential functions based on citations². We can draw some conclusions: (1) 1918 ~ 1962, an active period for developing pair-potential functions; (2) Highly cited Weeks-Chandler-Anderson (WCA, modified Lennard-Jones) potential developed in 1971. (3) Highly cited Hartree-Fock-dispersion model developed in 1975. (4) celebrated Tang-Toennies potential developed in 1984; (5) Korona potential (modified Tang-Toennies potential) developed in 1997; (6) most functions are applied to spectroscopy; (7) Molecular simulation still uses simple, functions such as WCA potential; (8) Rydberg-London potential developed in 2004 has been cited as the reliable one in the field of molecular simulation (to be noted, as present in section 1 and section 3 for the ground-states of H_2 , Li_2 , OH , NO , Ar_2 , and Kr_2 , Rydberg-London potential is not as accurate as the potential we have developed in this work); (9) potential functions are getting more and more complicate and involve many parameters.

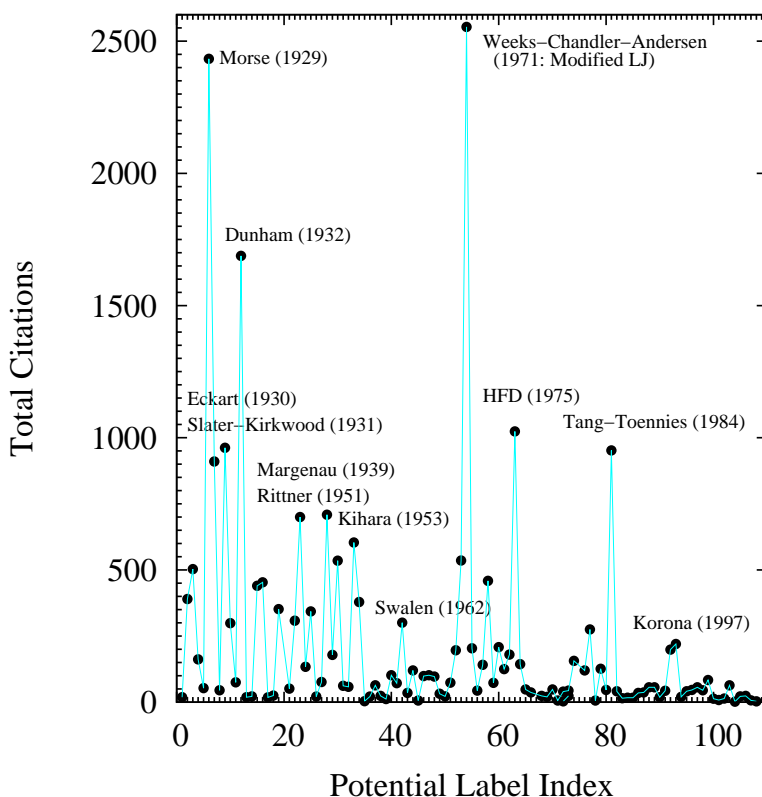


Fig.B.1.: Total citations of interatomic pair-potential functions developed from 1918 to 2013. Potential Label Index refers to the index listed in B.2 which presents the details of pair-potential functions.

²The citations for Lennard-Jones potential and some other potential functions are not accurate because they are highly cited as classical equations in textbooks. Thus, they are ignored by authors without citing them.

Table B.1.: Top pair-potential functions. Potential Label Index refers to the index listed in B.2 which list relevant potential functions developed during the period of 1918 to 2013. The citations are based on the Web of Science dated November 2013.

Potential Label Index	Potential	Year	Application Type	Total Citations
54	Weeks-Chandler-Andersen	1971	Simulation	2554
6	Morse	1929	Spectroscopy, Simulation	2433
12	Dunham	1932	Spectroscopy	1688
63	Hartree-Fock-dispersion	1975	Spectroscopy	1024
9	Slater-Kirkwood van der Waals	1931	Simulation, Spectroscopy	962
81	Tang-Toennies	1984	Spectroscopy, Simulation	952
7	Eckart	1930	Scattering	910
28	Rittner	1951	Ionic Bonding, Spectroscopy	709
23	Margenau	1939	Simulation, Spectroscopy	700
33	Rice-Hirschfelder	1954	Simulation	604
53	Barker-Fisher-Watts	1971	Simulation	536
30	Kihara	1953	Simulation	535
3	Lennard-Jones	1924	Simulation	503
58	Simon-Parr-Finlan	1973	Spectroscopy	459
16	Pekeris	1934	Spectroscopy	453
15	Pöschl-Teller	1933	Spectroscopy	440
2	Kratzer	1922	Spectroscopy	390
34	Varshni III	1957	Spectroscopy	379
19	Hellmann	1935	Spectroscopy, Ionic Bonding	352
25	Hulburt-Hirschfelder	1941	Spectroscopy	343
22	Exp-6	1938	Spectroscopy, Simulation	308
42	Swalen-Ibers	1962	Spectroscopy	301
10	Rosen-Morse	1932	Spectroscopy	299
77	Improved HFD	1982	Spectroscopy	275
93	Korona <i>et al.</i>	1997	Spectroscopy	220
60	Murrell-Sorbie	1974	Spectroscopy	208
55	Generalized Morse	1972	Spectroscopy	204
92	Modified Tang-Toennies I	1995	Spectroscopy	199
52	Exp-spline-Morse-spline-vdW	1971	Spectroscopy	196
62	Morse-van der Waals	1975	Spectroscopy	180
29	Lippincott	1953	Spectroscopy	179
4	Fues	1926	Spectroscopy	162
74	Ogilvie	1981	Spectroscopy	156
64	Perturbed Morse Oscillator	1976	Spectroscopy	144
57	Maitland-Smith	1973	Spectroscopy, Simulation	141
24	Linnett	1940	Spectroscopy	134
79	Extended Rydberg	1983	Spectroscopy	126
61	Thakkar	1975	Spectroscopy	125
76	Koide-Meath-Allnatt	1981	Spectroscopy	120
44	Varshni-Shukla II	1963	Spectroscopy, Ionic Bonding	120
40	Varshni-Shukla I	1961	Spectroscopy, Ionic Bonding	102
99	Bellert-Breckenridge	2002	Spectroscopy, Ionic Bonding	84
103	Morse-Long-Range	2006	Spectroscopy	64
97	Modified Lennard-Jones Oscillator	2000	Spectroscopy	56
98	Samuelis <i>et al.</i>	2001	Spectroscopy	45
100	Rydberg-London	2004	Simulation	13

B.2. List of Pair-Potential Functions

Advanced experimental techniques, with the help of semi-empirical or empirical analytical potential functions [112–117], provide an efficient and direct approach to determine very accurate interatomic potentials from the collected spectroscopy data. To date, many interatomic pair-potential functions have been reported. All of them can be roughly summarized in five kinds of analytical forms. The first three forms are: (i) the Dunham type expressed as a Taylor expansion of the interatomic potential $V(R)$ at the equilibrium internuclear distance R_e , (ii) suitable mathematical expressions such as Morse potential [6] that contain adjustable parameters, and (iii) direct use of polynomials such as Chebychev polynomials [106]. Since

different physical properties may be sensitive to different parts of the potential curve, a given empirical or semi-empirical potential function with parameters that are calibrated for one property, often describes other properties inadequately. The fourth form is a hybrid one such as Lennard-Jones (LJ) [3], Tang-Toennies (TT) [80], Hartree-Fock dispersion (HFD) [66], and Rydberg-London [98] potentials, which combine analytical potential functions in different interaction regions. The four forms usually focus on describing either strongly or weakly bound, covalent or ionic bound, neutral or singly-charged molecules and often lose their validity for either small or relatively large internuclear distance. The last analytical form is the one that uses piecewise analytical forms such as Exp-spline-Morse-spline-vdW (ESMSV) [51], in which different potential functions in different ranges of R are splined together to give a continuous, multi-parameter function defined for all R . Multi-parameter splined functions lack a certain uniqueness. One must make often arbitrary decisions as to where one function ends and the next begins.

In the following, we present in detail a list³ of interatomic pair-potential functions since 1918 when Born and Lande developed the Born-Lande potential function for ionic crystals. The citation number is based on the **Web of Science** dated November 2013. R , D_e , and R_e are the internuclear distance, the dissociation energy and the equilibrium distance, respectively.

1. Born-Lande Function (Year 1918): Ref. [1] Citations: 19

$$V = -\frac{1}{R} + \frac{b}{R^n}. \quad (6)$$

- Parameters: b , n
- Notes: Developed for investigating ionic crystals.

2. Kratzer Function (Year 1922): Ref. [2] Citations: 390

$$V = D_e \left(1 - \frac{R_e}{R}\right)^2 \quad (7)$$

- Parameters: D_e , R_e
- Notes: (1) Simple; (2) Kratzer (1920) considered the series of inverse powers of R and proposed above simplified formula; (3) Not applicable to molecular problems.

3. Lennard-Jones (LJ(n,m)) Potential (Year 1924): Ref. [3] Citations: 503

$$V = \frac{D_e}{n-m} \left(m \left(\frac{R_e}{R}\right)^n - n \left(\frac{R_e}{R}\right)^m \right) \quad (8)$$

- Parameter Numbers: D_e , R_e . Both n and m are usually fixed constant.
- Notes: (1) The repulsive forces dependent on the coefficient n and can be made sufficiently soft. (2) Having been used by a number of researchers to represent interatomic van der Waals potentials to hetero- and homo-nuclear complexes in a wide range of R . (3). The Lennard-Jones potential has only two parameters. (4)

³It is not a full list. This list is only based on the knowledge of the present authors and the key functions reported in the literature.

The potential diverges when two atoms approach one another. (5) Bonding has no directionality. (6) The twelfth-power term appearing in the potential is chosen for its ease of calculation for simulations and is not physically based. (7) The sixth-power term arises as a result of dipole-dipole interactions due to electron dispersion in noble gasses (London dispersion forces), but it does not represent other kinds of bonding well.

4. Fues Function (Year 1926): Ref. [4] Citations: 162

$$V = W_0 + \frac{W_1}{R} + \frac{W_2}{R^2} \quad (9)$$

- Parameters: W_0, W_1, W_2
- Notes: (1) Simple, and spectroscopy only. (2) It is actually a special case of Kratzer function (1922). (3) It is known to be a reasonably good representation of potential-energy curves for diatomic molecules for R near R_e , in spite of the fact that at first glance the R^{-1}, R^{-2} dependence of the potential seems overly strongly for covalently bonded systems. (4) The force constants predicted by this potential are surprisingly accurate. The predictions are quantitatively as good as calculations with Hartree-Fock wavefunctions.

5. Mecke-Sutherland Function (Year 1927): Ref. [5] Citations: 53

$$V = -\frac{a}{R^m} + \frac{b}{R^n} \quad (10)$$

- Parameters: a, b, m, n .
- Note: (1) Sometimes, a fifth parameter d is introduced by putting $R - d$ for R ; (2) Used to describe minima due to valence interactions as well as those due to van der Waals interaction; (3) It appears that for series of related molecules, m and n can be held constant.

6. Morse Potential (Year 1929): Ref. [6] Citations: 2433

$$V = D_e \left(1 - e^{-\alpha(R-R_e)}\right)^2 - D_e \quad (11)$$

- Parameters: D_e, R_e, α
- Notes: (1) Simple; (2) Spectroscopy and Simulation; (3) Its frequent use is due to the fact that the vibrational levels may be exactly calculated, and with reasonable values for the parameters D_e, α , and R_e , agree fairly well with observation for many molecules; (3) $V(R)$ not approaching to a finite value as R approaches zero; (4) Morse potential falls off too fast at large R ; (5) It cannot be adopted to give a more accurate fit; (6) It cannot be made to faithfully reproduce the potential curve shape in both short- and long-range limits; (7) Not suitable for using for a randomly chosen molecule.

7. Eckart Function (Year 1930): Ref. [7] Citations: 910

$$V = -abe^{-bR} \left(ae^{-bR} + 1 \right)^{-2} \quad (12)$$

- Parameters: a,b
- Notes: (1) Representing pure attraction or going through a minimum; (2) It is of interested in scattering problems since the $l = 0$ phase shift can be given in a closed form.

8. Rydberg Function (Year 1931): Ref. [8] Citations: 45

$$V = -D_e (1 + b(R - R_e)) e^{-b(R-R_e)} \quad (13)$$

- Parameters: D_e, R_e, b
- Notes: (1) Giving better performance than Morse or Hulburt-Hirschfelder function; (2) $V(R)$ goes to a finite value as $R \rightarrow 0$; (3) spectroscopy only; (4) Until the 1970's, it was received full attention and modified Rydberg function was developed, for example, Murrell-Sorbie (#60, 1974), extended Rydberg function I (# 79, 1983) and II (# 80, 1984).

9. Slater-Kirkwood van der Waals Function (Year 1931): Ref. [9] Citations: 962

$$V = -\frac{C_6}{R^6} \quad (14)$$

- Parameter: C_6
- Notes: (1) It was recognized that the van der Waals forces in gases have their origin in a mutual polarization of the molecules⁴; (2). A calculation of van der Waal's potential of two atoms at large separation was carried out for hydrogen and helium; (3) By means of above formula, the van der Waals cohesive pressure constant was calculated for Ne, A, N₂, H, O₂, and CH₄.

10. Rosen-Morse Function (Year 1932): Ref. [10] Citations: 299

$$V = A \tanh\left(\frac{R}{d}\right) - C \operatorname{sech}^2\left(\frac{R}{d}\right) \quad (15)$$

- Parameters: A, d, C
- Notes: (1) Simple; (2) $V(R)$ goes to a finite value as $R \rightarrow 0$; (3) For hydrogen halides, it gives results no better than Morse function; (4) see modified Rosen-Morse function (# 109, 2012).

11. Davidson Function (Year 1932): Ref. [11] Citations: 75

$$V = A \left(\frac{R}{R_e} - \frac{R_e}{R} \right)^2 \quad (16)$$

- Parameters: A, R_e
- Notes: (1) $k_e R_e^2 = 8A$ which is satisfied by ground states of hydrogen halides; (2) $V(R)$ does not go to a finite value as $R \rightarrow \infty$; (3) Spectroscopy only.

⁴The idea was suggested by Debye [see, Debye, Phys. Zeits. 21, 178 (1920)], but his calculation of intermolecular energies, based upon an electrostatic molecular model, did not meet with great success

12. Dunham Function (Year 1932): Ref. [12]..... Citations: 1688

$$V = a_0 \zeta^2 \left(1 + a_1 \zeta + a_2 \zeta^2 + a_3 \zeta^3 + \dots \right) \quad (17)$$

where $a_0 = \frac{\omega_e^2}{4B_e}$ and $\zeta = (R - R_e)/R_e$.

- Parameters: $R_e, a_0, a_1, a_2, \dots, a_n$.
- Notes: (1) widely used for spectroscopy analysis; (2) The expansion cannot converge for $R > 2R_e$; (3) Blow up as R approaches ∞ .

13. Born-Mayer Function (Year 1932): Ref. [13]..... Citations: 19

$$V = be^{-R/\sigma} - \frac{1}{R} \quad (18)$$

- Parameters: b, σ
- Notes: (1) Developed for alkali halide crystals; (2) Actually, the repulsive part $be^{-R/\sigma}$ has been widely used in later model potentials such as Buckingham (Exp-6) (#22, 1938), Rittner potential (#28, 1951), Hartree-Fock dispersion potential (#63, 1973), Tang-Toennies potential (#81, 1984), and so on.

14. Manning-Rosen-Newing Function (Year 1933): Ref. [14]..... Citations: 22

$$V = -\frac{Be^{-R/d} + Ce^{-2R/d}}{(1 - e^{-R/d})^2} \quad (19)$$

- Parameters: B, C, d
- Notes: (1) Simple; (2) Spectroscopy only; (3) Dissociation energy greater than that given by Morse function; (4) Giving $\omega_e \chi_e$ higher value.

15. Pöschl-Teller Function (Year 1933): Ref. [15]..... Citations: 440

$$V = A \operatorname{cosech}^2[\alpha(R - R_e)] - B \operatorname{sech}^2[\alpha(R - R_e)] \quad (20)$$

- Parameters: A, B, R_e, α
- Notes: (1) Simple; (2) Spectroscopy only; (3) Slightly superior to the Morse function.

16. Pekeris Potential (Year 1934): Ref. [16]..... Citations: 453

$$V = D_e \left(1 - e^{-\alpha(R - R_e)} \right)^2 + A \left(\frac{R_e}{R} \right)^2 \quad (21)$$

- Parameters: D_e, R_e, α, A
- Notes: (1) Add a centrifugal term to the Morse function; (2) Spectroscopy only.

17. Hylleraas Function (Year 1935): Ref. [17]..... Citations: 18

$$V = D_e \left(1 - \frac{(1+a)(1+c)(z+b)}{(z+a)(z+c)(1+b)} \right)^2 - D_e \quad (22)$$

with $z = e^{2(1+k)\beta(R - R_e)/R_e}$ and $\frac{1}{1+k} = \frac{1}{1+65} + \frac{1}{1+c} - \frac{1}{1+b}$.

- Parameters: a, b, c, R_e, D_e, β .
- Notes: (1) Giving Morse function for $a = b, c = 0$; (2) Giving Pöschl-Teller function for $k = 0$; (3) Difficult to determine 6 parameters; (4) Spectroscopy only.

18. Huggins Potential (Year 1935): Ref. [18] Citations: 25

$$V = ce^{-\alpha(R-R_{12})} - c'e^{-\alpha'(R-R_e)} \quad (23)$$

- Parameters: $\alpha, \alpha', c, c', R_e, R_{12}$.
- Notes: (1) The parameter α and R_{12} are chosen according to the inner-shell structure of the atom involved, and the others are determined from experiments; (3) This is a modified Morse function; (3) The resulting curve seems valid over a wider range of R than the unmodified Morse curve; (4) It can be used to justify Badger's rule; (5) Giving small values for higher anharmonicities and thus fail for cases where they are not small; (6) Spectroscopy only.

19. Hellmann Potential (Year 1935): Ref. [19] Citations: 352

$$V = A \frac{e^{-\alpha R}}{R} - \frac{1}{R} \quad (24)$$

- Parameters: A, α
- Notes: (1) Developed for ionic bonding; (2) Repulsive part is described by a Pauli repulsive term.

20. Wasastjerna Potential (Year 1935): Ref. [20] Citations: 0

$$V = CR^7 e^{-\beta R} - \frac{1}{R} \quad (25)$$

- Parameters: C, β
- Notes: Developed for Na, K, Rb and Cs halide crystals.

21. Morse Oscillators (Year 1938): Ref. [21] Citations: 51

$$V = D_e \sum_{n \geq 2} C_n (1 - e^{-\alpha(R-R_e)})^n \quad (26)$$

- Parameters: $D_e, R_e, \alpha, C_n (n \geq 2)$
- Notes: (1) Flexible; (2) Spectroscopy only; (3) Difficult to determine the parameter α ; (4) Losing its significance as taking more terms.

22. Buckingham (Exp-6) Potential (Year 1938): Ref. [22] Citations: 308

$$V = Ae^{-bR} - \frac{C_6}{R^6} \quad (27)$$

- Parameters: A, b, C_6

- Notes: (1) The generalized Ae^{-bR} exponent form introduced by Born and Mayer in 1932 for crystal forces, has been most frequently used in representations of short-range interatomic energy. (2) The Buckingham potential has been used extensively in simulations of molecular dynamics discussing the properties of rare gases; (3) Although the exponential term rises steeply as R decreases, it remains finite at $R = 0$, so the dispersion term dominates at very small R , and the potential reaches a maximum at a smaller value of R , and then tends to $-\infty$ as R approaches 0.

23. Margenau Function (Year 1939): Ref. [23] Citations: 700

$$V = ae^{-bR} - ce^{-dR} - \frac{e}{R^6} - \frac{f}{R^8} \quad (28)$$

- Parameter: a, b, c, d, e, f
- Notes: (1) Its purpose is to investigate the fundamental question concerning the additivity of first-order exchange and second-order van der Waals potentials; (2) It shows that the value of the dipole-dipole coefficient in the Slater-Kirkwood formula (#9, 1931) has been too high; (3) Highly cited as a model potential for studying van der Waals complexes; (4) Spectroscopy and simulation.

24. Linnett Function (Year 1940): Ref. [24] Citations: 134

$$V = \frac{a}{R^m} - be^{-nR} \quad (29)$$

- Parameters: $a > 0, m, n, b > 0$.
- Notes: (1) Buckingham (1938) and Margenau (1939) use this function with negative a and b for the rare gases. (2) Representing a valence attraction and an electrostatic repulsion; (3) Capable of giving rise to a low maximum between $R = R_e$ and $R \rightarrow \infty$.

25. Hulburt-Hirschfelder Function (Year 1941): Ref. [25] Citations: 343

$$V = D_e \left((1 - e^{-x})^2 + cx^2 e^{-2x} (1 + bx) \right) \text{ with } x = \frac{\omega_e}{2\sqrt{B_e D_e}} \frac{R - R_e}{R_e}; \quad (30)$$

- Parameters: $B_e, D_e, R_e, \omega_e, c, b$
- Notes: (1) b and c are simple algebraic functions of the five spectroscopic constants; (2) A great advantage is that the five parameters can be readily obtained from the study of band spectrum; (3) Not satisfactory in the region of $R < R_e$; (4) Spectroscopy only.

26. Wu-Yang Potential (Year 1944): Ref. [26] Citations: 21

$$V = a e^{-mR} - \frac{b}{R^n} \quad (31)$$

- Parameters: a, m, n, b
- Notes: (1) $V(R)$ is not a finite value as $R \rightarrow \infty$; (2) $V(R)$ goes to $-\infty$ as $R \rightarrow 0$; (3) Spectroscopy only.

27. Modified Buckingham-type Potential (Year 1947): Ref. [27] Citations: 76

$$V = Ae^{-bR} - \frac{C_6}{R^6} - \frac{C_8}{R^8} \quad (32)$$

- Parameters: A, b, C_6, C_8
- Notes: (1) The generalized Ae^{-bR} exponent form introduced by Born and Mayer in 1932 for crystal forces, has been most frequently used in representations of short-range interatomic energy; (2) This Buckingham potential has been used extensively in simulations of molecular dynamics; (3) Although the exponential term rises steeply as R decreases, it remains finite at $R \rightarrow 0$, the dispersion term dominates at very small R , the potential reaches a maximum, and then tends to $-\infty$ as R approaches 0; (4) Spectroscopy only.

28. Rittner Potential (Year 1951): Ref. [28] Citations: 709

$$V = Ae^{-R/\rho} - \frac{C}{R^6} - \frac{1}{R} - \frac{\alpha_+ + \alpha_-}{2R^4} - \frac{2\alpha_+\alpha_-}{R^7} \quad (33)$$

- Parameters: $A, \rho, C, \alpha_+, \alpha_-$
- Notes: (1) Developed for ionic bonding such as alkali halide and hydride molecules; (2) when applied to other diatomic molecules, the results have been unsatisfactory.

29. Lippincott Function (Year 1953): Ref. [29] Citations: 179

$$V = D_e \left(1 - e^{-n(R-R_e)^2/(2R)}\right) (1 + af(R)) \quad (34)$$

- Parameters: D_e, n, R_e, a
- Notes: (1) Useful in predicting unknown bond dissociation energies and anharmonicity constants for both diatomic and polyatomic molecules; (2) Spectroscopy only.

30. Kihara Potential (Year 1953): Ref. [30] Citations: 535

$$V = 4\epsilon \left[\left(\frac{\sigma - 2^{-1/6}\rho}{R - \rho} \right)^{12} - \left(\frac{\sigma - 2^{-1/6}\rho}{R - \rho} \right)^6 \right] \quad R \geq \rho; \\ = \infty \quad R < \rho. \quad (35)$$

- Parameters: ϵ, σ, ρ
- Notes: (1) It is a modified Lennard-Jones potential; (2) It has been claimed that this potential function is the best three-parameter potential⁵

31. Frost-Musulin Function (Year 1954): Ref. [31] Citations: 62

$$V = e^{-aR} \left(\frac{1}{R} - b \right) \quad (36)$$

⁵R.D. Weir, Mol. Phys. 11, 97 (1966)

- Parameters: a, b
- Notes: (1) Use Pauli-type repulsive term; (2) Spectroscopy only; (3) Satisfactory results for H_2^+ and H_2 .

32. Maitland-Smith Function (Year 1954): Ref. [32] Citations: 58

$$V = \frac{D_e}{n - m} \left(m e^{n(1-R/R_e)} - n(R_e/R)^m \right) \quad (37)$$

When $m = 6$, it turns to be Exp-6 potential model .

- Parameters: $D_e, R_e,$
- Notes: (1) Generalized Buckingham-type potential; (2) For $m = 6$, it turns to be Exp-6 potential; (3) Spectroscopy only.

33. Rice-Hirschfelder Potential (Year 1954): Ref. [33] Citations: 604

$$V = \frac{\epsilon}{1 - 6/\alpha} \left(\frac{6}{\alpha} e^{\alpha - \frac{\alpha R}{\sigma}} - \left(\frac{\sigma}{R} \right)^6 \right); \quad R > \sigma$$

$$= \infty \quad R \leq \sigma \quad (38)$$

- Parameters: $\epsilon, \alpha, \sigma.$
- Notes: (1) This is actually a modification of exp-6 potential; (2) Useful for second virial coefficient calculation.

34. Varshni III Function (Year 1957): Ref. [34] Citations: 379

$$V = D_e \left(1 - \frac{R_e}{R} e^{-\beta(R^2 - R_e^2)} \right)^2 \quad (39)$$

- Parameters: D_e, R_e, β
- Notes: (1) Spectroscopy only; (2) More accurate than Morse potential; (3) Not applied to a wide range of R .

35. Modified Frost-Musulin Function (Year 1957): Ref. [35] Citations: 4

$$V = e^{-aR} \left(\frac{c}{R} - b \right) \quad (40)$$

- Parameters: a, b, c
- Notes: (1) Satisfactory results for H_2^+ and H_2 ; (2) For hydrides and homonuclear molecules, the predicted third and fourth derivatives of $V(R)$ at R_e were not better than Morse function; (3) Spectroscopy only.

36. Frost-Woodson Function (Year 1958): Ref. [36] Citations: 21

$$V = \frac{c'}{R} + (c - c') \frac{e^{-aR}}{R} + U(R) \quad (41)$$

where $U(R)$ is supposed to include exchange and dispersion energies.

- Parameters: c' , c , a , and the coefficients in $U(R)$.
- Notes: (1) Previously proposed for covalent diatomic molecules and extended to apply to ionic molecules and to interaction of inert gas atoms; (2) A useful prediction of the dissociation energy and internuclear equilibrium distance of ionic molecules; (3) Spectroscopy only.

37. Buckingham Repulsive Function (Year 1958): Ref. [37] Citations: 64

$$V = (Z_A Z_B) p(R) \frac{e^{-\alpha R}}{R} \quad (42)$$

with $p(R) = 1 + \sum_{k=1} p_k R^k$

- Parameters: α , Z_A , Z_B , p_1 , p_2 , ..., p_k .
- Notes: (1) Developed for repulsive interaction only; (2) The region of R in which the van der Waals interaction dominates is not well represented; (3) The coefficients p_i are not arbitrary.

38. Simplified Rittner Potential (Year 1960): Ref. [38] Citations: 24

$$V = A e^{-R/\rho} - C/R^6 - 1/R - \alpha_{ave}/R^4 \quad (43)$$

- Parameters: A , ρ , α_{ave} , C .
- Notes: (1) a simplified version of Rittner potential; (2) ionic bonding

39. Rittner-Lawley Potential (Year 1961): Ref. [39] Citations: 12

$$V = A e^{-R/\rho} - \frac{C}{R^6} - \frac{1}{R} - \frac{\alpha_+ + \alpha_-}{2R^4} - \frac{2\alpha_+ \alpha_-}{R^7} - \frac{L}{R^{10}} \quad (44)$$

- Parameters: A , ρ , C , α_+ , α_- , L .
- Notes: Developed for ionic bonding only.

40. Varshni-Shukla I Potential (Year 1961): Ref. [40] Citations: 102

$$V = B e^{-kR^2} - \frac{1}{R} \quad (45)$$

- Parameters: B , k
- Notes: (1) Simple; (2) Developed for ionic bonding only.

41. Woolley Function (Year 1962): Ref. [41] Citations: 72

$$R/R_e = 1 + (V/D_e)^{1/2} \left(1 + \sum_{n=1} c_n (V/D_e)^{n/2} \right) \quad (46)$$

- Parameters: R_e , D_e , c_1 , ..., c_n .
- Notes: (1) This is an equivalent form of Sanderman (1940); (2) Such a process of root-taking gives fairly simple results for the Morse function $R/R_e = 1 - a^{-1} \ln[1 - (V/D_e)^{1/2}]$ and for the Lennard-Jones 12,6 potential, $R/R_e = [1 - (V/D_e)^{1/2}]^{-1/6}$.

42. Swalen-Ibers Function (Year 1962): Ref. [42]..... Citations: 301

$$V = \frac{1}{2}ax^2 + \frac{1}{2}bx^4 + v_0e^{-cx^2} \quad (47)$$

- Parameters: a, b, c, v_0 .
- Notes: Developed only for a symmetric double well potential.

43. Clinton Function (Year 1962): Ref. [43]..... Citations:35

$$V = \lambda_1 \ln(\lambda_2 R) / R^{\lambda_3} \quad (48)$$

- Parameters: $\lambda_1, \lambda_2, \lambda_3$
- Notes: (1) Spectroscopy only; (2) Yielding a considerably better potential curve than the Morse potential curve; (3) Having some theoretical foundation.

44. Varshni-Shukla II Function (Year 1963): Ref. [44]..... Citations: 120

$$V = A \frac{e^{-\alpha R}}{R^2} - \frac{1}{R} \quad (49)$$

- Parameters: A, α
- Notes: Developed only for ionic bonding.

45. Preuss Function (Year 1964): Ref. [45]..... Citations: 6

$$V = V(\infty) + \frac{Z_A Z_B}{R} + (E_0 - V(\infty)) \frac{\sum_{k=0}^{m-1} c_k R^k}{\sum_{l=0}^m d_l R^l} \quad (50)$$

with $c_0 = d_0 = 1$.

- Parameters: $c_1, c_2, \dots, c_{m-1}, d_1, d_2, \dots, d_m$.
- Notes: (1) Deriving a highly accurate curve for H_2 with 17 parameters and $m = 9$. (2) Very limited application. (3) Spectroscopy only.

46. Varshni-Shukla III Potential (Year 1965): Ref. [46]..... Citations: 99

$$V = AR^n e^{-\alpha R} - \frac{1}{R} \quad (51)$$

- Parameters: A, α .
- Notes: (1) A generalized function for ionic bonding; (2) When $n = -1, -2, 7$, it turns to Hellman, Varshni-II, and Wassastijerna potentials, respectively.

47. Varshni-Shukla IV Potential (Year 1965): Ref. [46]..... Citations: 99

$$V = B e^{-kR^p} - \frac{1}{R} \quad (52)$$

- Parameters: B, k, p

- Notes: (1) Developed for ionic bonding; (2) when $p = 2$, it turns to Varshni-Shukla I potential.

48. Waech-Bernstein Function (Year 1967): Ref. [47] Citations: 97

$$V = \sum_{n=0}^{32} a_n \left(\frac{R-5}{2.5} \right)^n \quad (53)$$

- Parameters: a_0, a_1, \dots, a_{32} .
- Notes: (1) Adequately describe all bound and quasi-bound states of $\text{H}_2(^1\Sigma_g^+)$. (2) Spectroscopy only.

49. Parr-White Function (Year 1968): Ref. [48] Citations: 32

$$V(\lambda) = w_0 + \sum_{n=1}^{\infty} (w_n - w_{n-1}) \lambda^n \quad (54)$$

where $\lambda = 1 - \frac{R_e}{R}$.

- Parameters: $R_e, w_0, w_1, \dots, w_n$.
- Notes: (1) This is an extension of Fues potential (# 4, 1926); (2) The quantities w_n are obtained simply as perturbation energies for a purely kinetic-energy perturbation at R_e . (3) Giving a simple physical interpretation to the coefficients of Fues potential, and also a derivation of the inverse power series by perturbation theory.

50. Redington Function (Year 1970): Ref. [49] Citations: 22

$$V = A_1 e^{-R/\rho} + A_2 e^{-R/(2\rho)} + A_3 e^{-R/(3\rho)} - \left(\frac{1}{R} + \frac{\alpha_1 + \alpha_2}{2R^4} + \frac{2\alpha_1\alpha_2}{R^7} \right) - \frac{C_6}{R^6} \quad (55)$$

- Parameters: $A_1, A_2, A_3, \rho, \alpha_1, \alpha_2, C_6$.
- Notes: (1) Developed for ionic bonding; (2) Good for dissimilar ions, such as LiI, CsF.

51. M-6-8 Potential (Year 1970): Ref. [50] Citations: 74

$$V = \frac{A}{R^m} - \frac{C_6}{R^6} - \frac{C_8}{R^8} \quad (56)$$

- Parameters: A, m, C_6, C_8
- Notes: (1) A four-parameter potential; (2) Developed for several fluids. (3) Better than some more complex functions due to the addition of the eighth power attraction. (4) Spectroscopy only.

52. Exp-spline-Morse-spline-vdW (ESMSV) (Year 1971): Ref. [51] Citations: 196

$$\begin{aligned} f(x) &= V(R)/D_e; x = R/R_e; & (57) \\ f &= A e^{-\alpha(x-1)}, & 0 < x \leq x_1; \\ f &= e^{a_1+(x-x_1)(a_2+(x-x_2)(a_3+(x-x_3)a_4))}, & x_1 < x < x_2; \\ f &= e^{-2\beta(x-1)} - 2e^{-\beta(x-1)}, & x_2 \leq x \leq x_3 \\ f &= b_1 + (x-x_3)(b_2 + (x-x_4)(b_3 + (x-x_3)b_4)), & x_3 < x < x_4; \\ f &= -c_6x^{-6} - c_8x^{-8} - c_{10}x^{-10}, & x_4 \leq x < \infty \end{aligned}$$

- Parameters: $D_e, R_e, A, \alpha, \beta, x_1, x_2, x_3, x_4, c_6, c_8, c_{10}, a_1, a_2, a_3, a_4, b_1, b_2, b_3, b_4$
- Notes: (1) Use cubic spline functions to join the various pieces of the potential; (2) Involve many parameters; (3) Spectroscopy only.

53. Barker-Fisher-Watts Function (Year 1971): Ref. [52] Citations: 536

$$V = e^{\alpha(1-R/R_e)} \sum_{k=0}^5 A_k \left(\frac{R}{R_e} - 1 \right)^k - \sum_{n=6,8,10} \frac{C_n}{\delta + (R/R_e)^n} \quad (58)$$

- Parameters: $R_e, \alpha, \delta, A_0, A_1, A_2, A_3, A_4, A_5, C_6, C_8, C_{10}$
- Note: (1) δ is a small non-physical parameter introduced to suppress the spurious singularity that would otherwise arise at $R \rightarrow 0$. (2) Highly accurate interatomic potential; (3) Specific to the noble gases such as Kr_2 ; (4) Spectroscopy only. Xe_2 .

54. Weeks-Chandler-Anderson (WCA) Function (Year 1971): Ref. [53] Citations: 2554

$$\begin{aligned} V &= 4\epsilon \left(\left(\frac{\sigma}{R} \right)^{12} - \left(\frac{\sigma}{R} \right)^6 \right) + \epsilon & R \leq 2^{1/6}\sigma; \\ &= 0 & R > 2^{1/6}\sigma \end{aligned} \quad (59)$$

- Parameters: σ, ϵ
- Notes: (1) A modified Lennard-Jones potential; (2) Compared with the Lennard-Jones potential, it is extremely short ranged so it can save considerable simulation time than the long ranged Lennard-Jones potential; (3) Compared with the hard-sphere potential, it is continuous and softer so it is more realistic than ideal; (4) As the transport properties of fluids are dominated by repulsive interactions, the essential physics is still retained by the WCA potential; (5) Not good for Xe_2 .

55. Generalized Morse Function (Year 1972): Ref. [54] Citations: 204

$$V = D_e \left(1 - e^{-\beta(R)(R-R_e)} \right)^2 - D_e \quad (60)$$

with $\beta(R) = \beta_0[1 + \gamma(R - R_e) + \lambda(R - R_e)^2]$

- Parameters: $D_e, R_e, \beta_0, \gamma, \lambda$
- Notes: (1) Better than Morse potential providing an adequate representation of the diatomic curves over the range of internuclear distances; (2) Spectroscopy only.

56. Morse-6 Hybrid Potential (Year 1972): Ref. [55] Citations: 44

$$\begin{aligned} V &= 4\epsilon(y^2 - y) & R \leq q_n; \\ &= -C_6/R^6 & R > q_n \end{aligned} \quad (61)$$

with $y = \exp[c(1 - R/\sigma)]$, where q_n is the internuclear separation at which the two potential pieces are joined together.

- Parameters: $\sigma, \epsilon, C_6, c, q_n$.

- Notes: (1) The subscript n on q denotes the order of the contact between the two forms. If $n = 0$, the potential is guaranteed only to be continuous at $R = q_0$; $n \geq 1$ means that the potential and its first n derivatives (with respect to R) are continuous at $R = q_n$. (2) As good as the very flexible Barker-Pompe-Bobetic empirical potential. (3) Spectroscopy only.

57. Maitland-Smith (n_0, n_1) Function (Year 1973): Ref. [56] Citations: 141

$$V = \frac{D_e}{n-6} \left[6 \left(\frac{R_e}{R} \right)^n - n \left(\frac{R_e}{R} \right)^6 \right] \quad (62)$$

with $n = n_0 + n_1 \left(\frac{R}{R_e} - 1 \right)$.

- Parameters: n_0, n_1, R_e, D_e .
- Notes: (1) There is one restriction concerning relation between the n_0 and n_1 coefficients. (2) If the requirement $V(R \rightarrow 0) \rightarrow \infty$ is to be satisfied, the condition $n_0 \geq n_1$ has to be fulfilled. Otherwise, $n_0 \leq n_1$, at very small R , the function reaches a maximum and then tends to $-\infty$ as R Approaches 0.

58. Simon-Parr-Finlan Potential (Year 1973): Ref. [57] Citations: 459

$$V = a \left(\rho^2 + \sum_{j=3} b_j \rho^j \right) \quad (63)$$

with $\rho = (R - R_e)/R$

- Parameters: $a, R_e, b_3, b_4, \dots, b_n$
- Note: (1) The procedure is similar to the well-known Dunham method except that the expansion parameter is $(R - R_e)/R$ instead of $(R - R_e)/R_e$. The new expansion, which has a formal theoretical basis, is shown to be superior in terms of both rate of convergence and region of convergence. (2) Extend to polyatomic molecules; (3) Blow up at $R = 0$.

59. Pade Approximation (Year 1974): Ref. [58] Citations: 73

$$V = [2, 2] = \frac{d_1 \zeta^2}{1 + e_1 \zeta + e_2 \zeta^2} \quad (64)$$

with $\zeta = (R - R_e)/R_e$.

- Parameters: R_e, d_1, e_1, e_2 .
- Notes: Good for ionic bonds.

60. Murrell-Sorbie Function (Year 1974): Ref. [59] Citations: 208

$$V = -D_e (1 + a_1 R + a_2 R^2 + a_3 R^3) e^{-a_1 R} \quad (65)$$

- Parameters: D_e, a_1, a_2, a_3 .

- Notes: (1) a_1 , a_2 and a_3 are obtained from the harmonic, cubic and quartic force constants. (2) This potential is superior to the Hulburt-Hirschfelder potential when tested on a least-squares basis against the spectroscopic RKR potential. (3) Successfully representing singly charged diatomic ions. (4) Not satisfactory for double charged diatomic ions.

61. Thakkar Potential (Year 1975): Ref. [63]..... Citations: 125

$$V = a \left(\rho^2 + \sum_{j=3} b_j \rho^j \right) \quad (66)$$

with $\rho = s(p)(1 - (R_e/R)^p)$, where p is non-zero real number, and $s(p) = 1$ if $p > 0$, and $s(p) = -1$ for $p < 0$.

- Parameters: a , p , R_e , b_3 , b_4 , ..., b_n .
- Notes: (1) If $p = -1$, the Thakkar potential coincides with the Dunham potential, and if $p = 1$, it coincides with the Simons-Par-Finlan potential. (2) It is superior to Dunham function or the Simons-Parr-Finlan function. (3) It is roughly as good as the Huffaker function or an RKR potential. (4) An expansion in a series of Lennard-Jones functions. (5) One fault of this function is occasional nonphysical behavior at the repulsive wall.

62. Morse-van der Waals Potential(Year 1975): Ref. [64]..... Citations: 180

$$V = D_e \left(e^{-B(R-R_e)} - 1 \right)^2 - D_e - C_6 \left(1 - e^{-(R/R_c)^{12}} \right) \left(\frac{R_c}{R} \right)^6. \quad (67)$$

- Parameters: B , D_e , R_c , R_e , C_6 .
- Notes: (1) Successfully applied to van der Waals complexes; (2) Spectroscopy only.

63. Hartree-Fock-dispersion (HFD) Potential (Year 1975): Ref. [66]..... Citations: 1024

$$V = A e^{-\alpha R - \beta R^2} - F(R) \sum_{n=3}^5 C_{2n} R^{-2n} \quad (68)$$

with $F(R) = e^{-(DR^{-1}-1)^2}$ for $R < D$ and $F(R) = 1$ for $R \geq D$.

- Parameters: A , α , β , D , C_6 , C_8 , C_{10}
- Notes: (1) Proposed originally by Hepburn *et al.* (1975) and modified slightly by Ahlrichs *et al.* (1977); (2) The Hartree-Fock part is obtained by SCF calculation and uses Born-Mayer repulsion function to fit the SCF energy. (3) Successfully applied to van der Waals complexes. (4) Spectroscopy only.

64. Perturbed Morse Oscillator (PMO) (Year 1976): Ref. [65]..... Citations: 144

$$V = D_e \left((1 - e^{-aq})^2 + b_4(1 - e^{-aq})^4 + b_5(1 - e^{-aq})^5 + \dots \right) \quad (69)$$

with $q = R - R_e$.

- Parameters: $D_e, R_e, a, b_4, b_5, \dots$
- Notes: (1) Spectroscopy only; (2) a suitable representation of rotating vibrators; (3) Suitable for fitting potentials with a minimum and a centrifugal type barrier.

65. Wicke-Harris Potential (Year 1976): Ref. [60] Citations: 48

$$V = D_e \left(1 - e^{-B(R-R_e)}\right)^2 + Ae^{-C(R-R_g)^2}. \quad (70)$$

- Parameters: D_e, R_e, A, B, C, R_g .
- Notes: (1) Limited to an unsymmetric double minimum potential; (2) Spectroscopy only.

66. Eaker-Parr Function (Year 1976): Ref. [61] Citations: 37

$$V = D_e e^{-a\beta x} \pm af(x)e^{-\beta x} \quad (71)$$

with $f(x) = (1 - bx)e^{bx(2-bx)/2}$ and $x = R - R_e$.

- Parameters: a, b, R_e, D_e, β
- Notes: (1) When $a = 2$ and $b = 0$, the function reduces to the usual Morse (–) and anti-Morse (+) function. (2) The local minimum occurs at $R = R_e$, and a local maximum (if any) occurs at $R > R_e$. (3) When this function is used, it forces a local maximum (albeit small) even if there is none in the original curve. (4) Spectroscopy only.

67. Schubert-Certain Function (Year 1977): Ref. [62] Citations: N/A

$$V = D_e \left(1 - \frac{R_e}{R} e^{-\beta(R^p - R_e^p)}\right)^2 - D_e \quad (72)$$

- Parameters: D_e, R_e, β, p ,
- Notes: (1) Successful applied to H_2 ($X^1 \Sigma_g^+$) and CH ($X^1 \Sigma^+$). (2) Spectroscopy only.

68. Kafri-Berry Function (Year 1977): Ref. [67] Citations: 24

$$V = D_e \left(1 - (R_e/R)e^{-\beta(R^p - R_e^p)}\right)^2 - D_e \quad (73)$$

with $\beta = \beta_0(1 + F(R - R_e))$, where $F(x) = b_0 e^{-b_1(x-b_2)^2}$. One set of (b_0, b_1) for $x < 0$ and another set for $x > 0$.

- Parameters: $D_e, R_e, \beta_0, b_0, b_1, b_2$
- Notes: (1) Since the Morse potential for the ground state of H_2 is a poor fit to the accurate potential at $R < R_e$ and even deviates significantly at long range ($> 2\text{\AA}$), Kafri and Berry proposed this function for solving the inadequacies of the Morse function. (2) Spectroscopy only.

69. Exp-Z4 Function (Year 1977): Ref. [68] Citations: 20

$$V = Ae^{-BR} - Z^2\alpha/(2R^4) \quad (74)$$

where α is the polarizability.

- Parameters: A, B, Z, α
- Notes: (1) Developed only for neutral-ionic interactions. (2) Spectroscopy only.

70. Engelke Potential (Year 1978): Ref. [69] Citations: 48

$$V = a \left(\rho^2 + \sum_{j=3} b_j \rho^j \right) \quad (75)$$

with $\rho = s(p)[1 - ((R/R_e + \beta)/(1 + \beta))^{-p}]$.

- Parameters: $R_e, a, p, \beta, b_3, \dots, b_n$.
- Notes: (1) For $\beta > 0$, if $p > 0$, ρ has no singularities on $0 \leq R \leq \infty$; (2) Not offer any advantage over the traditional series expansions. (3) Spectroscopy only.

71. Kafri Function (Year 1979): Ref. [70] Citations: 6

$$V = D_e \left(1 - \frac{R_e}{R} e^{-\beta(R^p - R_e^p)} \right)^2 - D_e \quad (76)$$

with $\beta = \beta_0(1 + F(R - R_e))$, where $F(x) = A_1 e^{-\beta_1 x}$ for $x < 0$ and $F(x) = (A_2 + A_3 x) e^{-\beta_2(x-x_0)^2}$ for $x \geq 0$.

- Parameters: $D_e, R_e, \beta_0, \beta_1, \beta_2, p, A_1, A_2, A_3$.
- Notes: (1) An improved version for Kafri-Berry function (#68, 1977). (2) Spectroscopy only.

72. Beckel Function (Year 1980): Ref. [71] Citations: 40

$$V[L/N] = \frac{p_0 + p_1 R + \dots + p_L R^L}{1 + q_1 R + \dots + q_N R^N} \quad (77)$$

with free polynomial degree L and $N = L + 6$

- Parameters: $L, p_0, p_1, \dots, p_L, q_1, q_2, \dots, q_{L+6}$.
- Notes: (1) Yielding accurate results in the extrapolated region. (2) The value of L in $[L/N]$ is constrained, based on the long-range behavior of the potential. (3) Spectroscopy only.

73. Mattera *et al* Function (Year 1980): Ref. [72] Citations: 44

$$V = a \left(\rho^2 + \sum_{j=3} b_j \rho^j \right) \quad (78)$$

with $\rho = 1 - (1 + \gamma(R/R_e - 1)/p)^{-p}$ ($\gamma \geq 0$).

- Parameters: $a, \gamma, R_e, p, b_3, \dots, b_n$.
- Note: (1) high flexibility of its leading term $V_0 = d_0(1 - (1 + \gamma(R/R_e - 1)/p)^{-p})^2$ which reduces to the Lennard-Jones ($p, 2p$) and Morse potentials for $p = \gamma R_e$ and $p = \infty$, respectively. (2) Spectroscopy only.

74. Ogilvie Function (Year 1981): Ref. [73] Citations: 156

$$V = a \left(\rho^2 + \sum_{j=3} b_j \rho^j \right) \quad (79)$$

with $\rho = 2(R - R_e)/(R + R_e)$

- Parameters a, R_e, b_3, \dots, b_n .
- Notes: (1) Spectroscopy only; (2) Having a finite value as R approaches 0 or infinity.

75. XC Model Potential (Year 1981): Ref. [74] Citations: N/A

$$V = (1 - \gamma(1 + 0.1R))E_C^{(1)} - \left(C_6 \frac{F_6(sR)}{R^6} + C_8 \frac{F_8(sR)}{R^8} + C_{10} \frac{F_{10}(sR)}{R^{10}} \right) G(sR) \quad (80)$$

where $G(sR) = 1 + 41.34e^{0.8588sR}$ with $s = 7.82/R_e$. F_n is a damping function and $E_C^{(1)}$ is the first order Coulomb energy.

- Parameters: $\gamma, R_e, C_6, C_8, C_{10}$,
- Notes: (1) The damped dispersion behaves in a reasonable manner at very short distances. (2) Spectroscopy only.

76. Koide-Meath-Allnatt Potential (Year 1981): Ref. [75] Citations: 120

$$V = Ae^{-\alpha R - \beta R^2} - \sum_{n=6,8,10}^5 F_n C_n R^{-n} \quad (81)$$

with $F_n(R) = [1 - \exp(-a_n R - b_n R^2 - d_n R^3)]^n$.

- Parameters: $A, \alpha, \beta, a_6, a_8, a_{10}, b_6, b_8, b_{10}, d_6, d_8, d_{10}, C_6, C_8, C_{10}$
- Notes: (1) The damped dispersion behaves in a reasonable manner at very short distances; (2) Involve many parameters; (3) Spectroscopy only.

77. Improved HFD Potential (Year 1982): Ref. [76] Citations: 275

$$V = Ae^{-\alpha R - \beta R^2} - \sum_{n=6,8,10}^5 F_n C_n R^{-n} \quad (82)$$

with $F_n(R) = g(\rho R) f_n(\rho R)$.

- Parameters: $A, \alpha, \beta, C_6, C_8, C_{10}$

- Notes: (1) This is an improved version of Hartree-Fock dipersion (HFD) function. (2) f_n is supposed to be a universal damping function correcting for charge-overlap effects (penetration) in the R^{-n} term. (3) g is a universal function correcting for exchange effects in all the dispersion terms. (4) ρ is a distance scaling factor. For example, for the H...H dispersion interaction ($\rho = 1$): $g(R) = 1 - R^{1.68}e^{-0.78R}$ and $f_n(R) = [1 - e^{-2.1R/n-0.109R^2/n^{1/2}}]^n$. (5) Spectroscopy only.

78. Navati-Korwar Function (Year 1983): Ref. [77] Citations: 6

$$V = D_e \left(1 - \frac{R_e}{R} e^{-\beta(R)(R^p - R_e^p)} \right)^2 - D_e \quad (83)$$

with $\beta(R) = \beta_0 e^{b((R_e/R)^2 - 1) + a((R_e/R) - 1)}$.

- Parameters: $D_e, R_e, \beta_0, a, b, p$
- Notes: Having not been tested in fitting ab initio potentials or others.

79. Extended Rydberg Function I (Year 1983): Ref. [78] Citations: 126

$$V = D_e \left(1 + a_1(R - R_e) + a_2(R - R_e)^2 + a_3(R - R_e)^3 \right) e^{-a_1(R - R_e)} \quad (84)$$

- Parameters: a_1, a_2, a_3, D_e, R_e .
- Notes: (1) Actually, it is Murrell-Sorbie function (#60, 1974) with R replaced by $R - R_e$; (2) It is better than Morse function in that in the polynomial multiplying the exponential term. (3) Convergence can be checked by adding more terms. (4) It is faster to obtain a direct nonlinear least squares fitting. (5) To locate the absolute minimum in the sum of the squares of the deviation in the parameter space, a_1 has to be altered and the linear fit repeated if using linear fitting. (6) Spectroscopy only.

80. Extended Rydberg Function II (Year 1984): Ref. [79] Citations: 46

$$V = D_e \left(1 + a_1 R + a_2 R^2 + a_3 R^3 \right) e^{-a_4 R} - \tanh \left(R - \frac{R_m}{2} \right) \left(\frac{C_6}{R^6} + \frac{C_8}{R^8} + \frac{C_{10}}{R^{10}} \right) \quad (85)$$

- Parameter Numbers: $a_1, a_2, a_3, a_4, R_m, C_6, C_8, C_{10}$
- Notes: (1) Add dispersion terms to the extended Rydberg function I (#79, 1983). (2) Successfully applied to rare-gas dimers. (3) Spectroscopy only.

81. Tang-Toennies Potential (Year 1984): Ref. [79] Citations: 952

$$V_{tt}(R) = A e^{-bR} - \sum_{n \geq 3}^{\infty} f_n(b, R) \frac{C_{2n}}{R^{2n}} \quad (86)$$

with $f_n(b, R) = 1 - e^{-bR} \sum_{k=0}^{2n} \frac{(bR)^k}{k!}$.

- Parameters: $A, b, C_6, C_8, C_{10}, \dots, C_{2n}$.

- Notes: (1) Having the merit of using no adjustable parameters; (2) Successfully applied to van der Waals complexes; (3) Having four modified versions I, II, III, and IV, which are listed in the following. (4) Spectroscopy and simulation.

82. Surkus-Rakauskas-Bolotin Potential (Year 1984): Ref. [81] Citations: 41

$$V = a \left(\rho^2 + \sum_{j=3} b_j \rho^j \right) \quad (87)$$

with $\rho = s(p)(R^p - R_e^p)/(R^p + nR_e^p)$, where n and p are real numbers with the conditions that $n = -1$ if $p = 0$.

- Parameters: $a, p, n, b_3, b_4, \dots, b_n$.
- Notes: (1) Developed for spectroscopy only; (2) The Dunham, Simons-Parr-Ftilan, Thakkar and Ogilvie potentials are particular cases of this function. (3) Reproducing the potential curve with sufficient accuracy even for the cases of small expansion length. (4) Involving many parameters.

83. Jordan-Siska Potential (Year 1984): Ref. [82] Citations: 15

$$V = \frac{D}{t-1} \left(e^{-ty} Q_R(y) - t e^{-y} Q_A(y) \right) + D' \quad (88)$$

with $y = \beta(R - R_e)/R_e$ and $Q_{A,R}(y) = 1 + q_4^{A,R} y^4 + q_5^{A,R} y^5$.

- Parameters: $D, t, D', \beta, R_e, q_4^A, q_4^R, q_5^A, q_5^R$.
- Note: (1) For $t = 2, D' = 0$, and $q_4^{A,R} = q_5^{A,R} = 0$, it turns to be Morse potential. (2) The Q's modify the behavior of the function in the neighborhood of the extremum beginning with the fourth derivative. (3) Choosing $D' > 0$ yields a Morse function with a shifted asymptote. (4) Choosing $t \neq 2$ allows variation of the repulsive exponent $t\beta$. (5) Different from the Hulbert-Hirschfelder function, the repulsive part of the standard Morse part is modified by using y^4 and y^5 terms. (6) Spectroscopy only.

84. Wright Function (Year 1988): Ref. [83] Citations: 17

$$V = D_e \sum_{m \geq 2} a_m \left(1 - \left(\frac{R_e}{R} \right)^n e^{-\beta(R)(R-R_e)} \right)^m - D_e \quad (89)$$

with $\beta(R) = \beta_0(1 + \lambda_1(R - R_e) + \lambda_2(R - R_e)^2)$, $\sum_{m \geq 2} a_m = 1, n = 0, 1/2, 1$ and $m = 2, 3, 4$.

- Parameters: $D_e, R_e, \lambda_1, \lambda_2, \beta_0, a_2, a_3, a_4 \dots$
- Notes: (1) When $n = 0$ and $m = 2$ and $\beta(R) = \beta_0$, it turns to Morse function. (2) When $n = 1$ and $m = 2$ and $\beta(R) = \beta_0$, it turns to Varshni II function. (3) The best 5-parameter functions are $\beta(R) = \beta_0(1 + \lambda_1(R - R_e) + \lambda_2(R - R_e)^2)$, $m = 2$, and $n = 0, 1, 1/2$, which are considerably superior to the Hulbert-Hirschfelder, extended Morse, and extended Rydberg functions. (3) Spectroscopy only.

85. Extended General Morse Function (Year 1988): Ref. [83]..... Citations: 17

$$V = D_e \left((1 - e^{-\beta(R-R_e)})^2 + \sum_{j=3}^n a_j (1 - e^{-\beta(R-R_e)})^j \right) \quad (90)$$

with $\beta = \beta_0(1 + \lambda_1(R - R_e) + \lambda_2(R - R_e)^2)$.

- Parameters: $D_e, R_e, \lambda_1, \lambda_2, \beta_0, a_2, a_3, a_4 \dots$
- Notes: (1) Much stable; (2) Giving excellent fits to H₂ and HF, much better than Simons-Parr-Finlan (#58, 1973), Ogilvie (#74, 1981), and perturbed Morse oscillator (#64, 1976). (2) Spectroscopy only.

86. Hua Function (Year 1990): Ref. [84]..... Citations: 35

$$V = D_e \left(\frac{1 - e^{-b(R-R_e)}}{1 - ce^{-b(R-R_e)}} \right)^2 \quad \text{with } b = a(1 - c) \quad (|c| < 1) \quad (91)$$

- Parameters: D_e, R_e, b, c
- Notes: As pointed out by Natanson⁶, Hua function is the well-known Tietz potential⁷, which in turn is a combination of the Rosen-Morse (# 10, 1932), Morse (# 6, 1929), and Manning-Rosen (# 14, 1933) potentials presented in a common form.

87. Zavitsas Potential (Year 1991): Ref. [85]..... Citations: 37

$$V = D_e |e^{-2\beta_{\pm}(R-R_e)} - 2e^{-\beta_{\pm}(R-R_e)}| \quad (92)$$

where $\beta_- = \beta_M(1 + mu^{1/2})$ for $R < R_e$ and $\beta_+ = \beta_M(1 + a_1u^{1/2} + a_2u^n + a_3u^{3n} + a_4u^{5n})$.

- Parameter Numbers: $a_1, a_2, a_3, a_4, \beta_M, n, \beta_M, m, \mu$.
- Notes: (1) Needs bond dissociation energy, infrared stretching frequency, equilibrium internuclear distance, electronegativity difference, effective nuclear charges, and masses. (2) Overall, deviations between calculated and reported potentials are within a factor of 2 of the estimated uncertainties of reported RKR points. (3) Applicable to polyatomic molecules. (3) Spectroscopy only.

88. Generalized Morse Oscillator (GMO) (Year 1991): Ref. [86]..... Citations: 60

$$V = D_e \left(1 - e^{-\beta_{GMO}(R)(R-R_e)} \right)^2 \quad (93)$$

with $\beta_{GMO}(R) = \sum_{m=0} \beta_m^{GMO}(R - R_e)^m$.

- Parameters: $D_e, R_e, \beta_0^{GMO}, \beta_1^{GMO}, \dots, \beta_n^{GMO}$
- Notes: (1) Developed for spectroscopy only; (2) Successfully applied to diatomic hydrides such as HBr and HI; (3) Involving many parameters.

⁶G. A. Natanson, Comment on "Four-parameter exactly solvable potential for diatomic molecules", Phys. Rev. A 44, 3377 (1991)

⁷Tietz Function (Year 1963) Ref. [111] (citations: 35): $V(R) = D_e + D_e \frac{(a+b)e^{-2\beta R} - be^{-\beta R}}{1 + ce^{-\beta R}}$,

89. Modified GMO (Year 1993): Ref. [87] Citations: 56

$$V = D_e \left(\frac{1 - e^{-\beta(R)}}{1 - e^{-\beta(\infty)}} \right)^2 \quad (94)$$

with $\beta(R) = Z \sum_{i=0} \beta_i z^i$, $\beta(\infty) = \sum_{i=0} \beta_i$, and $z = (R - R_e)/(R + R_e)$.

- Parameters: $D_e, R_e, \beta_0, \beta_1, \beta_2, \beta_3, \beta_4$.
- Notes: (1) A modified GMO function (1991); (2) Developed for spectroscopy only; (3) Successfully applied to AlCl and AlF.

90. Eggenberger Potential (Year 1993): Ref. [88] Citations: 19

$$V = A e^{-bR} + \frac{a}{R^{12}} - \sum_{n=3}^5 \frac{C_{2n}}{R^{2n}} \quad (95)$$

- Parameters: $A, b, a, C_6, C_8, C_{10}$
- Notes: Applied in classical molecular dynamics simulations to study the thermodynamical and structural properties of neon in the liquid and supercritical states.

91. Cvetko Potential (Year 1994): Ref. [89] Citations: 43

$$\begin{aligned} V(R) &= \frac{C_6}{10} (b/3)^6 (ae^{-bR} - \chi e^{-(2/3)bR} - e^{-(1/3)bR}), & bR \leq 16.6 \\ V(R) &= \frac{C_6}{10} (b/3)^6 ae^{-bR} - \frac{C_6}{R^6 - Q^2 R^4}, & bR \geq 16.6 \end{aligned} \quad (96)$$

- Parameters: a, b, Q, c_6, χ .
- Notes: (1) Developed for vander Waals atomic pairs; (2) Allows the potential energy of a given pair to be estimated with good accuracy from *ab initio* density functional calculations of the free-atom electron densities; (3) Spectroscopy only..

92. Modified Tang-Toennies I (Year 1995): Ref. [90] Citations: 199

$$V(R) = DR^{\frac{7}{2\beta}-1} e^{-2\beta R} - \sum_{n=3}^{\infty} \left(1 - e^{-bR} \sum_{k=0}^{2n} \frac{(bR)^k}{k!} \right) \frac{C_{2n}}{R^{2n}} \quad (97)$$

where $b = 2\beta - (\frac{7}{2\beta} - 1)/R$.

- Parameter: $D, \beta, b, C_6, C_8, C_{10}, \dots, C_{2n}$
- Notes: Modified Tang-Toennies potential for describing the ground state of He₂.

93. Korona *et al.* Potential (Year 1997): Ref. [91] Citations: 220

$$V = Ae^{-\alpha R + \beta R^2} - \sum_{n \geq 3}^8 f_n(b, R) C_{2n} / R^{2n} \quad (98)$$

with $f_n(b, R) = 1 - e^{-bR} \sum_{k=0}^{2n} \frac{(bR)^k}{k!}$.

- Parameters: $A, \alpha, \beta, b, C_6, C_8, c_{10}, C_{12}, C_{14}, C_{16}$
- Notes: (1) This is actually a modified Tang-Toennies potential. (2) Developed for rare-gas atomic pairs.

94. Zhu-Wang Potential (Year 1997): Ref. [92] Citations: 20

$$V = \frac{a_1}{\rho - a_2} - \frac{a_3}{\rho + a_4} \quad (99)$$

where $\rho = R - R_{min}$ is the displacement from the minimum R_{min} for diatomic ions with both potential minimum and maximum, and $\rho = R$ only for the repulsive states.

- Parameters: $a_1, a_2, a_3, a_4, R_{min}$
- Notes: Developed for describing the potential curves for doubly charged diatomic ions with both potential minimum and maximum.

95. Molski Series (Year 1999): Ref. [93] Citations: 21

$$V = a \left(\rho^2 + \sum_{j=3} b_j \rho^j \right) \quad (100)$$

with $\rho = (R - R_e)/(aR^p + (1 - a)R_e)$, where a is a free fitting parameter.

- Parameters: $a, R_e, p, b_3, b_4, \dots, b_n$.
- Notes: (1) This new expansion includes those of Dunham, SimonsParrFinlan, and Ogilvie as special cases. (2) Spectroscopy only.

96. Modified Tang-Toennies II (Year 1999): Ref. [94] Citations: 46

$$V(R) = A e^{-b_1 R - b_2 R^2} - \sum_{n=3}^8 \left(1 - e^{-b' R} \sum_{k=0}^{2n} \frac{(b' R)^k}{k!} \right) \frac{C_{2n}}{R^{2n}} \quad (101)$$

where $b' = b_1 + 2b_2 R$.

- Parameters: $A, b_1, b_2, C_6, C_8, C_{10}$
- Notes: Modified Tang-Toennies potential for describing Alkaline-earth Rare gas and Alkali-He systems

97. Modified Lennard-Jones Oscillator (Year 2000): Ref. [95] Citations: 56

$$V = D_e \left(1 - (R_e/R)^n e^{-\beta_{MLJ}(z)z} \right)^2 \quad (102)$$

with $\beta_{MLJ}(z) = \sum_{m=0}^M \beta_m z^m$ and $z = (R - R_e)/(R + R_e)$.

- Parameters: $D_e, R_e, \beta_0, \beta_1, \dots, \beta_M, n$.
- Notes: (1) Developed for spectroscopy only; (2) Flexible because of involving many parameters; (3) The model can be thought of as a generalization of the prototypical Lennard-Jones (2n,n) function.

98. Samuelis *et al.* Series (Year 2001): Ref. [96] Citations: 45

$$V = -D + a_0 + \sum_{j=1} a_j \zeta^j \quad (103)$$

with $\zeta = (R - R_e)/(R + bR_e)$.

- Parameters: $R_e, b, a_0, a_1, \dots, a_{39}$.
- Notes: (1) Developed for spectroscopy only; (2) more than 40 parameters for describing the ground state of Na_2 .

99. Bellert-Breckenridge (Year 2002): Ref. [97] Citations: 84

$$V = Ae^{-bR} - \frac{\alpha_{Rg}Z^2}{2R^4} - \frac{C_6}{R^6} - \frac{\alpha_{Rg,Q}Z^2}{2R^6} + \frac{B_{Rg}Z^3}{2R^7} - \frac{C_8}{R^8} - \frac{\alpha_{Rg,O}Z^2}{2R^8} - \frac{\gamma Z^4}{24R^8} \quad (104)$$

where Z is the effective charge on the ion, α_{Rg} , $\alpha_{Rg,Q}$, $\alpha_{Rg,O}$ are the dipole, quadrupole, and octopole polarizabilities of the rare-gas atom, B_{Rg} (negative value) is the higher-order dipole-quadrupole polarizability of the rare-gas atom, γ is the higher-order second dipole hyperpolarizability of the rare-gas atom, and C_6 and C_8 are Z -independent coefficients representing the first and second-terms in the dispersion interaction.

- Parameters: $A, b, \alpha_{Rg}, \alpha_{Rg,Q}, C_6, C_8, \gamma, B_{Rg}, \alpha_{Rg,O}$.
- Notes: Developed for the diatomic ions containing neutral rare-gas atom.

100. Rydberg-London Potential (Year 2004): Ref. [98] Citations: 13

$$V = a e^{-bR}(1 - cR) - \frac{d}{R^6 + eR^{-6}} \quad (105)$$

- Parameters: a, b, c, d, e
- Notes: (1) Much accurate than Morse, Lennard-Jones, and Hulburt-Hirschfelder potentials, (2) Demonstrated that Rydberg-London potential is more reliable than the Lennard-Jones potential to be used as starting geometries to obtain global minima of atom clusters. (3) Not accurate for covalent molecules in the repulsive and large- R region (4) $V(R \rightarrow 0)$ is given by a finite value.

101. Wang-Yang-Zhu Potential (Year 2004): Ref. [99] Citations: 8

$$V = \left(\sum_{n=0}^k a_n R^n \right) e^{-a_{k+1}R} + \frac{C}{R} \quad (106)$$

- Parameters: $a_0, a_1, \dots, a_k, a_{k+1}, C$
- Notes: This function can be used to describe the potential curves for doubly charged diatomic ions with both potential minimum and maximum, or without any stationary point.

102. Xie-Gong Function (Year 2005): Ref. [100] Citations: 13

$$E(R, \alpha, \beta, \gamma) = E_\infty + \frac{J_1(R, \gamma) + K_1(R, \alpha, \beta)}{1 + S_0(R)} \quad (107)$$

with

$$\begin{aligned} J_1(R, \gamma) &= e^{-2\gamma R} \left(\frac{1}{R} + 1 \right), \\ K_1(R, \alpha, \beta) &= e^{-\alpha R} \left(\frac{1}{R} - \beta R \right), \\ S_0(R) &= e^{-R} \left(1 + R + \frac{R^2}{3} \right), \end{aligned}$$

known as the Coulomb, exchange, and overlap integrals, respectively, where α, β, γ are the adjusting parameters, and E_∞ is the total energy of the system at the infinity.

- Parameters: α, β, γ
- Notes: (1) Simple, and only 3 parameters; (2) Able to describe the ground states of strongly or weakly bounded diatomic molecules with s-type or closed shell constituents; (3) Able to describe the meta-stable states of diatomic dications.; (4) Not accurate in the large- and short-R regions.

103. Morse-Long-Range Potential (Year 2006): Ref. [101] Citations: 64

$$V = D_e \left(1 - (u_{LR}(R)/u_{LR}(R_e)) e^{-\phi(R)y_p(R)} \right)^2 \quad (108)$$

with

$$\begin{aligned} y_p(R) &= (R^p - R_e^p)/(R^p + R_e^p), \\ \phi(R) &= (1 - y_p(R)) \sum_{i=0}^N \phi_i y_p(R)^i + y_p(R) \phi_\infty, \\ u_{LR}(R) &= \frac{C_n}{R^n} + \frac{C_m}{R^m}, \\ \phi_\infty &= \ln(2D_e/u_{LR}(R_e)) = \ln \left(2D_e R_e^n / [C_n(1 + Q_{m,n}/R_e^{m-n})] \right) \end{aligned}$$

- Parameters: $D_e, p, \phi_0, \dots, \phi_8, \phi_\infty, C_n, C_m$
- Notes: (1) Successfully applied to the ground state of N_2 ; (2) Involving many parameters. (3) Spectroscopy only.

104. General Form of MLJ and MLR Potential (Year 2006): Ref. [102] Citations: 2

$$V = D_e \left(1 - ((1 - b)(R_e/R)^n + b(R_e/R)^m) e^{-\beta(y)y} \right)^2 \quad (109)$$

with

$$\begin{aligned} \beta(y) &= \beta_0 + \beta_1 y + \beta_2 y^2 + \beta_3 y^3 + \dots, \\ y &= y_p(R) = (R^p - R_e^p)/(R^p + R_e^p) \end{aligned}$$

- Parameters: $D_e, R_e, b, p, n, m, \beta_0, \beta_1, \dots, \beta_n$
- Notes: (1) A general form of MLJ and MLR potentials. (2) Developed for spectroscopy only. (3) Involving many parameters.

105. Even-Tempered Gaussian (ETG) Function (Year 2007): Ref. [103] Citations: 19

$$V(R) = \sum_{k=0}^4 a_k e^{-\alpha \beta^k R^2} \quad (110)$$

where the coefficients a_k are obtained by nonlinear regression and the exponent parameters α and β by nonlinear minimization.

- Parameters: $a_0, a_1, a_2, a_3, a_4, \beta, \alpha$
- Notes: (1) Successfully applied to describe the ground states of F_2 and B_2 . (2) Spectroscopy only.

106. Modified Tang-Toennies III (Year 2009): Ref. [104] Citations: 22

$$V(R) = (A + BR + C/R + DR^2 + ER^3)e^{-\alpha R + \beta R^2} - \sum_{n=3}^8 \left(1 - e^{-bR} \sum_{k=0}^{2n} \frac{(bR)^k}{k!} \right) \frac{C_{2n}}{R^{2n}} + T_{dis} \quad (111)$$

- Parameters: $A, B, C, D, E, \alpha, \beta, C_6, C_8, C_{10}, C_{12}, C_{14}, C_{16}$
- Notes: Modified Tang-Toennies potential for describing the ground state of Be_2 .

107. Piecewise Continuous Approximants (Year 2010): Ref. [105] Citations: 24

$$\begin{aligned} V_{pw}(R) &= V_{IR}(R) & R_{SR} \leq R \leq R_{LR}; \\ &= V_{SR}(R) & R < R_{SR}; \\ &= V_{LR}(R) & R > R_{LR}; \end{aligned} \quad (112)$$

where

$$\begin{aligned} V_{IR} &= \sum_{i=0}^N a_i \left((R - R_e) / (R + \alpha R_e) \right)^i, \\ V_{SR} &= u_1 + u_2 / R^{N_s}, \\ V_{LR} &= - \sum_{i=1}^L C_{N_i} / R^{N_i} + A_{ex} R^\gamma e^{-\beta R} \end{aligned}$$

- Parameters: $R_{LR}, R_{SR}, \alpha, a_0, a_1, \dots, a_{25}, u_1, u_2, N_s, C_6, C_8, C_{10}, C_{26}, A_{ex}, \gamma, \beta$
- Notes: (1) Developed for spectroscopy only; (2) Successfully applied to Rb_2 ; (3) Involving many parameters.

108. Chebychev Polynomials (Year 2011): Ref. [106] Citations: 7

$$V(R) = T_{dis} - \frac{\sum_{k=0}^m c_k T_k(y_p)}{86 \left(1 + (R/R_{ref})^n \right)} \quad (113)$$

where T_{dis} is chosen such that the potential minimum has energy zero and $T_k(y)$ is the Chebychev polynomials of first kind and $-1 \leq y_p \leq 1$ is the reduced radial variable given by

$$y_p(R, R_e, R_{ref}) = \frac{R^p - R_{ref}^p}{R^p + R_{ref}^p - 2R_e}$$

- Parameters: $c_0, c_1, \dots, c_{24}, R_{ref}, R_e, p$
- Note: (1) Successfully applied to KCs; (2) Flexible due to many parameters. (3) Developed for Spectroscopy only.

109. Modified Rosen-Morse Potential (Year 2012): Ref. [107] Citations: 3

$$V = D_e \left(1 - \frac{e^{2(R_e - R_{ij})/d} + 1}{e^{2(R - R_{ij})/d} + 1} \right)^2 \quad \text{with } R_{ij} = R_e - \sqrt{\frac{KD_e}{k_e}} \quad (114)$$

- Parameters: D_e, R_e, R_{ij}, d
- Notes: (1) This modified potential is found to be more accurate than the Morse and Rosen-Morse potentials. (2) Spectroscopy only.

110. Generalized Morse Long-Range Potential (GMLR) (Year 2013): Ref. [108]. Citations: 1

$$V(R) = T_e + D_e \left(a_0 Z^2(R) + a_1 Z^3(R) + a_2 Z^4(R) + \dots \right) \quad (115)$$

where

$$\begin{aligned} a_0 &= 1 - \sum_{n=1} a_n, \\ Z(R) &= 1 - (b_0(R_e/R)^{n_1} + b_1(R_e/R)^{n_2} + \dots) e^{-\beta(y)y(R)}, \\ b_0 &= 1 - \sum_{n=1} b_n, \\ \beta(y) &= \beta_0 + \beta_1 y + \beta_2 y^2 + \dots, \\ y(R) &= \frac{R^p - R_e^p}{\epsilon R^p + \alpha R_e^p} \end{aligned}$$

- Parameters: $D_e, R_e, \epsilon, \alpha, p, \beta_0, \beta_1, \dots, \beta_n, b_0, b_1, \dots, n_1, n_2, \dots, a_0, a_1, \dots,$
- Notes: (1) A general version of Morse Long-Range potential. (2) Developed for spectroscopy only. (3) Involves many parameters.

111. Modified Tang-Toennies IV (Year 2013): Ref. [109] Citations: 0

$$V(R) = A e^{-bR} - \sum_{n=3}^{\infty} \left(1 - e^{-bR} \sum_{k=0}^{2n} \frac{(bR)^k}{k!} \right) \frac{C_{2n}}{R^{2n}} + T_{dis} \quad (116)$$

where T_{dis} is chosen such that the potential minimum has energy zero and the R-dependent parameter b is given by

$$b = b_0 + \frac{R_c}{R + R_c} \sum_{i=1}^m b_i \left(\frac{R - R_e}{R + R_e} \right)^i$$

- Parameters: $A, b_0, R_e, b_1, b_2, \dots, b_6, R_e, C_6, C_8, C_{10}$
- Notes: (1) Developed for spectroscopy only; (2) Successfully applied to Mg_2 ; (3) Involves many parameters.

112. Modified Tang-Toennies V (Year 2013): Ref. [110].....Citations: 0

$$V(R) = Ae^{-bR} + De^{-eR-fR^2} - \sum_{n=3}^8 \left(1 - e^{-bR} \sum_{k=0}^{2n} \frac{(bR)^k}{k!} \right) \frac{C_{2n}}{R^{2n}} \quad (117)$$

where the second term is a new term added to the Tang-Toennies potential.

- Parameters: $A, b, D, e, f, C_6, C_8, C_{10}, C_{12}, C_{14}, C_{16}$.
- Notes: (1) Modified Tang-Toennies function; (2) Applied to the ground state of Be_2 .

References

- [1] M. Born and A. Lande, *Verhandl. Deut. Physik. Ges.* 20, 210 (1918); M. Born, *Concerning the electronic nature of the power of cohesion of solid matter*, *Ann. Physik* (Liepzig), 61, 87 (1920).
- [2] A. Kratzer, *The rotation spectrum of halogen hydrogens*, *Z. Physik*, 3, 289-307 (1920); A. Kratzer, *Band system which follow the standard*, *Ann. Physik* 67, 127-153 (1922).
- [3] J.E. Lennard-Jones, *On the Determination of Molecular Fields. II. From the equation of state of a gas*, *Proc. Roy. Soc. (Lond)* A 106, 463-477 (1924).
- [4] E. Fues, *The natural frequency spectrum of two atom molecules in the mechanics of undulation*, *Ann. Physik*, 80, 367-396 (1926).
- [5] R. Mecke, *Band spectra and the periodic classification of the elements*, *Z. Physik* 42, 390-425 (1927); G. B. B. M. Sutherland, *Proc. Indian Acad. Sci.* 8, 341 (1938); G.B.B. M. Sutherland, *The Determination of Internuclear Distances and of Dissociation Energies from Force Constants*, *J. Chem. Phys.* 8, 161 (1940).
- [6] P.M. Morse, *Diatomic molecules according to the wave mechanics. II. Vibrational levels*, *Phys. Rev.* 34, 57-64 (1929).
- [7] C. Eckart, *The penetration of a potential barrier by electrons*, *Phys. Rev.* 35, 1303-1309 (1930); V. Bargmann, *On the Connection between phase shifts and scattering potential*, *Rev. Mod. Phys.* 21, 488-493 (1949); T. J. P. O'Brien and R. B. Bernstein, *Investigation of the Hylleraas Method for Determining the Potential Energy Function from the Phase Shift*, *J. Chem. Phys.* 51, 5112-5117 (1969).
- [8] R. Rydberg, *Graphical Representation of some bound spectroscopic Results*, *Z. Phys.* 73, 376-385 (1931).
- [9] J.C. Slater and J.G. Kirkwood, *The van der waals forces in gases*, *Phys. Rev.* 37, 682-297 (1931).
- [10] N. Rosen and P.M. Morse, *On the vibrations of polyatomic molecules*, *Phys. Rev.* 42, 210-217 (1932).
- [11] P.M. Davidson, *Eigenfunctions for calculating electronic vibrational intensities*, *Proc. Roy. Soc. (London)* A135, 459-472 (1932).
- [12] J.L. Dunham, *The Energy Levels of a Rotating Vibrator*, *Phys. Rev.* 41, 721-731 (1932).
- [13] M. Born and J.E. Mayer, *For the lattice theory of ionic crystals*, *Physica B-Condensed Matter* 75, 1-18 (1932)
- [14] M.F. Manning and N. Rosen, *Phys. Rev.* 44, 953-953 (1933); R.A. Newing, *Note on the interrelation of the equilibrium nuclear distance with other molecular constants for diatomic molecules*, *Phil. Mag.* 19, 759-767 (1935); R.A. Newing, *On the interrelation of molecular constants for diatomic molecules - II* *Phil. Mag.* 29, 298 (1940).
- [15] G. Pöschl and E. Teller, *Comments on the quantum mechanics of the anharmonic oscillator*, *Z. Physik* 83, 143-151 (1933).
- [16] C.L. Pekeris, *The Rotation-Vibration Coupling in Diatomic Molecules*, *Phys. Rev.* 45, 98-103 (1934).
- [17] E.A. Hylleraas, *Analytical representation of potential atomic molecules and their determination from spectroscopic data*, *Z. Physik* 96, 643-660 (1935); E.A. Hylleraas, *Energy Formula and Potential Distribution of Diatomic Molecules*, *J. Chem. Phys.* 3, 595 (1935); E.A. Hylleraas, *A new approach for the course of the potential of two-atomic homopolaric molecules-Application on CdH and N-2*, *Physik. Z.* 36, 599-600(1935).
- [18] M.L. Huggins, *Molecular Constants and Potential Energy Curves for Diatomic Molecules*, *J. Chem. Phys.* 3, 473-479 (1935); M.L. Huggins, *Molecular Constants and Potential Energy Curves for Diatomic Molecules II.*, *J. Chem. Phys.* 4, 308-312 (1936);
- [19] H. Hellmann, *A New Approximation Method in the Problem of Many Electrons*, *J. Chem. Phys.* 3, 61-61 (1935). H. Hellmann, *Combination of the approximation method of computation in the problem of many electrons*, *ACTA Physicochimica URSS* 1, 913-940 (1935).
- [20] J. A. Wasastjerna, *Soc. Sci. Fennica, Commentationes Phys.Math.* 8, 21 (1935); J. A. Wasastjerna, *On the forces acting between atoms and ions and the physical properties of matter in bulk*, *Phil. Trans. Roy. Soc. London* 237, 105 (1939).
- [21] A.S. Coolidge, H.M. James, E.L. Vernon, *On the Determination of Molecular Potential Curves from Spectroscopic Data*, *Phys. Rev.* 54, 726-738 (1938).
- [22] R.A. Buckingham, *The classical equation of state of gaseous helium, neon and argon*, *Proc. Roy. Soc.* 168, 264-283 (1938)
- [23] H. Margenau, *Van der Waals Forces*, *Rev. Mod. Phys.* 11, 1-35 (1939). H. Margenau, *Van der Waals Potential in Helium*, *Phys. Rev.* 56, 1000 (1939).

- [24] J.W. Linnett, *The relation between potential energy and interatomic distance in some diatomic molecules*, Trans. Faraday Soc. 36, 1123 (1940); J.W. Linnett, *The relation between potential energy and interatomic distance in some di-atomic molecules II.*, Trans. Faraday Soc. 38, 1 (1942);
- [25] H.M. Hulburt and J.O. Hirschfelder, *Potential Energy Functions for Diatomic Molecules*, J. Chem. Phys. 9, 61-69 (1941); Erratum: J. Chem. Phys. 35, 1901 (1961).
- [26] C.K. Wu and C.T. Yang, *The relation between the force constant and the interatomic distance of a diatomic linkage*, J. Phys. Chem. 48, 295-303 (1944).
- [27] R.A. Buckingham, *Tables of 2nd virial and low-pressure Joule-Thomson coefficients for intermolecular potentials with exponential repulsion*, Proc. Roy. Soc. 189, 118-129 (1947)
- [28] E.S. Rittner, *Binding Energy and Dipole Moment of Alkali Halide Molecules*, J. Chem. Phys. 19, 1030-1035 (1951).
- [29] E.L. Lippincott, *A New Relation between Potential Energy and Internuclear Distance*, J. Chem. Phys. 21, 2070-2071 (1953) [92]; E.L. Lippincott, *A New Relation between Potential Energy and Internuclear Distance*, J. Chem. Phys. 23, 603-603 (1955) [87]
- [30] T. Kihara, *Virial Coefficients and Models of Molecules in Gases*, Rev. Mod. Phys. 25, 831 (1953).
- [31] A.A. Frost and B. Musulin, *Semiempirical Potential Energy Functions. I. The H_2 and H_2^+ Diatomic Molecules*, J. Chem. Phys. 22, 1017 (1954).
- [32] G.C. Maitland, M. Rigby, E.B. Smith, W.A. Wakchem, *Intermolecular Forces*, Clarendon Press, Oxford, 1987; William E. Rice and Joseph O. Hirschfelder, *Second Virial Coefficients of Gases Obeying a Modified Buckingham (ExpSix) Potential*, J. Chem. Phys. 22, 187-192 (1954)
- [33] W.E. Rice and J.O. Hirschfelder, *Second Virial Coefficients of Gases Obeying a Modified Buckingham (ExpSix) Potential*, J. Chem. Phys. 22, 187 (1954); E.A. Mason and W.E. Rice, *The intermolecular potentials of Helium and Hydrogen*, J. Chem. Phys. 22, 522-535 (1954); E.A. Mason and W.E. Rice, *The Intermolecular potentials for some simple nonpolar molecules*, J. Chem. Phys. 22, 843-851 (1954).
- [34] Y.P. Varshni, *Comparative study of potential energy functions for diatomic molecules*, Rev. Mod. Phys. 29, 664-682 (1957).
- [35] P.S.K. Chen, M. Geller, A.A. Frost, *Semiempirical potential energy functions. 2. General Diatomic Molecules*, J. Phys. Chem. 61, 828-829 (1957).
- [36] A.A. Frost and J.H. Woodson, *Semiempirical Potential Energy Functions. III. Generalization for Ionic Molecules and the Inclusion of London Forces*, J. Am. Chem. Soc. 80, 2615-2618 (1958).
- [37] R.A. Buckingham, *The repulsive interaction of atoms in S states*, Trans. Faraday Soc. 54, 453-459 (1958).
- [38] E.J. Finn and C.L. Beckel, *Power Series Expansions of Vibrational Potentials. II. Two Classical Potentials for Ionic Molecules*, J. Chem. Phys. 33, 1887-1888 (1960); E.J. Finn, *Vibrational Energy Levels of Ionic Molecules Bound by Classical Forces*, J. Chem. Phys. 39, 2423 (1963).
- [39] K. P. Lawley, *Influence of hyperpolarizability on some properties of ion pairs*, Trans. Faraday Soc. 67, 1809 (1961).
- [40] Y.P. Varshni and R.C. Shukla, *New Potential Function for Alkali Halide Molecules*, J. Chem. Phys. 35, 582 (1961).
- [41] H.W. Woolley, *Realistic Diatomic Potential Function*, J. Chem. Phys. 37, 1307-1316 (1962).
- [42] J.D. Swalen and J.A. Ibers, *Potential Function for the Inversion of Ammonia*, J. Chem. Phys. 36, 1914-1918 (1962).
- [43] W.L. Clinton, *New potential energy function. I. Empirical*, J. Chem. Phys. 36, 555-555 (1962); W.L. Clinton, *New potential energy function. II. Theoretical*, J. Chem. Phys. 36, 556-556 (1962).
- [44] Y.P. Varshni and R.C. Shukla, *Alkali hydride molecules: potential energy curves and the nature of their binding*, Rev. Mod. Phys. 35, 130-144 (1963).
- [45] H. Preuss, *Eine neue Näherung für die Energiekurven zweiatomiger System*, Theor. Chim. Acta 2, 102-113 (1964).
- [46] Y.P. Varshni and R.C. Shukla, *Potential Energy Functions for Alkali Halide Molecules*, J. Mol. Spectro. 16, 63-83 (1965).
- [47] T. G. Waech and R.B. Bernstein, *Calculated Spectrum of Quasibound States for $H_2(1\sum_g^+)$ and Resonances in $H + H$ Scattering*, J. Chem. Phys. 46, 4905-4911 (1967).

- [48] R. G. Parr and R. J. White, *Perturbation Theoretic Approach to Potential Energy Curves of Diatomic Molecules*, J. Chem. Phys. 49, 1059-1062 (1968).
- [49] R.L. Redligton, *Internuclear Potential Energy Functions for Alkali Halide Molecules*, J. Phys. Chem. 74, 181-186 (1970). Y. P. Varshni and R.C. Shukla, *Potential Energy Functions for Alkali Halide Molecules*, J. Mol. Spectro. 16, 63-83 (1965).
- [50] M. Klein and H.J.M. Hanley, *M-6-8 Potential Function*, J. Chem. Phys. 53, 4722 (1970).
- [51] P.E. Siska, J.M. Parson, T.P. Schafer, and Y.T. Lee, *Intermolecular potentials from crossed beam differential elastic scattering measurements. III. He + He and Ne + Ne*, J. Chem. Phys. 55, 5762-5770 (1971).
- [52] J.A. Barker, R.A. Fisher, and R.O. Watts, *Liquid argon: Monte Carlo and Molecular Dynamics Calculations*, Molecular Physics, 21, 657 (1971).
- [53] John D. Weeks, David Chandler, and Hans C. Andersen, *Role of Repulsive Forces in Determining the Equilibrium Structure of Simple Liquids*, J. Chem. Phys. 54, 5237-5247 (1971).
- [54] P.J. Kuntz and A.C. Roach, *Ion-molecule reactions of rare-gas with hydrogen. 1. Diatomics-in-molecules potential-energy surface for ArH_2^+* J. Chem. Soc. Faraday Trans. 2, 68, 259-280 (1972).
- [55] D.D. Konowalow and D.S. Zakheim, *Morse-6 Hybrid Potentials for Pair Interactions of Rare Gas Atoms*, J. Chem. Phys. 57, 4375 (1972).
- [56] G.C. Maitland and E.B. Smith, *A simplified representation of intermolecular potential energy*, Chem. Phys. Lett. 22, 443-446 (1973).
- [57] G. Simons, R.G. Parr, and J.M. Finlan, *New alternative to the Dunham potential for diatomic molecules*, J. Chem. Phys. 59, 3229-3234 (1973).
- [58] K. D. Jordan, J. L. Kinsey, and R. Silbey, *Use of Pade approximants in the construction of diabatic potential energy curves for ionic molecules*, J. Chem. Phys. 61, 911-917 (1974).
- [59] J.N. Murrell and K.S. Sorbie, *New Analytic Form for the Potential Energy Curves of Stable Diatomic States*, J. Chem. Soc. Faraday Trans. II. 70, 1552-1556 (1974).
- [60] B.G. Wicke and D.O. Harris, *Comparison of three numerical techniques for calculating eigenvalues of an unsymmetrical double minimum oscillator*, J. Chem. Phys. 64, 5236-5242 (1976).
- [61] C. W. Eaker and C.A. Parr, *Optimization of diatomic state mixing in diatomics-in-molecules theory: The CH_n potential-energy surfaces*, J. Chem. Phys. 64, 1322 (1976).
- [62] J.G. Schubert and P.R. Certain, unpublished; cited in E. Herbst, Chem. Phys. Lett. 47, 517 (1977).
- [63] A. J. Thakkar, *A new generalized expansion for the potential energy curves of diatomic molecules*, J. Chem. Phys. 62, 1693-1701 (1975).
- [64] G. York, R. Scheps, and A. Gallagher, *Continuum radiation and potentials of Na-noble gas molecules*, J. Chem. Phys. 63, 1052-1064 (1975).
- [65] J.N. Huffaker, *Diatomic molecules as perturbed Morse oscillators. I. Energy levels*, J. Chem. Phys. 64, 3175-3181 (1976).
- [66] R. Ahlrichs, R. Penco, G. Scoles, *Intermolecular forces in simple systems*, Chem. Phys. 19, 119 (1977); R. A. Aziz and H. H. Chen, *An accurate intermolecular potential for argon*, J. Chem. Phys. 67, 5719 (1977); J. Hepburn, G. Scoles, and R. Penco, *A simple but reliable method for the prediction of the intermolecular potentials*, Chem. Phys. Lett. 36, 451-456 (1975). A.K. Dham, A.R. Allnatt, W.J. Meath, R.A. Aziz, Mol. Phys. 67, 1291-1307 (1989).
- [67] O. Kafri and M.J. Berry, *A New Empirical Potential Hypersurface for Bimolecular Reaction Systems*, Faraday Discuss. Chem. Soc. 62, 127-137 (1977).
- [68] J.H. Goble, D.C. Hartman, and J.S. Winn, *Recovery of the long range potential in $BeAr^+$ by potential inversion methods*, J. Chem. Phys. 67, 4206-4211 (1977).
- [69] R. Engelke, *Diatomic molecule vibrational potentials: Accuracy of representations*, J. Chem. Phys. 68, 3514-3521 (1978).
- [70] O. Kafri, *Modified Morse Function Fitting Procedure For Diatomic Potentials*, Chem. Phys. Lett. 61, 538 (1979).

- [71] C.L. Beckel and P.R. Findley, *Rational fraction representation of diatomic vibrational potentials. Application of H_2^+ ground state*, J. Chem.Phys. 73, 3517-3518 (1980); C.L. Beckel, R.B. Kwong, and A. HashemiAttar, *Rational fraction representation of diatomic vibrational potentials. II. Application to H_2 ground state*, J. Chem.Phys. 73, 5385-5386 (1980); C.L. Beckel, E.R. Scaggs, and R.B. Kwong, *Rational fraction representation of diatomic vibrational potentials. III. Application to H_2^+ $2p\Pi_u$ electronic state*, J. Chem.Phys. 73, 5398-5390 (1980); S.A. Sonnleitner and C. L. Beckel, *Rational fraction representation of diatomic vibrational potentials. IV. The $2p\sigma_u$ van der Waals state of H_2^+* , J. Chem.Phys. 73, 5404-5405 (1980);
- [72] L. Mattera, C. Salvo, S. Terreni and F. Tommasini, *A simple and flexible atom-surface potential with easy-to-handle vibrational spectrum*, Surface Sci. 97, 158-170 (1980).
- [73] J.F. Ogilvie, *A general potential-energy function for diatomic molecules*, Proc. Roy. Soc. London, Ser. A 378, 287-300 (1981).
- [74] W.J. Meath, D.J. Margoliash, B.L. Jhanwar, A. Koide and G.D. Zeiss, in: *Intermolecular Forces*, ed. B. Pullman, (Reidel, Dordrecht, 1981) p. 101.
- [75] A. Koide, W.J. Meath, and A.R. Allnatt, *Second order charge overlap effects and damping functions for isotropic atomic and molecular interactions*, Chem. Phys. 58, 105-119 (1981).
- [76] C. Douketis, G. Scoles, S. Marchetti, M. Zen, and A. J. Thakkar, *Intermolecular forces via hybrid HartreeFockSCF plus damped dispersion (HFD) energy calculations. An improved spherical model*, J. Chem. Phys. 76, 3057-3063 (1982).
- [77] B.S. Navati and V.M. Korwar, *Pramana* 20, 457 (1983).
- [78] P. Huxley and J. N. Murrell, *Ground-state diatomic potentials*, J. Chem. Soc. Faraday Trans. 2, 79, 323-328 (1983).
- [79] P. Huxley, D.B. Knowles, J. N. Murrell, and J. D. Watts, *Ground-state diatomic potentials Part 2. Van der waals Molecules*, J. Chem. Soc.Faraday Trans. 2, 80, 1349-1361 (1984).
- [80] K. T. Tang and J. P. Toennies, *An improved simple model for the van der Waals potential based on universal damping functions for the dispersion coefficients*, J. Chem. Phys. 80, 3726-3741 (1984).
- [81] A.A. Surkus, R.J. Rakauskas, and A.B. Bolotin, *The generalized potential energy function for diatomic molecules*, Chem. Phys. Lett. 105, 291 (1984).
- [82] R. M. Jordan and P. E. Siska, *Potential energy curves for the $A^1 \sum_u^+$ and $C^1 \sum_g^+$ states of He_2 obtained by combining scattering, spectroscopy, and ab initio theory*, J. Chem. Phys. 80, 5027-5035 (1984).
- [83] J.S. Wright, *Accuracy of diatomic potential functions*, J. Chem. Soc. Faraday Trans. 2, 84, 219-226 (1988).
- [84] W. Hua, *Four-parameter exactly solvable potential for diatomic molecules*, Phys. Rev. A 42, 2524-2529 (1990).
- [85] A.A. Zavitsas, *Energy-Distance Relationship in Chemical Bonding. Accurate Calculation of Potential Energy Curves*, J. Am. Chem. Soc. 113, 4755-4767 (1991).
- [86] J.A. Coxon and P.G. Hajigeorgiou, *Isotopic Dependence of Born-Oppenheimer Breakdown Effects in Diatomic Hydrides: The $X^1 \sum^+$ States of HI / DI and HBr/ DBr*, J. Mol. Spectro. 150, 1-27 (1991).
- [87] H. G. Hedderich, M. Dulick, and P. F. Bernath, *High resolution emission spectroscopy of AlCl at 20*, J. Chem. Phys. 99, 8363-8370 (1993).
- [88] R. Eggenberger, S. Gerber, H. Huber, D. Searles, and M. Welker, *Thermodynamical and structural properties of neon in the liquid and supercritical states obtained from ab initio calculations and molecular dynamics simulations*, J. Chem. Phys. 99, 9163-9169 (1993). R. Eggenberger, S. Gerber, H. Huber, D. Searles, *Ab initio calculation of the 2nd virial-coefficient of Neon and the potential-energy curve of Ne_2* , Chem. Phys. 156, 395-401 (1991).
- [89] D. Cvetko, A. Lausi, A. Morgante, F. Tommasini, P. Cortona, and M. G. Doni, *A new model for atomatom potentials*, J. Chem. Phys. 100, 2052-2057 (1994).
- [90] K.T. Tang, J.P. Toennies, and C.L. Yiu, *Accurate analytical He-He van der Waals Potential Based on Perturbation Theory*, Phys.Rev. Lett. 74, 1546-1549 (1995).
- [91] T. Korona, H.L. Williams, R. Bukowski, B. Jeziorski, and K. Szalewicz, *Helium dimer potential from symmetry-adapted perturbation theory calculations using large Gaussian geminal and orbital basis sets*, J. Chem. Phys. 106, 5109-5122 (1997)
- [92] Z. H. Zhu, F. H. Wang, B. Chen, M. L. Tan, and H. Y. Wang, *New analytical potential energy function for doubly charged diatomic ions*, Molecular Physics 92, 1061-1065 (1997). Z.H. Zhu, *Atomic and Molecular Reaction Statics* (Beijing: Science Press, 1997); Z.H. Zhu, and H.G. Yu, *Molecular Structure and Molecular Potential Energy Function*, (Beijing: Science Press, 1997); F.H. Wang, D.L. Jiang, D. L., and Z.H. Zhu, *J. SU.*, 34, 198 (1997).

- [93] M. Molski, *Application of Deformational Self-Consistent Procedure and New Potential Expansion to Effective Reduction of Wavenumbers of Rotational and VibrationRotational Transitions of GeS $X^1 \Sigma^+$* , J. Mol. Spectro. 193, 244-248(1999).
- [94] U. Kleinekathöfer, M. Lewerenz, and M. Mladenovic, *Long Range Binding in Alkali-Helium Pairs*, Phys. Rev. Lett. 83, 4717-4720 (1999).
- [95] G. Hajigeorgiou and R.J. Le Roy, *A modified Lennard-Jones oscillator model for diatom potential functions*, J. Chem. Phys. 112, 3949-3957 (2000).
- [96] C. Samuelis, E. Tiesinga, T. Laue, M. Elbs, H. Knöckel, and E. Tiemann, *Cold atomic collisions studied by molecular spectroscopy*, Phys. Rev. A 63, 012710 (2001).
- [97] D. Bellert and W.H. Breckenridge, *Bonding in Ground-State and Excited-State $A^+ .Rg$ van der Waals Ions (A) Atom, $Rg=Rare-Gas$ Atom): A Model-Potential Analysis*, Chem. Rev. 102, 1595-1622 (2002).
- [98] K. Cahill and V. A. Parsegian, *Rydberg-London potential for diatomic molecules and unbonded atom pairs*, J. Chem. Phys. (Communication), 121, 10839-10842 (2004).
- [99] F.H. Wang, C.L. Yang, and Z.H. Zhu, *New analytical potential energy function for diatomic cations*, J. Mol.Struct. 684, 9-13 (2004); F.H. Wang, C.L. Yang, Z.H. Zhu, and F.Q. Jing, *New analytical potential energy function for doubly charged diatomic molecules*, Chin. Phys. 14, 317-322 (2005).
- [100] R.H.Xie and J.B. Gong, Phys. Rev. Lett. **95**, 263202 (2005).
- [101] R. J. Le Roy, Y.Y. Huang, and C. Jary, *An accurate analytic potential function for ground-state N_2 from a direct-potential-fit analysis of spectroscopic data*, J. Chem. Phys. 125, 164310 (2006).
- [102] V.B. Sovkov, V.S. Ivanov, Z. Chen, L. Li, and S. Magnier, *Analysis of the $Na_2 4^3 \Sigma_g^+$ state above and below the $3s + 3d$ atomic limit*, J. Mol. Spectro. 236, 35-41 (2006).
- [103] L. Bytautas, N. Matsunaga, T. Nagata, M. S. Gordon, and K. Ruedenberg, J. Chem. Phys. 127, 204313 (2007).
- [104] K. Patkowski, V. Spirko, and K. Szalewicz, *On the Elusive Twelfth Vibrational State of Beryllium Dimer*, Science. 326, 1382-1384 (2009).
- [105] C. Strauss, T. Takekoshi, F. Lang, K. Winkler, R. Grimm, J. H. Denschlag, and E. Tieman, *Hyperfine, rotational, and vibrational structure of the $a^3 \Sigma_u^+$ state of $^{87}Rb_2$* , Phys. Rev. A: 82, 052514 (2010).
- [106] L. Busevica, I. Klincare, O. Nikolayeva, M. Tamanis, R. Ferber, V. V. Meshkov, E. A. Pazyuk, and A. V. Stolyarov, *Fourier transform spectroscopy and direct potential fit of a shelllike state: Application to $E(4)^1 \Sigma^+$ KCs*, J. Chem. Phys. 134, 104307 (2011).
- [107] G.D. Zhang, J. Y. Liu, L. H. Zhang, W. Zhou, and C.S. Jia, *Modified Rosen-Morse potential-energy model for diatomic molecules*, Phys. Rev. A 86, 062510 (2012)
- [108] V. B. Sovkov, V. S. Ivanov, K. V. Minaev, and M. S. Aleksandrov, *Multiparameter Model Functions in Problems of Approximating ab initio Potentials and Spectroscopic Data of Diatomic Molecules*, Optics and Spectroscopy, 114, 167-176 (2013).
- [109] H. Knöckel, S. Rühmann, and E. Tiemann, *The $X^1 \Sigma_g^+$ ground state of Mg_2 studied by Fourier-transform spectroscopy*, J. Chem. Phys. 138, 094303 (2013).
- [110] X. W. Sheng, X. Y. Kuang, P. Li, and K. T. Tang, *Analyzing and modeling the interaction potential of the ground-state beryllium dimer*, Phys. Rev. A 88, 022517 (2013).
- [111] T. Tietz, *Potential-Energy function for diatomic molecules*, J. Chem. Phys. 38, 3036 (1963).
- [112] I.M. Torrens, *Interatomic Potentials* (Academic Press, New York ,1972).
- [113] J. Goodisman, *Diatomic Interaction Potential Theory: Vol. 1: Fundamentals, and Vold. 2: Applications*. (Academic Press, New York, 1973).
- [114] A.R. Leach, *Molecular Modelling: Principles and Applications* (Pearson Education, New Delhi, 2003).
- [115] I.G. Kaplan, *Intermolecular Interactions: Physical Picture, Computational Methods, and Model Potentials* (John Wiley & Sons, New Jersey, 2006).
- [116] M. Finnis, *Interatomic Forces in Condensed Matter* (Oxford University Press, Oxford, 2010)

- [117] A. J. Stone, *The Theory of Intermolecular Forces* (2nd Edition) (Oxford University Press, Oxford, 2013).
- [118] J. Cizek, *J. Chem. Phys.* **45**, 4256 (1966).
- [119] Gaussian 09, Revision D.01, M. J. Frisch, G. W. Trucks, H. B. Schlegel, G. E. Scuseria, M. A. Robb, J. R. Cheeseman, G. Scalmani, V. Barone, B. Mennucci, G. A. Petersson, H. Nakatsuji, M. Caricato, X. Li, H. P. Hratchian, A. F. Izmaylov, J. Bloino, G. Zheng, J. L. Sonnenberg, M. Hada, M. Ehara, K. Toyota, R. Fukuda, J. Hasegawa, M. Ishida, T. Nakajima, Y. Honda, O. Kitao, H. Nakai, T. Vreven, J. A. Montgomery, Jr., J. E. Peralta, F. Ogliaro, M. Bearpark, J. J. Heyd, E. Brothers, K. N. Kudin, V. N. Staroverov, R. Kobayashi, J. Normand, K. Raghavachari, A. Rendell, J. C. Burant, S. S. Iyengar, J. Tomasi, M. Cossi, N. Rega, J. M. Millam, M. Klene, J. E. Knox, J. B. Cross, V. Bakken, C. Adamo, J. Jaramillo, R. Gomperts, R. E. Stratmann, O. Yazyev, A. J. Austin, R. Cammi, C. Pomelli, J. W. Ochterski, R. L. Martin, K. Morokuma, V. G. Zakrzewski, G. A. Voth, P. Salvador, J. J. Dannenberg, S. Dapprich, A. D. Daniels, Ö. Farkas, J. B. Foresman, J. V. Ortiz, J. Cioslowski, D. J. Fox, Gaussian, Inc., Wallingford, CT, 2009.
- [120] W. Kolos and J. Rychlewski, *J. Chem. Phys.* **98**, 3960 (1993); W. Kolos, C.C.J.Roothaan, *Rev. Mod. Phys.* **32**, 219 (1960).
- [121] R. Rydberg, *Z. Phys.* **73**, 376 (1932); O. Klein, *Z. Phys.* **76**, 226 (1932); A. L. G. Rees, *Proc. Phys. Soc. London* **59**, 998 (1947).
- [122] I. Tobias and J. T. Vanderslice, *J. Chem. Phys.* **35**, 1852 (1961).
- [123] B. Barakat, R. Bacis, F. Carrot, S. Churassy, P. Crozet, F. Martin, *Chem. Phys.* **102**, 215 (1986).
- [124] K. Cahill, *Euro. Phys. J. D* **44**, 459 (2007).
- [125] G.L. Guo, K.T. Tang, J.P. Toennies, and C.L. Yiu, *J. Chem. Phys.* **98**, 8777 (1993).
- [126] H. Bredohl, I. Dubois, P. Nzohabonayo, *J. Mol. Spectrosc.* **93**, 281 (1982); H. Bredohl, I. Dubois, F. Melen, *J. Mol. Spectrosc.* **121**, 128 (1987).
- [127] L. Bytautas, N. Matsunaga, G. E. Scuseria, and K. Ruedenberg, *J. Phys. Chem. A* **116**, 1717 (2012).
- [128] W.Y. Jiang and A. K. Wilson, *J. Chem. Phys.* **134**, 034101 (2011); A. J. C. Varandas, *J. Chem. Phys.* **129**, 234103 (2008); D. L. Kokkin, G.B. Bacskay, and T.W. Schmidt, *J. Chem. Phys.* **126**, 084302 (2007); C.D. Sherrill and P. Piecuch, *J. Chem. Phys.* **122**, 124104 (2005); R. K. Chaudhuri and K. F. Freed, *J. Chem. Phys.* **122**, 154310 (2005).
- [129] M. L. Abrams and C. David Sherrill, *J. Chem. Phys.* **121**, 9211 (2004).
- [130] R.J. Gdanitz, *Chem. Phys. Lett.* **283**, 253 (1998).
- [131] X.Z. Li and J. Paldus, *J. Chem. Phys.* **129**, 054104 (2008).
- [132] P. G. Hajigeorgiou, *J. Chem. Phys.* **138**, 014309 (2013).
- [133] L. Bytautas, N. Matsunaga, and K. Ruedenberg, *J. Chem. Phys.* **132**, 074307 (2010).
- [134] L. Bytautas, N. Matsunaga, T. Nagata, M. S. Gordon, and K. Ruedenberg, *J. Chem. Phys.* **127**, 204301 (2007).
- [135] E. A. Colbourn, M. Dagenais, A. E. Douglas, and J. W. Raymond, *Can. J. Phys.* **54**, 1343 (1976).
- [136] W.C. Tung, M. Pavanello, and L. Adamowicz, *J. Chem. Phys.* **134**, 064117 (2011).
- [137] Y.C. Chan, D.R. Harding, W.C. Stwalley, and C. R. Vidal, *J. Chem. Phys.* **85**, 2436 (1986); W. C. Stwalley and W. T. Zemke, *J. Phys. Chem. Ref. Data* **22**, 87 (1993).
- [138] W. Cencek and J. Rychlewski, *Chem. Phys. Lett.* **320**, 549 (2000); X. Li and J. Paldus, *J. Chem. Phys.* **118**, 2470 (2003).
- [139] J. Koput, *J. Chem. Phys.* **135**, 244308 (2011).
- [140] R. J. Le Roy, D. R. T. Appadoo, R. Colin, and P. F. Bernath, *J. Mol. Spectrosc.* **236**, 178 (2006).
- [141] J.M.C. Marques, F.V. Prudente, F.B Pereira, M.M. Almeida, A M Maniero, and C.E. Fellows, *J. Phys. B* **41**, 085103 (2008).
- [142] M.Steinke, H. Knckel, and E. Tiemann, *Phys. Rev.A* **85**,042720 (2012).
- [143] C.E. Fellows, *J. Chem. Phys.* **94**, 5855 (1991).
- [144] J.B.White, M.Dulick, and P.F. Bernath, *J. Mol. Spectrosc.* **169**, 410(1995).

- [145] J.M. Peek, J. Chem. Phys. 43, 3004 (1965); J. Patel, J. Chem. Phys. 47, 770 (1967).
- [146] A. Ruzsinszky, J. P. Perdew, G. I. Csonka, J. Phys. Chem. A 109 (2005) 11006.
- [147] J.P. Karr and L. Hilico, J. Phys. B 39, 2095-2105 (2006).
- [148] L. Wolniewicz, J. Chem. Phys. 43, 1087 (1965).
- [149] W. Kolos and J. M. Peek, Chem. Phys. 12, 381 (1976); D. M. Bishop and L. M. Cheung, J. Mol. Spectrosc. 75, 462 (1979).
- [150] M. Stanke, D. Kedziera, M. Molski, S. Bubin, M. Barysz, and L. Adamowicz, Phys. Rev. Lett. 96, 233002 (2006); S. Bubin, M. Stanke, D. Kedziera, and L. Adamowicz, Phys. Rev. A 76, 022512 (2007); W.C. Tung, M. Pavanello, and L. Adamowicz, J. Chem. Phys. 137, 164305 (2012).
- [151] K. Pachucki, Phys. Rev. A 85, 042511 (2012).
- [152] W. Kolos, Int. J. Quantum Chem. 10, 217 (1976); T. R. Singh, Chem. Phys. Letters 11, 598 (1971).
- [153] W.C.Tung, M.P. Pavanello, and L. Adamowicz, J. Chem. Phys. 137, 164305 (2012).
- [154] W.C.Tung, M.P. Pavanello, and L. Adamowicz, J. Chem. Phys. 136, 104309 (2012).
- [155] J. Koput, J. Chem. Phys. 139, 104309 (2013).
- [156] J. A. Coxon and R. Colin, J. Mol. Spectrosc. 181, 215 (1997).
- [157] D.T. Chang, K.Reimann, G.Surratt,G.I. Gellene, P.Lin, and R.R.Lucchese, J. Chem. Phys. 117, 5757 (2002).
- [158] B. Liu, K. O-Ohata, and K. KirbyDocken, J. Chem. Phys. 67, 1850 (1977).
- [159] R. S. Ram, M. Dulick, B. Guo, K.-Q. Zhang, and P. F. Bernath, J. Mol. Spectrosc. 183, 360 (1997).
- [160] W. Kolos and L. Wolniewicz, J. Chem. Phys. **43**, 2429 (1965).
- [161] K. T. Tang, J. Peter Toennies, and C. L. Yiu, Theor.Chim. Acta. **88**, 169 (1994).
- [162] E. J. Bredford and F. Engelke, J. Chem. Phys. 71, 1994 (1979).
- [163] K. T. Tang, J. P. Toennies, J. Chem. Phys. **118**, 4976 (2003).
- [164] R. A. Aziz, V. P. S. Nain, J. S. Carley, W. L. Taylor, and O. T. McConville, J. Chem. Phys. **70**, 4330 (1979).
- [165] R. Feltgen, H. Kirst, K. A. Köhler, H. Pauly, and F. Torello, J. Chem. Phys. **76**, 2360 (1982).
- [166] B. Liu and A. D. McLean, J. Chem. Phys. **91**, 2348 (1989)
- [167] R. A. Aziz and M. J. Slaman, J. Chem. Phys. **94**, 8047 (1991).
- [168] J.B. Anderson, C. A. Traynor, and B.M. Boghosian, J. Chem. Phys. **99**, 345 (1993).
- [169] K. T. Tang, J. P. Toennies, and C. L. Yiu, Phys. Rev. Lett. **74**, 1546 (1995).
- [170] R.A. Aziz, W.J. Meath, and A.R. Allnatt, Chem. Phys. 78, 295 (1983).
- [171] R.A. Aziz, M.J.Slaman, Chem.Phys.130, 187 (1989)
- [172] R.J. LeRoy. M.L. Klein, and L.J. NgGee, Mol. Phys. 28 , 587 (1974); Y. Tanaka and K. Yoshino, J. Chem. Phys. 57, 2964 (1972).
- [173] B. Fernandez and H. Koch, J. Chem. Phys. **109**, 10255 (1998).
- [174] R.A. Aziz, J. Chem. Phys. **99**, 4518 (1993).
- [175] K.T. Tang and J.P. Toennies, J. Chem. Phys. **118**, 4976 (2003).
- [176] D.R. Lide and H.V. Kehiaian, *CRC Handbook of Thermophysical and Thermochemical Data* (CRC Press, Boca Raton, 1994). pp.69-71.
- [177] R. Islampour, M. Gharibi, and A. Khavaninzadch, J. Struct. Chem. 52, 664 (2011).

- [178] K.K. Docken and T.P. Schafer, *J. Mol. Spectro.* 46, 454 (1973).
- [179] P. R. Herman, P. E. LaRocque, and B. P. Stoicheff, *J. Chem. Phys.* 89, 4535 (1988).
- [180] P. Slavek, R. Kalus, P. Paska, I. Odvarkova, P. Hobza, and A. Malijevsky, *J.Chem.Phys.* 119, 2102 (2003).
- [181] J.M.C. Mareques, F.V. Prudente, F.B. Pereira, M.M. Almeida, A. M. Maniero and C E Fellows, *J. Phys. B* 41, 085103 (2008).
- [182] K. Patkowski, G. Murdachaew, C.M. Fou, and K. Szalewicz, *Mol. Phys.* 103, 2031 (2005).
- [183] A.K. Dham, W.J. Meath, A.R. Allnatt, R.A. Aziz, and M.J. Slaman, *Chem. Phys.* 142, 173 (1990).
- [184] Y. Tanaka, K. Yoshino, and D. E. Freeman, *J. Chem. Phys.* 59, 5160 (1973).
- [185] P. E. LaRocque, R. H. Lipson, P. R. Herman, and B. P. Stoicheff, *J. Chem. Phys.* 84, 6627 (1986).
- [186] D. E. Freeman, K. Yoshino, and Y. Tanaka, *J. Chem. Phys.* 61, 4880 (1974).
- [187] M.S.A. Kader, *Chem. Phys.* 352, 311 (2008).
- [188] W.J. Balfour and R.F. Whitlock, *Can. J. Phys.* 53, 472(1975).
- [189] C.R. Vidal, *J. Chem. Phys.* 72, 1864 (1980).
- [190] O. Allard, A. Pashov, H. Knöckel, and E. Tiemann, *Phys. Rev. A* 66, 042503 (2002); O. Allard, C. Samuelis, A. Pashov, H. Knöckel, E. Tiemann, *Eur. Phys. J. D* 26, 155 (2003).
- [191] D.D.Yang, P.Li, and K.T.Tang, *J.Chem.Phys.*131, 154301 (2009).
- [192] A. Stein, H. Knöckel, and E. Tiemann, *Phys. Rev.A* 78, 042508 (2008).
- [193] G. P. Yin, P. Li, and K. T. Tang, *J.Chem.Phys.*132, 074303 (2010)
- [194] Y.N.M. de Escobar, P.G. Mickelson, P. Pellegrini, S.B. Nagel, A. Traverso, M. Yan, R. Cote, and T. C. Killian, *Phys.Rev.A* 78, 062708 (2008).
- [195] A. Stein, H. Knöckel, and E. Tiemann, *Euro. Phys. J. D* 57, 171 (2010).
- [196] W.J. Balfour and A.E. Douglas, *Can. J. Phys.* **48**, 901 (1970).
- [197] C. R. Vidal and H. Scheingraber, *J. Mol. Spectrosc.* **65**, 46 (1977).
- [198] H. Knöckel, S. Rühmann, and E. Tiemann, *J. Chem. Phys.* 138, 094303 (2013).
- [199] P. Li, W. Xie, and K. T. Tang, *J.Chem.Phys.* **133**, 084308 (2010).
- [200] E. Tiesinga, S. Kotochigova, and P. S. Julienne, *Phys. Rev. A* **65**, 042722 (2002)
- [201] U. Kleinekathöfer, M. Lewerenz, and M. Mladenovic, *Phys. Rev. Lett.* 83, 4717 (1999).
- [202] N. Tariq, N. A. Taisan, V. Singh, and J. D. Weinstein, *Phys. Rev. Lett.* 110, 153201 (2013).
- [203] R. Brühl and D. Zimmermann, *J.Chem.Phys.*115, 7892 (2001)
- [204] D. Schwarzhans and D. Zimmermann, *Eur. Phys. J. D* 22, 193198 (2003)
- [205] G. Aepfelbach, A. Nunnemann, and D. Zimmermann, *Chem. Phys. Lett.* 96, 311 (1983).
- [206] R.E. Smalley, D.A. Auerbach, P.S.H. Fitch, D.H. Levy, and L. Wharton, *J. Chem. Phys.* 66, 3778 (1977).
- [207] F. Bokelmann and D. Zimmermann, *J. Chem. Phys.* 104, 923 (1996)
- [208] R. Bruhl, J. Kapetanakis and D. Zimmermann, *J.Chem.Phys.*94, 5865 (1991)
- [209] U.Kleinekathöfer, *Chem.Phys.Lett* 324, 403 (2000).
- [210] J. Koperski, *Phys. Rep.* 369, 177 (2002).

- [211] L. M. Wei, P. Li, L. W. Qiao, and K. T. Tang, *J. Chem. Phys.* 139, 154306 (2013).
- [212] E. Pahl, D. Figgen, A. Borschevsky, K. A. Peterson, and P. Schwerdtfeger, *Theor. Chem. Acc.* 129, 651 (2011).
- [213] M. Czajkowski and J. Koperski, *Spectrochim. Acta, Part A* 55, 2221 (1999).
- [214] M. Strojceki, M. Krosnicki, P. Zgoda, and J. Koperski, *Chem. Phys. Lett.* 489, 20 (2010).
- [215] E. Pahl, D. Figgen, C. Thierfelder, K. A. Peterson, F. Calvo, and P. Schwerdtfeger, *J. Chem. Phys.* 132, 114301 (2010).
- [216] L.J. Munro, J.K. Johnson, and K.D. Jordan, *J. Chem. Phys.* 114, 5545 (2001); K.T. Tang and J.P. Toennies, *Mol. Phys.* 106, 1645 (2008)
- [217] L.W. Qiao, P. Li, and K.T. Tang, *Chem.Phys.Lett.* 532, 19 (2012).
- [218] U. Buck, H.O. Hoppe, F. Huisken, and H. Pauly, *J. Chem. Phys.* 60, 4925 (1974).
- [219] J. Koperski and M. Czajkowski, *Eur. Phys.J. D* 10, 363(2000)
- [220] B.Backlund, A.Shih, and G.I. Gellene, *J.Chem.Phys* 121, 11798 (2004).
- [221] K.T. Tang and J.P. Toennies, *Chem. Phys.* 156, 413 (1991).
- [222] J.N. Murrella, T.G. Wright, S.D. Bosanac, *J. Mol. Struct.* 591, 1 (2002).
- [223] A.M. Gardner, R.J. Plowright, M.J. Watkins, T.G. Wright, and W.H. Breckenridge *J. Chem. Phys.*132, 184301 (2010).
- [224] N.Brahms, B. Newman, C. Johnson, T. Greytak, D. Kleppner, and J. Doyle, *Phys. Rev. Lett.* 101, 103002 (2008).
- [225] J. Y. Zhang, J. Mitroy, H. R. Sadeghpour, M. W. J. Bromley, *Phys.Rev.A* 78, 062710 (2008)
- [226] F. Cargnoni, T. Kus, M. Mella, and R. J. Bartlett, *J. Chem. Phys.* 129, 204307 (2008)
- [227] J.S. Winn, *Acc. Chem. Res.* 14, 341 (1981).
- [228] V. Aquilanti, E. Luzzatti, F. Pirani, and G.G. Volpi, *J.Chem.Phys.* 89, 6165 (1988).
- [229] C. H. Becker, P. Casavecchia and Y. T. Lee, *J. Chem. Phys.* 69, 2377 (1978).
- [230] C. H. Becker, P. Casavecchia and Y. T. Lee, *J. Chem. Phys.* 70, 2986 (1979).
- [231] L. Pauling, *J. Chem. Phys.* 1, 56 (1933).
- [232] H. Yagisawa, H. Sato, and T. Watanabe, *Phys. Rev. A* 16, 1352 (1977).
- [233] A. Metropoulos, C.A. Nicolaides, R.J. Buenker, *Chem.Phys.*114, 1 (1987); C. A. Nicolaides, *Chem. Phys. Lett.* 161, 547 (1989);
- [234] A. Belkacem, E. P. Kanter, R. E. Mitchell, Z. Vager, and B. J. Zabransky, *Phys. Rev. Lett.* 63, 2555 (1989).
- [235] J. Ackermann and H. Hogreve, *J. Phys. B* 25, 4069 (1992).
- [236] M. Kolbuszewski and J.P. Gu, *J. Chem. Phys.* 103, 7649 (1995).
- [237] L. Wolniewicz, *J. Phys. B* 32, 2257 (1999).
- [238] C. A. Nicolaides, M. Chrysos, P. Valtazanos, *J. Phys. B* 23, 791 (1990).